MQOM: MQ on my Mind

Algorithm Specifications and Supporting Documentation (Version 2.1)

Ryad Benadjila Charles Bouillaguet Thibauld Feneuil

Matthieu Rivain

September 22, 2025

CryptoExperts, Sorbonne Université

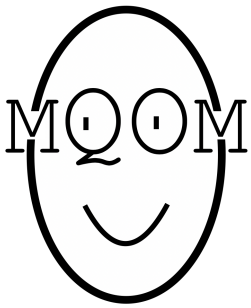

Contents

Changelog

2025-09-22: Version 2.0 → Version 2.1

We have replaced the field-embedding batching with the packing strategy. While both approaches are syntactically equivalent from a security perspective, packing allows us to shift the arithmetic overhead from $\mathbb{F}$ to $\mathbb{K}$. We have also updated the definition of the evaluation domain Ω: instead of relying on field elements ordered lexicographically, we now use Gray code, which improves the efficiency of the folding step. Although these two changes do not affect the security analysis of the scheme, they modify the structure of the public key and the signature. Consequently, the *known answer tests* have been updated.

We have also introduced a new scheme variant whose security relies on the hardness of solving the multivariate quadratic problem over the field $\mathbb{F}_{16}$. In contrast, the previous variants relied on $\mathbb{F}_2$ and $\mathbb{F}_{256}$. This new variant offers both competitive signature sizes and running times: the $\mathbb{F}_2$ variant suffers from limited computational performance, while the $\mathbb{F}_{256}$ variant incurs relatively large signature sizes.

Finally, we have provided benchmark results for new highly-optimized implementations targeting both `x86` platforms and embedded devices.

1 Introduction

MQOM (MQ-On-my-Mind) is a signature scheme derived from a zero-knowledge proof-of-knowledge of a secret solution to a random MQ instance. This zero-knowledge proof leverages the MPC-in-the-Head (MPCitH) paradigm [IKO+07] and is converted into a signature scheme using the Fiat-Shamir heuristic. This document specifies MQOM v2, the second version of the MQOM signature scheme, a second round candidate to the NIST *call for additional digital signature schemes for the post-quantum cryptography standardization process* [NIS22].

The proof system in MQOM v2 builds upon the Threshold-Computation-in-the-Head (TCitH) framework [FR23b]. Like the proof system in MQOM v1 [FR23a; BFR24], this framework transforms an MPC protocol into a zero-knowledge proof-of-knowledge via the MPCitH paradigm, while committing to secret sharings using GGM seed trees (as first proposed in [KKW18]). However, the TCitH framework utilizes threshold (Shamir) secret sharing instead of additive secret sharing. This shift reduces the computational cost of MPC emulation and enables the exploitation of multiplication homomorphism, offering significant performance improvements. The TCitH proof system in MQOM v2 can also be interpreted as a variant of VOLE-in-the-Head [BBD+23], where small VOLE correlations are directly applied in parallel repetitions, rather than being combined into a larger VOLE correlation.

By transitioning from the original MPCitH proof system (relying on additive secret sharing) to the TCitH proof system, the size of MQOM signatures has been roughly halved. In particular, for Category I, MQOM v2 achieves signatures of 2.8–4.2 KB against 6.3–7.9 KB for MQOM v1. Unless otherwise specified, MQOM should refer to MQOM v2 in the rest of this documentation.

Organization of the document. Section 2 gives an overview of the MQOM signature scheme as well as a detailed description of the key generation, signature and verification algorithms and their underlying subroutines. Section 3 explains the selection of parameters and depicts the proposed instances and their performances. Section 4 provides a security analysis of the MQOM signature scheme. Section 5 discusses the design choices of MQOM, while Section 6 addresses its advantages and limitations.

2 Description of the MQOM signature scheme

2.1 Overview

The Threshold-Computation-in-the-Head (TCitH) framework specializes the MPC-in-the-Head paradigm with threshold (Shamir) secret sharing [FR23c; FR23b]. In this framework, the prover commits to a Shamir secret sharing $[\![x]\!]$ of the secret value x and simulates an MPC protocol to verify the validity of x (e.g., as the solution to a public MQ instance). During this process, the prover reveals the publicly broadcast sharings $[\![\alpha]\!]$ to the verifier. The verifier, in turn, checks certain properties of $[\![\alpha]\!]$ to assess the validity of x and finally challenges the prover to open specific parties to verify the correctness of the MPC simulation. The TCitH framework is closely related to the VOLE-in-the-Head (VOLEitH) framework [BBD+23], where the prover commits to VOLE correlations of the form $x \cdot \Delta + r_x$ (for a random r_x). The prover then executes a protocol that computes and transmits to the verifier VOLE correlations of the form $\alpha \cdot \Delta + r_\alpha$ (analogous to the broadcast sharings $[\![\alpha]\!]$), before ultimately revealing $x \cdot \Delta + r_x$ for a challenge value of Δ.

Both frameworks can be interpreted as composing of a *polynomial interactive oracle proof* (polynomial IOP or PIOP) and a (zero-knowledge) *polynomial commitment scheme* (PCS), an increasingly common approach in the design of proof systems [SZ22; Tha23]. In the case of TCitH, committing to a Shamir secret sharing $[\![x]\!]$ corresponds to committing to the underlying polynomial P_x. Revealing a share $[\![x]\!]_i$ is equivalent to disclosing an evaluation $P_x(\omega_i)$. Similarly, VOLEitH commits to a VOLE correlation, which corresponds to a degree-1 polynomial $P_x(\Delta) = x \cdot \Delta + r_x$, with the prover later revealing an evaluation of this polynomial.

This section provides an overview of the MQOM signature scheme and the underlying TCitH-Π_{PC} proof system [FR23b] within the PIOP+PCS formalism. We begin by recalling the definition of the MQ problem. Next, we introduce the PIOP and PCS components that define the MQOM zero-knowledge proof of knowledge (ZK PoK). Finally, we discuss the compilation of this ZK PoK into the MQOM signature scheme using parallel repetitions, the Fiat-Shamir transform, and additional optimizations.

2.1.1 MQ problem

We recall the definition of the MQ problem (in matrix form) which is the core hardness assumption of the MQOM signature scheme.

Definition 1 (Multivariate Quadratic Problem)**.** *Let $\mathbb{F}$ be a finite field and let m, n be positive integers. The Multivariate Quadratic (MQ) problem with parameters $(\mathbb{F}, m, n)$ is the following problem:*

Let $(A_i)_{i\in[m]}$, $(b_i)_{i\in[m]}$, x and $y = (y_1, \ldots, y_m)$ be such that:

1. *x is uniformly sampled from $\mathbb{F}^n$,*
2. *for all $i \in [m]$, A_i is uniformly sampled from $\mathbb{F}^{n\times n}$,*
3. *for all $i \in [m]$, b_i is uniformly sampled from $\mathbb{F}^n$,*
4. *for all $i \in [m]$, y_i is defined as $y_i := x^\intercal A_i x + b_i^\intercal x$.*

From $\big(\{A_i\}, \{b_i\}, y\big)$, find x.

2.1.2 MQOM polynomial IOP

Formally, a PIOP is an interactive proof in which the prover can send a *polynomial oracle* $[P_1, \ldots, P_n]$ to the verifier for polynomials $P_1, \ldots, P_n \in \mathbb{K}[X]$ of prescribed degree d. From such a polynomial oracle, the verifier can then query some evaluations. Namely, for a query r to the oracle, the latter provides the verifier with the polynomial evaluations $P_1(r), \ldots, P_n(r)$. The verifier has the guarantee that some polynomials of degree d are embedded in the oracle and that their evaluations in r match the oracle's response.

In the MQOM PIOP, the prover aims to convince the verifier that they know an MQ solution $x \in \mathbb{F}^n$ such that $F(x) = (0, \ldots, 0) \in \mathbb{F}^m$, where

$$F = (f_1, \ldots, f_m) \quad \text{with} \quad f_i : x \mapsto x^\intercal A_i x + b_i^\intercal x - y_i \ . \tag{1}$$

This protocol is the PIOP equivalent of the QuickSilver protocol [YSW+21] within the VOLE-in-the-Head framework [BBD+23] or the Π_{PC} MPC protocol within the TCitH framework [FR23b].

Packing. Let $\mathbb{K}$ be a degree-μ extension field of $\mathbb{F}$. Let $\beta_1, \ldots, \beta_\mu$ be an $\mathbb{F}$-basis of $\mathbb{K}$ and let

$$\phi : (e_1, \ldots, e_\mu) \in \mathbb{F}^\mu \mapsto \sum_{i=1}^{\mu} e_i \cdot \beta_i \in \mathbb{K} \ .$$

be the associated $\mathbb{F}$-linear field-embedding isomorphism.

The MQOM PIOP performs computation in the field extension $\mathbb{K}$, and its efficiency depends on the number of degree-2 constraints over $\mathbb{K}$. The above constraint $F(x) = 0$ corresponds to m degree-2 constraints over $\mathbb{F}$. To reduce the number of constraints, we apply a packing technique similar to that in [BBM+24]. Specifically, we define:

$$\begin{array}{rclcrcl}
\hat{A}_1 & = & \phi(A_1, \ldots, A_\mu) \ , & \ldots & \hat{A}_{\hat{m}} & = & \phi(A_{m-\mu+1}, \ldots, A_m) \ , \\
\hat{b}_1 & = & \phi(b_1, \ldots, b_\mu) \ , & \ldots & \hat{b}_{\hat{m}} & = & \phi(b_{m-\mu+1}, \ldots, b_m) \ , \\
\hat{y}_1 & = & \phi(y_1, \ldots, y_\mu) \ , & \ldots & \hat{y}_{\hat{m}} & = & \phi(y_{m-\mu+1}, \ldots, y_m) \ ,
\end{array}$$

with $\hat{m} = m/\mu$ (assuming m is a multiple of μ). Instead of proving that $x \in \mathbb{F}^n$ satisfies $F(x) = (0, \ldots, 0)$, the MQOM PIOP proves that x satisfies $\hat{F}(x) = (0, \ldots, 0) \in \mathbb{K}^{\hat{m}}$, where

$$\hat{F} = (\hat{f}_1, \ldots, \hat{f}_{\hat{m}}) \quad \text{with} \quad \hat{f}_i : x \mapsto x^\intercal \hat{A}_i x + \hat{b}_i^\intercal x - \hat{y}_i \ . \tag{2}$$

By $\mathbb{F}$-linearity of ϕ, this new statement is strictly equivalent to the original one, but it involves $\hat{m} = m/\mu$ degree-2 constraints over $\mathbb{K}$ instead of m degree-2 constraints over $\mathbb{F}$. To avoid repeated conversions, MQOM key generation outputs the MQ instance directly in packed form $(\hat{A}_i, \hat{b}_i, \hat{y}_i)_{i \in [\hat{m}]}$, and the signing and verification algorithms operate exclusively on this packed representation.

Notions. Let $\Omega \subseteq \mathbb{K}$ an *evaluation domain* (i.e. the points on which the polynomial oracle can be queried). We denote $\mathbb{K}[X]^{\leqslant d}$ the set of polynomials of degree $\leq d$ with coefficients in $\mathbb{K}$ and we shall consider *vector polynomials*, which are vectors with polynomial coordinates. We consider the homogeneous application of $\hat{F}$ to a degree-1 vector polynomial $P \in \left(\mathbb{K}[X]^{\leqslant 1}\right)^n$, which results in a degree-2 vector polynomial $\hat{F}(P) \in \left(\mathbb{K}[X]^{\leqslant 2}\right)^{\hat{m}}$ such that

$$\hat{F}(P)(X) = (P(X)^\intercal \hat{A}_i P(X) + \hat{b}_i^\intercal P(X) \cdot X - \hat{y}_i \cdot X^2)_i \ .$$

We shall denote by $P(\infty) \in \mathbb{K}^n$ the leading coefficient vector of a vector polynomial P. In particular, for $P \in \mathbb{K}[X]^{\leqslant 1}$, $P(\infty)$ denotes the degree-1 coefficient vector, while for $\hat{F}(P) \in \mathbb{K}[X]^{\leqslant 2}$, $\hat{F}(P)(\infty)$ denotes the degree-2 coefficient vector. For some vector polynomial $P_x \in \left(\mathbb{K}[X]^{\leqslant 1}\right)^n$ such that $P_x(\infty) = x$, we thus obtain $\hat{F}(P)(\infty) = \hat{F}(x)$, which is the all-0 vector if and only if x is the MQ solution associated to F (and $\hat{F}$).

PIOP: simple version. We start with a simplified version of the PIOP underlying MQOM, which is depicted in Figure 1. The prover first picks random vector polynomials $P_x \in \left(\mathbb{K}[X]^{\leqslant 1}\right)^n$ and $P_u \in \left(\mathbb{K}[X]^{\leqslant 1}\right)^{\hat{m}}$ such that $P_x(\infty) = x$ (while P_u is fully random). Then they send an oracle to these polynomials to the verifier. The prover further computes $P_\alpha = P_u + \hat{F}(P_x)$ and sends it in clear (i.e. not as an oracle) to the verifier. The verifier samples a random point r in the evaluation domain Ω and queries the oracle to obtain the evaluations $P_x(r), P_u(r)$. They finally check that $P_\alpha(r) = P_u(r) + \hat{F}(P_x(r))$.

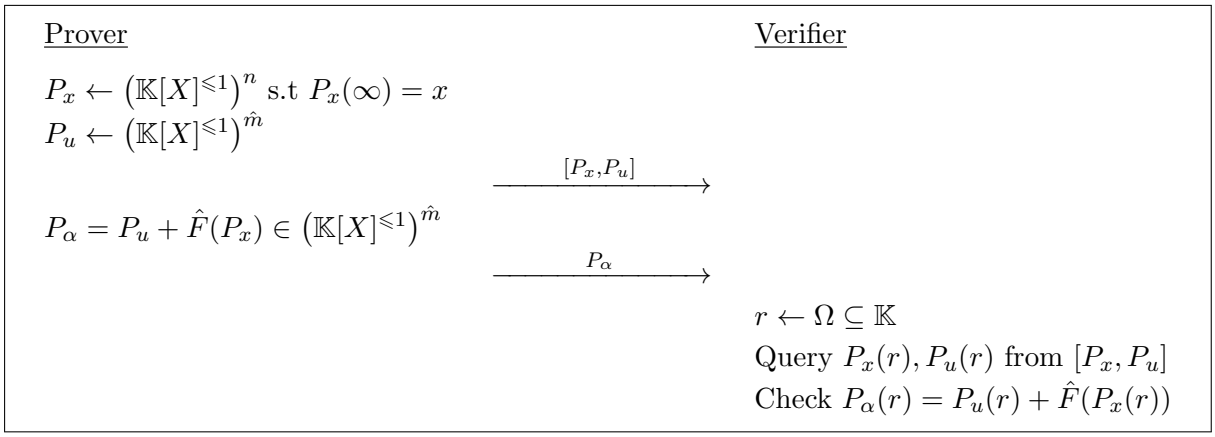

Figure 1: Polynomial IOP underlying MQOM (simple version).

The vector polynomial $P_z := \hat{F}(P_x)$ is of degree 1 if and only if $P_z(\infty) = \hat{F}(P_x(\infty)) = (0, \ldots, 0) \in \mathbb{K}^{\hat{m}}$, meaning that $x = P_x(\infty)$ is a valid solution to the MQ instance defined by F. The soundness of this protocol follows from the Schwartz–Zippel lemma. Assume that $P_\alpha(r) = P_u(r) + \hat{F}(P_x(r))$ holds for 3 different points $r \in \Omega$, then because P_x, P_u, P_α are guaranteed to be of degree 1, we must have $P_\alpha = P_u + \hat{F}(P_x)$ and hence $\hat{F}(x) = 0$ (i.e. the prover indeed knows a solution x). Conversely, in the presence of a malicious prover (who does not know a correct solution x), we can only have $P_\alpha(r) = P_u(r) + \hat{F}(P_x(r))$ for at most two values r of Ω. The soundness error of the PIOP is hence of $2/|\Omega|$.

The zero-knowledge property of this protocol holds for two reasons. First, thanks to the addition of the random vector polynomial P_u, the vector polynomial P_α is further uniformly random. Then, any evaluations $P_x(r), P_u(r)$ are independent of x thanks to the randomness involved in these polynomials.

Remark 1. *The original TCitH-Π_{PC} protocol does not encode the secret x as the leading coefficient of P_x but as its constant term (as for the original Shamir's secret sharing). While this choice neither impacts the soundness nor the communication, choosing the leading term has some advantages in terms of computation (see Section 5 for further discussion).*

Besides the polynomial oracle, the communication cost of the above PIOP is the size of P_α which is made of $2\hat{m}$ elements of the extension field $\mathbb{K}$. We now describe a method to batch the coordinates of P_α, enabling to lower this communication cost.

Batching with random combinations. To reduce the size of P_α, we can use the standard approach to batch the verification of several relations using random linear combinations. In our context, this means batching the $\hat{m}$ coordinates of $\hat{F}(P_x)$ into η random linear combinations for some parameters $\eta \in \mathbb{N}$. Let $\Gamma \in \mathbb{K}^{\eta \times \hat{m}}$ be a matrix randomly sampled by the verifier. The prover now defines P_α as:

$$P_\alpha = P_u + \Gamma \cdot P_z \in \left(\mathbb{K}[X]^{\leqslant 1}\right)^\eta$$

with $P_u \in \left(\mathbb{K}[X]^{\leqslant 1}\right)^\eta$ and $P_z = \hat{F}(P_x) \in \left(\mathbb{K}[X]^{\leqslant 1}\right)^{\hat{m}}$. We then have:

$$\Pr\left[\Gamma \cdot P_z(\infty) = (0, \ldots, 0) \mid P_z(\infty) \neq (0, \ldots, 0)\right] \;\leq\; \frac{1}{|\mathbb{K}|^\eta} \,.$$

For a target λ-bit security, selecting $\eta := \lceil \lambda / \log_2 |\mathbb{K}| \rceil$ makes the above soundness error $\leq 2^{-\lambda}$.

PIOP: full version. Figure 2 provides the description of the PIOP integrating the optional batching strategy. When the batching is disabled, the PIOP skips the step of sampling Γ by the verifier and sending it to the prover (represented between dashed lines on Figure 2). Γ is then simply defined as the identity matrix $\Gamma = I_\eta \subseteq \mathbb{K}^{\eta \times \eta}$ with $\eta = \hat{m}$.

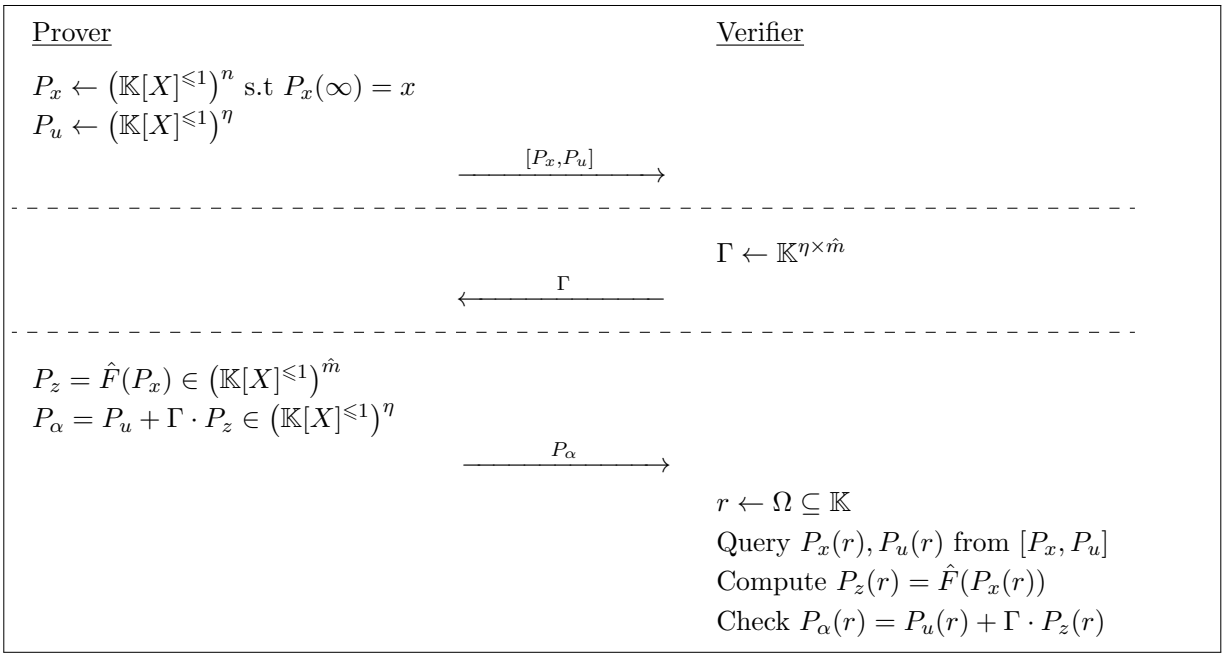

Figure 2: Polynomial IOP underlying MQOM (full version).

Disabling random-combination batching makes the MQOM zero-knowledge proof-of-knowledge a simple sigma protocol. This comes at a moderate communication cost (depending of the parameters) thanks to the packing strategy which significantly reduces the communication overhead in the context. On the other hand, when random-combination batching is enabled, the main purpose of the packing is to reduce the computation overhead. More precisely, we could replace $\hat{F}$ by F and sample a larger matrix $\Gamma \in \mathbb{K}^{\eta \times m}$. While this would not change the communication or the soundness of the PIOP, this would make sampling Γ as well as computing the product $\Gamma \cdot P_z$ heavier.

2.1.3 Line commitment scheme

To compile the above polynomial IOP into a zero-knowledge proof of knowledge (ZK-PoK), the polynomial oracle is replaced by a polynomial commitment scheme. This means that the prover sends a commitment $\mathsf{Com}(P_x, P_u)$ to the polynomials P_x, P_u in place of the oracle. Later on, the query from the verifier to the oracle is replaced by an evaluation opening protocol:

1. the verifier sends the evaluation point r to the prover,
2. the prover replies with evaluations $v_x = P_x(r), v_u = P_u(r)$ along with an opening proof π,
3. the verifier checks π and, in case of success, accepts v_x, v_u as valid evaluations.

The commitment scheme should be:

- *binding*: the commitment $\mathsf{Com}(P_x, P_u)$ defines unique polynomials P_x, P_u and it should be hard for a mallicious prover to later come up with evaluations v_x, v_u and an opening proof π passing the verification while $v_x \neq P_x(r)$ or $v_u \neq P_u(r)$;
- *hiding/zero-knowledge*: the verifier does not learn anything more than v_x, v_u about P_x, P_u.

In the context of this specification, the polynomials P_x and P_u are limited to be of degree 1. In consequence, we shall use the terminology of *line commitment scheme*. We explain the line commitment scheme used in MQOM hereafter. This construction relies on a GGM seed tree.

GGM seed tree. A GGM seed tree consists in pseudorandomly expanding a root seed `rseed` into N leaf seeds `lseed[0]`, ..., `lseed[`$N-1$`]` using a binary tree. The process is summarized by

$$\begin{cases} \texttt{node[1]} \leftarrow \texttt{rseed} \\ (\texttt{node[}2i\texttt{]}, \texttt{node[}2i+1\texttt{]}) \leftarrow \mathsf{SeedDerive}(\texttt{node[}i\texttt{]}) \quad \text{for } 1 \leq i \leq N-1 \end{cases} \tag{3}$$

where SeedDerive is a seed derivation function. The leaf seeds are then defined as the last N nodes, namely `lseed[`i`]` := `node[`$N+i$`]` for all $i \in [0, N-1]$. The structure of a GGM seed tree and underlying node numbering are illustrated on Figure 3. In the scope of the present specification, the number of leaves N is always a power of two.

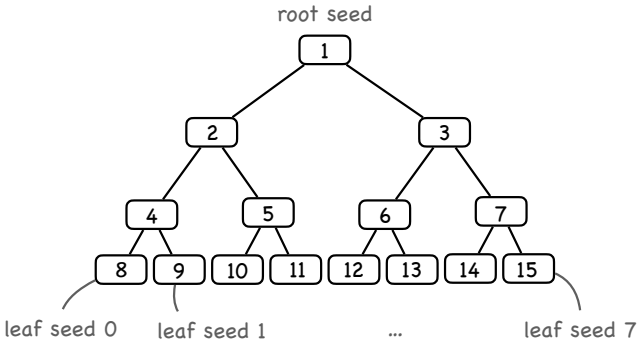

Figure 3: GGM tree structure and node numbering.

The GGM tree structure enables to reveal all-but-one leaf seeds from $\log_2(N)$ nodes of the tree. Let $i^* \in [0, N-1]$ be the index of the leaf seed that should remain hidden. Any node on

the path from the hidden leaf $\texttt{lseed}[i^*] = \texttt{node}[N + i^*]$ to the root of the tree should remain hidden (since $\texttt{lseed}[i^*]$ can be derived from any of those nodes). The indexes of the node on this hidden path belong to the following set:

$$\mathcal{H} = \{\lfloor (N + i^*)/2^j \rfloor \mid 0 \leq j \leq \log_2(N) - 1\} \ .$$

On the other hand, the *sibling path*, which is made of the siblings of the hidden nodes, can be revealed without giving any information $\texttt{lseed}[i^*]$. According to the binary tree structure, the sibling of $\texttt{node}[i]$ is $\texttt{node}[i \oplus 1]$. The sibling path of $\texttt{lseed}[i^*]$ is hence defined as:

$$\texttt{path} = \{\texttt{node}[i \oplus 1] \mid i \in \mathcal{H}\} \ .$$

By running the tree derivation of Equation 3 from all the seeds in the sibling path, one reconstructs a partial tree composed of all the nodes but the hidden path. In particular, this partial tree includes all the leaves but the hidden leaf $\texttt{lseed}[i^*]$.

GGM seed trees have been introduced in the context of MPC-in-the-Head to commit additive secret sharings with efficient opening of all-but-one shares [KKW18]. From a random root seed `rseed`, one expands a GGM seed tree to obtain the leaf seeds $\texttt{lseed}[0], \ldots, \texttt{lseed}[N-1]$. Then, each leaf seed is expanded into a share:

$$\bar{x}_i \in \mathbb{F}^n \leftarrow \mathsf{PRG}(\texttt{lseed}[i]) \ ,$$

and a correction value Δ_x is defined as:

$$\Delta_x = x - \sum_{i=0}^{N-1} \bar{x}_i \ . \tag{4}$$

By definition, $(\bar{x}_0 + \Delta_x)$, $\bar{x}_1$, $\ldots$, $\bar{x}_{N-1}$ forms an additive secret sharing of x. This additive sharing is committed by deriving a commitment for each seed:

$$\texttt{ls\_com}[i] \leftarrow \mathsf{SeedCommit}(\texttt{lseed}[i])$$

and sending a global commitment:

$$\texttt{com} \leftarrow \mathsf{Commit}(\texttt{ls\_com}[0], \ldots, \texttt{ls\_com}[N-1], \Delta_x)$$

to the verifier. Later on, the verifier can challenge the prover to open all the additive shares of x but one, say the share of index i^*. The prover then reveals the sibling path of $\texttt{lseed}[i^*]$, the correction value Δ_x and the commitment $\texttt{ls\_com}[i^*]$. From all the leaf seeds (but $\texttt{lseed}[i^*]$), the verifier can expand all the shares $\bar{x}_i$ (but $\bar{x}_{i^*}$) and correct $\bar{x}_0$ with Δ_x. The verifier can also recompute the commitments $\texttt{ls\_com}[i]$, for all $i \neq i^*$, and together with $\texttt{lseed}[i^*]$ and Δ_x, recompute and check the global commitment.

Line commitment from GGM seed tree. As described in the TCitH framework [FR23b], one can use a sharing conversion technique from [CDI05] to turn an all-but-one additive secret sharing (a.k.a. *replicated secret sharing*) into a Shamir's secret sharing, with underlying polynomial P_x encoding x. Then, revealing all-but-one additive shares of x amounts to revealing one Shamir's share of x, i.e., one evaluation of the polynomial P_x. A similar technique was also previously described in the VOLE-in-the-Head framework [BBD+23] to commit small VOLE correlations based on the small-field VOLE construction from [Roy22].

The committed degree-1 polynomial (or line) is defined as:

$$P_x = \Delta_x P_0 + \sum_{i=0}^{N-1} \bar{x}_i P_i \ \in \mathbb{K}[X]^{\leqslant 1} \tag{5}$$

where $P_0, \ldots, P_{N-1} \in \mathbb{K}[X]^{\leqslant 1}$ are fixed degree-1 polynomials defined as:

$$\begin{cases} P_i(\omega_i) = 0 \\ P_i(\infty) = 1 \end{cases} \tag{6}$$

for some predefined evaluation points $\Omega = \{\omega_0, \ldots, \omega_{N-1}\} \subseteq \mathbb{K}$. From this definition, we have that P_x encodes the secret x by:

$$P_x(\infty) = \Delta_x + \sum_{i=0}^{N-1} \bar{x}_i = x \ .$$

Moreover, the evaluation of P_x in a point $\omega_{i^*} \in \Omega$ can be derived from the all-but-one additive sharing of index i^*. Namely, from all the $\bar{x}_i$ but $\bar{x}_{i^*}$, the verifier can recompute:

$$P_x(\omega_{i^*}) = \Delta_x P_0(\omega_{i^*}) + \sum_{i=0}^{N-1} \bar{x}_i P_i(\omega_{i^*}) = \Delta_x P_0(\omega_{i^*}) + \sum_{i \neq i^*} \bar{x}_i P_i(\omega_{i^*})$$

where the above equality holds because $P_{i^*}(\omega_{i^*}) = 0$. Since any other evaluation of P_x would require the knowledge of $\bar{x}_{i^*}$, the verifier only learns $P_x(\omega_{i^*})$ from the all-but-one opening.

Following Equation 5 and Equation 6, and assuming $\omega_0 = 0$, we have $P_i(X) = X - \omega_i$ for all $i \in [0, N-1]$, and:

$$P_x(X) = x \cdot X - \sum_{i=0}^{N-1} \omega_i \cdot \bar{x}_i \ .$$

Remark 2. *As mentionned in Remark 1, the original TCitH scheme [FR23b] does not encode the secret x as $P_x(\infty)$ but as $P_x(0)$ (as in the original Shamir's secret sharing). For this reason, the P_i polynomials are defined such that $P_i(\omega_i) = 0$ and $P_i(0) = 1$ in [FR23b]. In the present specification, we choose to encode x in $P_x(\infty)$ which offers some advantages, as discussed in Section 5.*

Committing the random polynomial P_u works the same way but without correction value. Namely, the additive shares $\bar{u}_i \in \mathbb{K}^\eta$ are also pseudorandomly sampled from the leaf seeds $\texttt{lseed}[i]$ for all $i \in [0, N-1]$ and P_u is defined as:

$$P_u(X) = \sum_{i=0}^{N-1} \bar{u}_i P_i = \Big(\sum_{i=0}^{N-1} \bar{u}_i \Big) \cdot X - \sum_{i=0}^{N-1} \omega_i \cdot \bar{u}_i \ \in \big(\mathbb{K}[X]^{\leqslant 1}\big)^\eta \ .$$

Correlated tree optimization. The correlated half-tree technique introduced in [GYW+23] enables to slightly reduce the communication cost of a GGM all-but-one sharing commitment. For a fixed $\delta \in \{0,1\}^\lambda$ (where $\{0,1\}^\lambda$ is the definition space of the seeds), the correlated tree technique maintains the following invariant. At any given level in the tree, the XOR of all the seeds equal δ. To enforce this property, the definition of the tree is modified as follows:

$$\begin{cases} \texttt{node}[2] \leftarrow \texttt{rseed} \\ \texttt{node}[3] \leftarrow \texttt{rseed} \oplus \delta \end{cases} \quad \text{and} \quad \begin{cases} \texttt{node}[2i] \leftarrow \mathsf{SeedDerive}(\texttt{node}[i]) \\ \texttt{node}[2i+1] \leftarrow \texttt{node}[2i] \oplus \texttt{node}[i] \end{cases}$$

for $1 \leq i \leq N-1$. One can indeed check that, for any $j \geq 1$, we thus get:

$$\begin{aligned}\delta &= \texttt{node}[2] \oplus \texttt{node}[3] \\ &= \texttt{node}[4] \oplus \texttt{node}[5] \oplus \texttt{node}[6] \oplus \texttt{node}[7] \\ &\vdots \\ &= \bigoplus_{i=2^j}^{2^{j+1}-1} \texttt{node}[i] \ .\end{aligned}$$

Then redefining:

$$\bar{x}_i \in \mathbb{F}^n \leftarrow \texttt{lseed}[i] \parallel \mathsf{PRG}(\texttt{lseed}[i]) \ ,$$

we get that the λ first bits of $\sum_{i=0}^{N-1} \bar{x}_i$ equal δ (assuming that $\mathbb{F}$ is a binary field so that the field addition matches the XOR). By defining δ as the λ first bits of x, Equation 4 then implies that the λ first bits of Δ_x equal 0^λ (the all-0 λ-bit string). We can thus save λ bits in the communication of Δ_x.

Wrapping up. When plugging the above line commitment scheme into the PIOP of Figure 2, we obtain the MQOM ZK PoK depicted in Figure 4. Note that this PoK is extractable knowledge sound under an idealized assumption on the SeedCommit primitive (e.g. in the random oracle or ideal cipher model). This leads to a tight EUF-CMA security since the reduction can extract the secret from any valid commitment.

2.1.4 Compilation to signature scheme

The MQOM signature scheme is constructed in two steps: first, we amplify the soundness of the MQOM ZK PoK (Figure 4) through parallel repetitions; then, we apply the Fiat-Shamir transform to render it non-interactive and message-bound. In addition, we introduce some tweaks to lower the signature size and improve security and performances.

Parallel repetitions. The MQOM ZK PoK (Figure 4) has round-by-round soundness with soundness error $\epsilon_1 = 1/|\mathbb{K}|^\eta$ for the (optional) batching round and $\epsilon_2 = 2/|\Omega| = 2/N$ for the next round (see Section 2.1.2). To achieve a soundness error below $2^{-\lambda}$ for a target security of λ bits, η is fixed to $\eta = \lambda / \log_2 |\mathbb{K}|$ (the result of this division is always an integer for our considered parameters). For the next round, we rely on parallel repetitions. Namely, the protocol is repeated τ times to make $(2/N)^\tau$ sufficiently small.

Specifically, the considered line commitment is turned into a *batch line commitment* (BCL), which commits τ pairs of polynomials $(P_x^{(0)}, P_u^{(0)}), \ldots, (P_x^{(\tau-1)}, P_u^{(\tau-1)})$. For each of them, a polynomial $P_\alpha^{(e)} = P_u^{(e)} + \Gamma \cdot \hat{F}(P_x^{(e)})$ is computed and sent to the verifier, where (in case of batching) the matrix Γ is the same for each repetition. The verifier then picks τ indexes $i^*[0], \ldots, i^*[\tau-1]$, each leading to an evaluation point $r^{(e)} \in \Omega$. The prover finally reveals the opening data for the verifier to check and compute the evaluations $P_x^{(e)}(r^{(e)}), P_u^{(e)}(r^{(e)})$.

Concretely, the BCL scheme relies on τ parallel GGM trees, each giving rise to its own set of leaf seeds $(\texttt{lseed}[e][i])_{0 \leq i < N}$, corresponding commitments, $(\texttt{ls\_com}[e][i])_{0 \leq i < N}$, and correction value $\Delta_x[e]$, for $e \in [0, \tau-1]$. The global commitment is then defined as:

$$\texttt{com} \leftarrow \mathsf{Commit}(c^{(0)}, \ldots, c^{(\tau-1)}, \Delta_x[0], \ldots, \Delta_x[\tau-1])$$

where $c^{(e)} \leftarrow \mathsf{Commit}(\texttt{ls\_com}[e][0], \ldots, \texttt{ls\_com}[e][\tau-1])$. Finally, the global opening consists of the opening tuple $(\texttt{path}[e], \Delta_x[e], \texttt{ls\_com}[e][i^*[e]])$ for each execution $e \in [0, \tau-1]$.

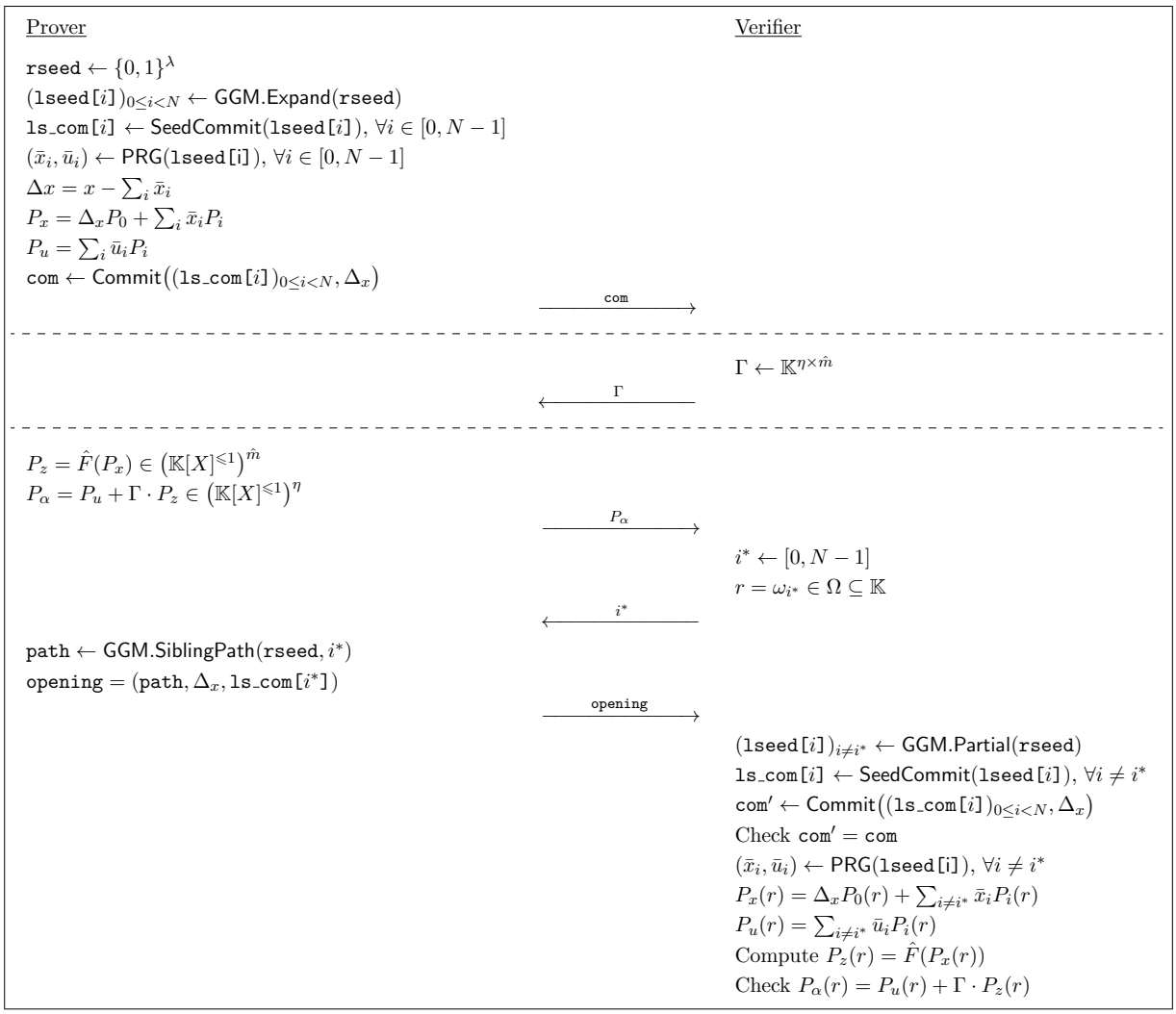

Figure 4: MQOM zero-knowledge proof of knowledge.

Hash commitment of P_α. To reduce the communication of the ZK PoK protocol, a standard optimization is to send a hash commitment of the polynomials $P_\alpha^{(0)}, \ldots, P_\alpha^{(\tau-1)}$ instead of transmitting them in full. Doing so, the prover only needs to send the leading coefficient $\alpha_1^{(e)} \in \mathbb{K}^\eta$ for each of these polynomial rather than the full pair of coefficients $(\alpha_0^{(e)}, \alpha_1^{(e)}) \in (\mathbb{K}^\eta)^2$. From the open evaluations $P_x^{(e)}(r^{(e)})$, $P_u^{(e)}(r^{(e)})$, the verifier deduces $P_\alpha^{(e)}(r^{(e)})$ and computes a candidate value for the constant term:

$$\alpha_0^{(e)} = P_\alpha^{(e)}(r^{(e)}) - \alpha_0^{(e)} \cdot r^{(e)} \ .$$

Finally, the verifier checks this against the hash commitment. This technique effectively halves the communication cost (or signature footprint) associated with the polynomials $P_\alpha^{(0)}, \ldots, P_\alpha^{(\tau-1)}$.

Fiat-Shamir transform. In the following, we shall denote by $\texttt{com}_1$ the BLC commitment and $\texttt{com}_2$ the hash commitment of the polynomials $P_\alpha^{(0)}, \ldots, P_\alpha^{(\tau-1)}$ following the above optimization.

In the first (optional) round, the application of Fiat-Shamir consists in deriving the matrix

$\Gamma \in \mathbb{K}^{\eta \times \frac{m}{\mu}}$ from the commitment by a call to an extendable output hash function:

$$\Gamma \leftarrow \mathsf{XOF}(\mathtt{com}_1) \ .$$

In the second round, the application of Fiat-Shamir consists in deriving the challenge indexes $i^*[0], \ldots, i^*[\tau-1]$ from the commitments $\mathtt{com}_1$ and $\mathtt{com}_2$. We further input the message as well as the public key is this hash computation, which gives:

$$(i^*[0], \ldots, i^*[\tau-1]) \leftarrow \mathsf{XOF}(\mathtt{pk}, \mathtt{com}_1, \mathtt{com}_2, \mathtt{msg}) \ .$$

Grinding. To reduce the number of parallel repetitions, we employ *grinding*. Namely, we include a w-bit proof-of-work increasing the number of iterations of the second hash by a factor of 2^w on average for a grinding parameter w. The number of repetitions is then relaxed to satisfy

$$\left(\frac{2}{N}\right)^{\tau} \leq \frac{1}{2^{\lambda-w}} \ , \tag{7}$$

namely, we fix $\tau := \lceil (\lambda - w)/(\log_2(N) - 1) \rceil$.

The second Fiat-Shamir hash is then performed as follows. One first compute a hash value

$$\mathtt{hash} \leftarrow \mathsf{Hash}(\mathtt{pk}, \mathtt{com}_1, \mathtt{com}_2, \mathtt{msg})$$

and then iterates

$$(i^*, \mathtt{val}) \leftarrow \mathsf{XOF}(\mathtt{hash}, \mathtt{nonce})$$

where $i^* = (i^*[0], \ldots, i^*[\tau-1]) \in [0, N-1]^\tau$, $\mathtt{val} \in [0, 2^w - 1]$, and $\mathtt{nonce} \in [0, 2^{32} - 1]$ a 32-bit counter. The above computation is repeated by increasing $\mathtt{nonce}$ until obtaining $\mathtt{val} = 0$. The succeeding $\mathtt{nonce}$ value is included into the signature so that the verifier only needs to run the right XOF computation once. The verifier further checks that the XOF output satisfies $\mathtt{val} = 0$ to accept the signature.

In the random oracle model (ROM), any attempt to forge a signature requires the adversary to make a random oracle query to get the associated challenge i^*. Using grinding, each such random oracle query has only a probability 2^{-w} to yield a valid grinding value $\mathtt{val} = 0$. As a result, the (amplified) second-round soundness error scales from $\epsilon_1 = (2/N)^\tau$ down to $\epsilon_1 \cdot 2^{-w}$ from which we get the relaxation of Equation 7. The reader is referred to [Sta21] for a formal argument.

Seed derivation and commitment in GGM trees. The functions $\mathsf{SeedDerive}$, $\mathsf{SeedCommit}$, and PRG are defined based on a block cipher:

$$\mathsf{Enc} : (\mathtt{key}, \mathtt{ptx}) \in \{0,1\}^\lambda \times \{0,1\}^\lambda \mapsto \mathtt{ctx} \in \{0,1\}^\lambda \ , \tag{8}$$

which is instantiated as AES-128 (for $\lambda = 128$) or Rijndael-256-256 (for $\lambda = 192$ and $\lambda = 256$). This choice ensures efficiency by leveraging the AES hardware instructions available on modern CPUs.

For security, the derivation, commitment and expansion of seeds must incorporate a random salt, which is sampled at the beginning of the signing process and included as part of the signature. Since seeds are only λ bits long, using this salt mitigates the risk of collisions in tree derivation and prevents accelerated exhaustive searches for hidden seeds. Additionally, this salt is modified to enforce domain separation between different calls to $\mathsf{SeedDerive}$ and $\mathsf{SeedCommit}$ within a single signature computation.

We employ a Davies-Meyer construction to transform the block cipher Enc into the seed derivation and commitment primitives. Here, the salt acts as the key, while the seed is used as the plaintext and also introduced in the output through a feed-forward mechanism. Given the XOR-invariant properties of correlated GGM tree optimizations, a simple XOR-based feed-forward would make the seed derivation process invertible. Instead, as suggested in [GKW+20], we use a $\mathbb{F}_2$-linear orthomorphism ψ, defined as:

$$\psi : (x_l \parallel x_r) \in \{0,1\}^\lambda \mapsto (x_l \oplus x_r \parallel x_l) \ . \tag{9}$$

Concretely, we define encryption with feed-forward (EncFF) as follows:

$$\mathsf{EncFF} : (\mathsf{seed}, \mathtt{tweak}) \mapsto \mathsf{Enc}(\mathtt{salt} \oplus \mathtt{tweak}, \mathsf{seed}) \oplus \psi(\mathsf{seed}) \ . \tag{10}$$

This allows us to define the seed derivation function as:

$$\mathsf{SeedDerive}(\mathsf{seed}, \mathtt{tweak}) = \mathsf{EncFF}(\mathsf{seed}, \mathtt{tweak}) \ , \tag{11}$$

and the seed commitment function as:

$$\mathsf{SeedCommit}(\mathsf{seed}, \mathtt{tweak}) = \mathsf{EncFF}(\mathsf{seed}, \mathtt{tweak}) \parallel \mathsf{EncFF}(\mathsf{seed}, \mathtt{tweak} \oplus 1) \ . \tag{12}$$

The domain-separator tweaks are defined to ensure security. For seed derivation, we assign a unique $\mathtt{tweak}$ for each pair (e, j), where $e \in [0, \tau - 1]$ denotes the execution index, and $j \in [0, \log_2(N) - 1]$ represents the height of the current node in the tree. This guarantees that any two seeds in the revealed sibling paths result from distinct derivation functions, preventing accelerated preimage attacks. For commitment, we use a distinct pair $(\mathtt{tweak}, \mathtt{tweak} \oplus 1)$ per execution index $e \in [0, \tau - 1]$ (and which are also disjoint from the seed derivation tweaks), ensuring that hidden seed commitments are derived from separate commitment functions, thereby thwarting accelerated preimage attacks.

2.2 Notations

Mathematical notations. We summarize the mathematical notations used in the algorithmic description of MQOM in Table 1. The concrete instantiations of $\mathbb{F}$ and $\mathbb{K}$, with underlying irreducible polynomials, the evaluation points $\omega_0, \ldots, \omega_{N-1}$, and the $\mathbb{F}$-basis of $\mathbb{K}$, $\beta_1, \ldots, \beta_\mu$, are defined in Section 3.

Table 1: Mathematical notations.

$\mathbb{F}$	The base field, a finite field of characteristic 2
$\mathbb{K}$	The extension field, a finite extension of $\mathbb{F}$
$\Omega = \{\omega_0, \ldots, \omega_{N-1}\}$	The evaluation domain, a subset of $\mathbb{K}$
$\{\beta_1, \ldots, \beta_\mu\}$	An $\mathbb{F}$-basis of $\mathbb{K}$
$\mathbb{F}[X]^{\leqslant 1}$	Set of polynomials of degree ≤ 1 with coefficients from $\mathbb{F}$
$\mathbb{K}[X]^{\leqslant 1}$	Set of polynomials of degree ≤ 1 with coefficients from $\mathbb{K}$
ψ	Linear orthomorphism $\psi : \{0,1\}^\lambda \to \{0,1\}^\lambda$
$\lvert\cdot\rvert_2$	Bit-size of a field-element vector
$\lvert\cdot\rvert_8$	Byte-size of a field-element vector
I_η	Identity matrix on $\mathbb{K}^{\eta\times\eta}$
0^ℓ	All-0 ℓ-bit string

We let ψ be the $\mathbb{F}_2$-linear orthomorphism defined as:

$$\psi : (x_l \parallel x_r) \in \{0,1\}^\lambda \mapsto (x_l \oplus x_r \parallel x_l) \ . \tag{13}$$

Notations for MQOM parameters. The notations for the various parameters of MQOM are summarized in Table 2. The specific instantiations of these parameters, which define the different instances of MQOM, are provided in Section 3.

Table 2: Parameters of the MQOM signature scheme.

MQ parameters:	
$\mathbb{F}$	Base field
n	Number of unknowns
m	Number of equations
Proof system parameters:	
λ	Security parameter
μ	Extension degree $\mu = [\mathbb{K} : \mathbb{F}]$
$\hat{m}$	Number of packed equations $\hat{m} = m/\mu$
N	Size of the evaluation domain $N = \lvert\Omega\rvert$
η	Number of internal repetitions of the proof system
τ	Number of external repetitions of the proof system
w	Grinding proof-of-work parameter

Notations for algorithmic description. The variables used in the algorithmic description of MQOM, along with their respective definition domains, are summarized in Table 3.

Table 3: Notations of the MQOM signature scheme.

x	Secret MQ solution	$\mathbb{F}^n$
$\hat{A}_i$	Quadratic-part matrix of the i-th MQ packed equation	$\mathbb{K}^{n\times n}$
$\hat{b}_i$	Linear-part vector of the i-th MQ packed equation	$\mathbb{K}^n$
$\hat{y}_i$	Constant part of the i-th MQ packed equation	$\mathbb{K}$
`seed_key`	Master seed for key generation	$\{0,1\}^{2\lambda}$
`seed_eq`$[i-1]$	Seed for MQ equations $\{\hat{A}_i\}$, $\{\hat{b}_i\}$	$\{0,1\}^{2\lambda}$
$\texttt{com}_1$	BLC commitment	$\{0,1\}^{2\lambda}$
$\texttt{com}_2$	Hash commitment $\texttt{com}_2 = \mathsf{Hash}(\alpha_0, \alpha_1)$	$\{0,1\}^{2\lambda}$
`key`	BLC opening key $\texttt{key} = (\texttt{node}, \Delta_{x'})$	–
`opening`	BLC opening $\texttt{opening} = (\texttt{path}, \texttt{out\_ls\_com}, \Delta_{x'})$	–
i^*	Hidden-leaf indexes $i^* = (i^*[0], \ldots, i^*[\tau-1])$	$[0, N-1]^\tau$
`nonce`	Grinding nonce	$[0, 2^{32}-1]$
`val`	Grinding test value	$[0, 2^w-1]$
`batching`	Boolean for enabling / disabling the batching variant	$\{\mathsf{True}, \mathsf{False}\}$
x_0	Coefficient array $x_0 = (x_0[0], \ldots, x_0[\tau-1])$	$\left(\mathbb{K}^n\right)^\tau$
u_0	Coefficient array $u_0 = (u_0[0], \ldots, u_0[\tau-1])$	$\left(\mathbb{K}^\eta\right)^\tau$
u_1	Coefficient array $u_1 = (u_1[0], \ldots, u_1[\tau-1])$	$\left(\mathbb{K}^\eta\right)^\tau$
α_0	Coefficient array $\alpha_0 = (\alpha_0[0], \ldots, \alpha_0[\tau-1])$	$\left(\mathbb{K}^\eta\right)^\tau$
α_1	Coefficient array $\alpha_1 = (\alpha_1[0], \ldots, \alpha_1[\tau-1])$	$\left(\mathbb{K}^\eta\right)^\tau$
`x_eval`	Evaluation array $\texttt{x\_eval} = (\texttt{x\_eval}[0], \ldots, \texttt{x\_eval}[\tau-1])$	$(\mathbb{K}^n)^\tau$
`u_eval`	Evaluation array $\texttt{u\_eval} = (\texttt{u\_eval}[0], \ldots, \texttt{u\_eval}[\tau-1])$	$(\mathbb{K}^\eta)^\tau$
`mseed`	Signature master seed	$\{0,1\}^\lambda$
`salt`	Signature salt	$\{0,1\}^\lambda$
`rseed`	Array $\texttt{rseed} = (\texttt{rseed}[0], \ldots, \texttt{rseed}[\tau-1])$	–
`rseed`$[e]$	GGM root seed for execution e	$\{0,1\}^\lambda$
`lseed`	Array $\texttt{lseed} = (\texttt{lseed}[0], \ldots, \texttt{lseed}[\tau-1])$	–
`lseed`$[e]$	Array $\texttt{lseed}[e] = (\texttt{lseed}[e][0], \ldots, \texttt{lseed}[e][N-1])$	–
`lseed`$[e][i]$	Leaf seed of index i for execution e	$\{0,1\}^\lambda$
`ls_com`	Array $\texttt{ls\_com} = (\texttt{ls\_com}[0], \ldots, \texttt{ls\_com}[\tau-1])$	–
`ls_com`$[e]$	Array $\texttt{ls\_com}[e] = (\texttt{ls\_com}[e][0], \ldots, \texttt{ls\_com}[e][N-1])$	–
`ls_com`$[e][i]$	Leaf seed commitment of index i for execution e	$\{0,1\}^{2\lambda}$
`node`	Array $\texttt{node} = (\texttt{node}[0], \ldots, \texttt{node}[\tau-1])$	–
`node`$[e]$	Array $\texttt{node}[e] = (\texttt{node}[e][2], \ldots, \texttt{node}[e][2N+1])$	–
`node`$[e][j]$	Node seed of index j for execution e	$\{0,1\}^\lambda$
`path`	Array $\texttt{path} = (\texttt{path}[0], \ldots, \texttt{path}[\tau-1])$	–
`path`$[e]$	Array $\texttt{path}[e] = (\texttt{path}[e][0], \ldots, \texttt{path}[e][\log_2(N)-1])$	–
`path`$[e][j]$	Sibling-path seed of index j (from leaf to root) for execution e	$\{0,1\}^\lambda$
`exp`$[e][i]$	Expanded leaf seed	$\{0,1\}^{\lvert x\rvert_2+\lvert u\rvert_2-\lambda}$

2.3 Data representation

The elementary data type in MQOM is a byte string. Any other data types, such as bit-strings, vectors of field elements, tuples or arrays, are serialized and represented as byte strings in input and output of the MQOM algorithms. We detail hereafter how these data types are serialized into byte strings.

In the algorithms presented in the following sections, we use the Serialize routine to explicitly apply the serialization process depicted below. On the other hand, the Parse routine peforms the inverse operation with the output format implicit from the context.

Bit-string. A bit-string is an element from $\{0,1\}^\ell$ for some $\ell \in \mathbb{N}$ (most of the time $\ell = \lambda \in \{128, 192, 256\}$ or $\ell = 2\lambda \in \{256, 384, 512\}$). A bit-string is naturally represented as a byte-string of size $\lceil \ell/8 \rceil$. Whenever ℓ is not a multiple of 8, the last ($\ell \bmod 8$) bits of the bit-string are the least significant bits in the last byte.

The different variants of MQOM involve three different fields: $\mathbb{F}_2$, $\mathbb{F}_{256}$ and $\mathbb{F}_{2^{16}}$. Below, we describe the serialization process for vectors of field elements for each of these fields.

Vectors of $\mathbb{F}_2$-elements. An element of $\mathbb{F}_2$ is naturally represented on a single bit. Vectors from $\mathbb{F}_2^\ell$ are only serialized for ℓ a multiple of 8. A vector $v = (v_1, \ldots, v_\ell) \in \mathbb{F}_2^\ell$ is serialized as:

$$\mathsf{Serialize}(v) = \mathsf{B}(v_1, \ldots, v_8) \,\|\, \ldots \,\|\, \mathsf{B}(v_{\ell-7}, \ldots, v_\ell)$$

where B is the byte-grouping function defined as:

$$\mathsf{B}(b_0, \ldots, b_7) = \sum_{i=0}^{7} 2^i \cdot \mathsf{int}(b_i)$$

with int the natural mapping $\mathbb{F}_2 \to \{0,1\} \subseteq \mathbb{N}$.

Vectors of $\mathbb{F}_{16}$-elements. An element of $\mathbb{F}_{16}$ is naturally represented as a half byte, commonly referred to as a *nibble*. Specifically, an element $e \in \mathbb{F}_{16}$ is represented as a tuple $(e_0, \ldots, e_3) \in \mathbb{F}_2^4$ such that $e = \sum_{i=0}^{3} e_i \cdot \rho^i$ for ρ a primitive element of $\mathbb{F}_{16}$ over $\mathbb{F}_2$ (i.e. $\mathbb{F}_{16} = \mathbb{F}_2[\rho]$). The byte representation of a pair $(e_1, e_2) \in \mathbb{F}_{16}^2$ is defined as:

$$\mathsf{byte}(e_1, e_2) = \mathsf{B}(e_{1,0}, e_{1,1}, e_{1,2}, e_{1,3},\ e_{2,0}, e_{2,1}, e_{2,2}, e_{2,3}) \quad \Leftrightarrow \quad e_i = \sum_{j=0}^{3} e_{i,j} \cdot \rho^j \ ,\ \forall i \in \{1,2\} \ .$$

Vectors from $\mathbb{F}_{16}^\ell$ are only serialized for ℓ a multiple of 2. A vector $v = (v_1, \ldots, v_\ell) \in \mathbb{F}_{16}^\ell$ is naturally serialized as:

$$\mathsf{Serialize}(v) = \mathsf{byte}(v_1, v_2) \,\|\, \ldots \,\|\, \mathsf{byte}(v_{\ell-1}, v_\ell) \ .$$

Vectors of $\mathbb{F}_{256}$-elements. An element of $\mathbb{F}_{256}$ is naturally represented as a byte. Specifically, an element $e \in \mathbb{F}_{256}$ is represented as a tuple $(e_0, \ldots, e_7) \in \mathbb{F}_2^8$ such that $e = \sum_{i=0}^{7} e_i \cdot \xi^i$ for ξ a primitive element of $\mathbb{F}_{256}$ over $\mathbb{F}_2$ (i.e. $\mathbb{F}_{256} = \mathbb{F}_2[\xi]$). The byte representation of such an element is defined as:

$$\mathsf{byte}(e) = \mathsf{B}(e_0, \ldots, e_7) \quad \Leftrightarrow \quad e = \sum_{i=0}^{7} e_i \cdot \xi^i \ .$$

A vector $(v_1, \ldots, v_\ell) \in \mathbb{F}_{256}^\ell$ is naturally serialized as:

$$\mathsf{Serialize}(v) = \mathsf{byte}(v_1) \parallel \ldots \parallel \mathsf{byte}(v_\ell) \ .$$

Vectors of $\mathbb{F}_{2^{16}}$-elements. An element $e \in \mathbb{F}_{2^{16}}$ is represented as a pair $(e_0, e_1) \in \mathbb{F}_{256} \times \mathbb{F}_{256}$ such that $e = e_0 + e_1 \cdot \nu$ for ν a primitive element of $\mathbb{F}_{2^{16}}$ over $\mathbb{F}_{256}$ (i.e. $\mathbb{F}_{2^{16}} = \mathbb{F}_{256}[\nu]$). Such an element of $\mathbb{F}_{2^{16}}$ is serialized as $\mathsf{byte}(e_0) \parallel \mathsf{byte}(e_1)$. A vector $(v_1, \ldots, v_\ell) \in \mathbb{F}_{2^{16}}^\ell$ is hence naturally serialized as:

$$\mathsf{Serialize}(v) = \mathsf{byte}(v_{1,0}) \parallel \mathsf{byte}(v_{1,1}) \parallel \ldots \parallel \mathsf{byte}(v_{\ell,0}) \parallel \mathsf{byte}(v_{\ell,1})$$

where $v_i = v_{i,0} + v_{i,1} \cdot \nu$ for all $i \in [1, \ell]$.

The concrete values of ρ, ξ and ν which define the representation of $\mathbb{F}_{16}$, $\mathbb{F}_{256}$ and $\mathbb{F}_{2^{16}}$ are provided in Section 3.

Tuples and arrays. MQOM further manipulates tuples of elements that might be of different natures. Such a tuple is naturally serialized as:

$$\mathsf{Serialize}((e_1, \ldots, e_\ell)) = \mathsf{Serialize}(e_1) \parallel \ldots \parallel \mathsf{Serialize}(e_\ell) \ .$$

In the same way, an array $\texttt{arr} = (\texttt{arr[0]}, \ldots, \texttt{arr}[\ell - 1])$ is serialized as

$$\mathsf{Serialize}(\texttt{arr}) = \mathsf{Serialize}(\texttt{arr[0]}) \parallel \ldots \parallel \mathsf{Serialize}(\texttt{arr}[\ell - 1]) \ .$$

2.4 Main algorithms

2.4.1 Key generation

The key generation of MQOM consists in pseudorandomly generating a (packed) MQ instance, with triangular matrices $\hat{A}_i$. It randomly draws a master seed `seed_key` from which it derives the secret MQ solution x and another seed `mseed_eq` from which the packed MQ equations $\{\hat{A}_i\}, \{\hat{b}_i\}$ are derived. The MQ output $\hat{y}$ is then computed from $\{\hat{A}_i\}, \{\hat{b}_i\}$ and x. Finally, the key pair is defined and returned as $\mathtt{pk} := (\mathtt{mseed\_eq}, \hat{y})$ and $\mathtt{sk} := (\mathtt{pk}, x)$. The key generation is depicted in Algorithm 1. The subroutine ExpandEquations is invoked to expand the MQ equations from the seed `mseed_eq`. Subseeds $\mathtt{seed\_eq}[0], \ldots, \mathtt{seed\_eq}[\hat{m}-1]$ are first derived from `mseed_eq`, then $(\hat{A}_i, \hat{b}_i)$ is expanded from $\mathtt{seed\_eq}[i]$ for every $i \in [1, \hat{m}]$.

Algorithm 1 KeyGen()

Output: a secret key `sk`, a public key `pk`

1: $\mathtt{seed\_key} \leftarrow \{0,1\}^{2\lambda}$
2: $(x, \mathtt{mseed\_eq}) \leftarrow \mathsf{Parse}(\mathsf{XOF}_0(\mathtt{seed\_key}, \mathtt{len} := |x|_2 + 2\lambda))$ ▷ $x \in \mathbb{F}^n, \mathtt{mseed\_eq} \in \{0,1\}^{2\lambda}$
3: $(\{\hat{A}_i\}, \{\hat{b}_i\}) \leftarrow \mathsf{ExpandEquations}(\mathtt{mseed\_eq})$ ▷ $\hat{A}_i \in \mathbb{K}^{n\times n}, \hat{b}_i \in \mathbb{K}^n$
4: **for** $i = 1$ **to** $\hat{m}$ **do**
5: $\quad \hat{y}_i \leftarrow x^\intercal \hat{A}_i x + \hat{b}_i^\intercal x$ ▷ $\hat{y}_i \in \mathbb{K}$
6: $\hat{y} \leftarrow (\hat{y}_1, \ldots, \hat{y}_{\hat{m}})$ ▷ $\hat{y} \in \mathbb{K}^{\hat{m}}$
7: $\mathtt{pk} \leftarrow \mathsf{Serialize}(\mathtt{mseed\_eq}, \hat{y})$
8: $\mathtt{sk} \leftarrow \mathsf{Serialize}(\mathtt{pk}, x)$
9: **return** $(\mathtt{pk}, \mathtt{sk})$

Algorithm 2 ExpandEquations(`mseed_eq`)

Input: a seed key $\mathtt{mseed\_eq} \in \{0,1\}^{2\lambda}$
Output: Packed MQ equations $(\{\hat{A}_i\}, \{\hat{b}_i\})$

1: Let $nf_{\text{eq}} = n + \sum_{j=1}^{n} j$ ▷ Number of field elements for $(\hat{A}_i, \hat{b}_i)$
2: Let $nb_{\text{eq}} = nf_{\text{eq}} \cdot \frac{\log_2 |\mathbb{K}|}{8}$ ▷ Number of PRG bytes for $(\hat{A}_i, \hat{b}_i)$
3: **for** $i = 1$ **to** $\hat{m}$ **do**
4: $\quad \mathtt{seed\_eq}[i-1] \leftarrow \mathsf{XOF}_1((\mathtt{mseed\_eq}, \mathsf{Bits}_{16}(i-1)), \mathtt{len} := \lambda)$
5: $\quad (\mathtt{row}_{i,1}, \ldots, \mathtt{row}_{i,n}, \hat{b}_i) \leftarrow \mathsf{Parse}(\mathsf{PRG}(0^\lambda, 0, \mathtt{seed\_eq}[i-1], nb_{\text{eq}}))$ ▷ $\mathrm{row}_{i,j} \in \mathbb{K}^j, \hat{b}_i \in \mathbb{K}^n$
6: $\quad$ **for** $j = 1$ **to** n **do**
7: $\quad\quad \hat{A}_{i,j} \leftarrow (\mathtt{row}_{i,j} \,\|\, 0_{\mathbb{K}^{n-j}})$ ▷ $\hat{A}_{i,j} \in \mathbb{K}^n$, jth row of $\hat{A}_i$
8: $\quad \hat{A}_i \leftarrow (\hat{A}_{i,1}, \ldots, \hat{A}_{i,n})$ ▷ $\hat{A}_i \in \mathbb{K}^{n\times n}$
9: **return** $(\{\hat{A}_i\}, \{\hat{b}_i\})$

2.4.2 Signing

The MQOM signing process is depicted in Algorithm 3 while the challenge sampling subroutine (implementing the grinding tweak) is depicted in Algorithm 4. The subroutines for the BLC commitment and computation of P_α are depicted in Section 2.5.

Algorithm 3 Sign($\mathtt{sk}, \mathtt{msg}$)

Input: a secret key $\mathtt{sk}$, a message $\mathtt{msg}$
Output: a signature sig

1: $(\mathtt{pk}, x) = \mathsf{Parse}(\mathtt{sk})$
2: $(\mathtt{mseed\_eq}, \hat{y}) = \mathsf{Parse}(\mathtt{pk})$
3: $\mathtt{mseed} \leftarrow \{0,1\}^\lambda$
4: $\mathtt{salt} \leftarrow \{0,1\}^\lambda$
5: $\mathtt{msg\_hash} \leftarrow \mathsf{Hash}_2(\mathtt{msg})$
6: $(\mathtt{com}_1, \mathtt{key}, x_0, u_0, u_1) \leftarrow \mathsf{BLC.Commit}(\mathtt{mseed}, \mathtt{salt}, x)$
7: $(\alpha_0, \alpha_1) \leftarrow \mathsf{ComputePAlpha}(\mathtt{com}_1, x_0, u_0, u_1, x, \mathtt{mseed\_eq})$
8: $\mathtt{com}_2 \leftarrow \mathsf{Hash}_3(\alpha_0, \alpha_1)$
9: $\mathtt{hash} \leftarrow \mathsf{Hash}_4(\mathtt{pk}, \mathtt{com}_1, \mathtt{com}_2, \mathtt{msg\_hash})$
10: $(i^*, \mathtt{nonce}) \leftarrow \mathsf{SampleChallenge}(\mathtt{hash})$
11: $\mathtt{opening} \leftarrow \mathsf{BLC.Open}(\mathtt{key}, i^*)$
12: **return** sig $:= \mathsf{Serialize}(\mathtt{salt}, \mathtt{com}_1, \mathtt{com}_2, \alpha_1, \mathtt{opening}, \mathtt{nonce})$

Algorithm 4 SampleChallenge($\mathtt{hash}$)

Input: Fiat-Shamir hash digest $\mathtt{hash} \in \{0,1\}^{2\lambda}$
Output: challenge indexes $i^* \in [0, N-1]^\tau$, a grinding counter $\mathtt{nonce} \in [0, 2^{32}-1]$

1: $\mathtt{nonce} \leftarrow 0$ ▷ $\mathtt{nonce} \in [0, 2^{32}-1]$
2: $(i^*, \mathtt{val}) \leftarrow \mathsf{Parse}(\mathsf{XOF}_5((\mathtt{hash}, \mathtt{nonce}), \mathtt{len} := \tau \cdot \log_2(N) + w))$ ▷ $i^* \in [0, N-1]^\tau$
3: **while** $\mathtt{val} \neq 0$ **do** ▷ $\mathtt{val} \in [0, 2^w - 1]$
4: $\quad \mathtt{nonce} \leftarrow \mathtt{nonce} + 1$
5: $\quad (i^*, \mathtt{val}) \leftarrow \mathsf{Parse}(\mathsf{XOF}_5((\mathtt{hash}, \mathtt{nonce}), \mathtt{len} := \tau \cdot \log_2(N) + w))$
6: **return** $(i^*, \mathtt{nonce})$

2.4.3 Verification

The MQOM verification process is depicted in Algorithm 5. The subroutines for the BLC evaluation and recomputation of P_α are depicted in Section 2.5.

Algorithm 5 $\mathsf{Verif}(\mathtt{pk}, \mathtt{msg}, \mathsf{sig})$

Input: a public key $\mathtt{pk}$, a message $\mathtt{msg}$, a signature sig
Output: True or False

1: $(\mathtt{mseed\_eq}, \hat{y}) = \mathsf{Parse}(\mathtt{pk})$
2: $(\mathtt{salt}, \mathtt{com}_1, \mathtt{com}_2, \alpha_1, \mathtt{opening}, \mathtt{nonce}) = \mathsf{Parse}(\mathsf{sig})$
3: $\mathtt{msg\_hash} \leftarrow \mathsf{Hash}_2(\mathtt{msg})$
4: $\mathtt{hash} \leftarrow \mathsf{Hash}_4(\mathtt{pk}, \mathtt{com}_1, \mathtt{com}_2, \mathtt{msg\_hash})$
5: $(i^*, \mathtt{val}) \leftarrow \mathsf{Parse}(\mathsf{XOF}_5((\mathtt{hash}, \mathtt{nonce}), \mathtt{len} := \tau \cdot \log_2(N) + w))$
6: **if** $\mathtt{val} \neq 0$ **then return** False
7: $(\mathtt{ret}, \mathtt{x\_eval}, \mathtt{u\_eval}) \leftarrow \mathsf{BLC.Eval}(\mathtt{salt}, \mathtt{com}_1, \mathtt{opening}, i^*)$
8: **if** $\mathtt{ret} \neq$ True **then return** False
9: $\alpha_0 \leftarrow \mathsf{RecomputePAlpha}(\mathtt{com}_1, \alpha_1, \mathtt{x\_eval}, \mathtt{u\_eval}, \mathtt{mseed\_eq}, \hat{y})$
10: $\mathtt{com}_2' \leftarrow \mathsf{Hash}_3(\alpha_0, \alpha_1)$
11: **if** $\mathtt{com}_2' \neq \mathtt{com}_2$ **then return** False
12: **return** True

2.5 Subroutines

2.5.1 Arithmetic routines

The main arithmetic routine of the signing process is ComputePAlpha which computes the polynomials $P_\alpha = P_u + \hat{F}(P_x)$, for all the executions $e \in [0, \tau - 1]$, where $\hat{F} = (\hat{f}_1, \ldots, \hat{f}_{\hat{m}})$ with $\hat{f}_i(x) = x^\intercal \hat{A}_i x + \hat{b}_i^\intercal x - \hat{y}_i$. The resulting polynomials are returned as arrays of coefficient vectors: $\alpha_0 = (\alpha_0[0], \ldots, \alpha_0[\tau - 1])$ and $\alpha_1 = (\alpha_1[0], \ldots, \alpha_1[\tau - 1])$ such that for a given execution e, the polynomial P_α is defined as: $P_\alpha = \alpha_0[e] + \alpha_1[e] \cdot X$. This function relies on the subroutine ComputePz which computes $P_z = \hat{F}(P_x)$ from P_x. The batching (a.k.a. 5-round) variant is enabled/disabled with the Boolean `batching`.

Algorithm 6 ComputePAlpha$(\texttt{com}, x_0, u_0, u_1, x, \texttt{mseed_eq})$

Input: a BLC commitment `com`, coefficient arrays x_0, u_0, u_1, MQ secret solution x, seed `mseed_eq` of the packed MQ equations $\{\hat{A}_i\}, \{\hat{b}_i\}$
Output: coefficient arrays α_0, α_1

1: **if** batching **then** ▷ batching = True ⇒ 5-round variant
2: $\quad \Gamma \in \mathbb{K}^{\eta \times \hat{m}} \leftarrow$ Parse(XOF$_8$(`com`, `len` $:= \eta \cdot \hat{m} \cdot \log_2 |\mathbb{K}|$))
3: **else** ▷ batching = False ⇒ 3-round variant
4: $\quad \Gamma \leftarrow I_\eta$ ▷ Identity matrix $I_\eta \in \mathbb{K}^{\eta \times \eta}$ with $\eta = \hat{m}$
5: $(\{\hat{A}_i\}, \{\hat{b}_i\}) \leftarrow$ ExpandEquations(`mseed_eq`)
6: **for** $e = 0$ **to** $\tau - 1$ **do**
7: $\quad (z_0, z_1) \leftarrow$ ComputePz$(x_0[e], x, \{\hat{A}_i\}, \{\hat{b}_i\})$ ▷ $P_z = z_0 + z_1 \cdot X \in \left(\mathbb{K}[X]^{\leqslant 1}\right)^{\hat{m}}$
8: $\quad \alpha_0[e] \leftarrow u_0[e] + \Gamma \cdot z_0$
9: $\quad \alpha_1[e] \leftarrow u_1[e] + \Gamma \cdot z_1$ ▷ $P_\alpha = \alpha_0[e] + \alpha_1[e] \cdot X \in \left(\mathbb{K}[X]^{\leqslant 1}\right)^{\eta}$
10: **return** (α_0, α_1)

Algorithm 7 ComputePz$(x_0[e], x, \{\hat{A}_i\}, \{\hat{b}_i\})$

Input: coefficient vectors $x_0[e] \in \mathbb{K}^n$, $x \in \mathbb{F}^n$, MQ equations $\{\hat{A}_i\}, \{\hat{b}_i\}$
Output: coefficients $z_0, z_1 \in \mathbb{K}^{\hat{m}}$

▷ Compute $P_{z,i} = {P_x}^\intercal \hat{A}_i P_x + \hat{b}_i^\intercal P_x \cdot X - y_i \cdot X^2$ for all $i \in [1, \hat{m}]$
▷ Skip computation of degree-2 coefficients (known to be 0)

1: **for** $i = 1$ **to** $\hat{m}$ **do**
▷ Compute $P_t = t_0 + t_1 \cdot X := \hat{A}_i \cdot P_x + \hat{b}_i \cdot X$
2: $\quad t_0 \leftarrow \hat{A}_i \cdot x_0[e]$ ▷ $t_0 \in \mathbb{K}^n$
3: $\quad t_1 \leftarrow \hat{A}_i \cdot x + \hat{b}_i$ ▷ $t_1 \in \mathbb{F}^n$
▷ Compute $P_{z,i} = z_{0,i} + z_{1,i} \cdot X = P_t^\intercal P_x - y_i \cdot X^2$
4: $\quad z_{0,i} \leftarrow t_0^\intercal \cdot x_0[e]$ ▷ $z_{0,i} \in \mathbb{K}$
5: $\quad z_{1,i} \leftarrow t_0^\intercal \cdot x + t_1^\intercal \cdot x_0[e]$ ▷ $z_{1,i} \in \mathbb{K}$
6: $z_0 \leftarrow (z_{0,1}, \ldots, z_{0,\hat{m}})$ ▷ $z_0 \in \mathbb{K}^{\hat{m}}$
7: $z_1 \leftarrow (z_{1,1}, \ldots, z_{1,\hat{m}})$ ▷ $z_1 \in \mathbb{K}^{\hat{m}}$
8: **return** (z_0, z_1)

Remark 3. *In* ComputePz*, the variable* $t_1 = \hat{A}_i \cdot x + \hat{b}_i$ *takes a different value for each* i*, but for*

a fixed i, its value remains constant across all executions $e = 0, \ldots, \tau - 1$. This implies that the $\hat{m}$ values of t_1 (corresponding to $i \in [1, \hat{m}]$) can be computed once and reused for all executions. Furthermore, since these values depend only on the secret key `sk`*, they could be precomputed and used for every call to the signing algorithm. We do not consider this optimization here to keep the description simple but it could be easily integrated to enhance the efficiency of a concrete implementation.*

The main arithmetic routine of the verification process is RecomputePAlpha which recomputes the polynomials P_α from the coefficients α_1 and the opened evaluations $P_x(r)$, $P_u(r)$ for all the executions $e \in [0, \tau - 1]$. Namely, this function recomputes and returns the missing coefficients α_1. It makes use of the subroutine ComputePzEval which computes the evaluation $P_z(r)$ from $P_x(r)$, $P_u(r)$ for a single execution.

Algorithm 8 RecomputePAlpha($\mathtt{com}, \alpha_1, i^*, \mathsf{x\_eval}, \mathsf{u\_eval}, \mathtt{mseed\_eq}, \{\hat{y}_i\}$)

Input: a BLC commitment `com`, coefficient array α_1, index array i^*, evaluation arrays `x_eval`, `u_eval`, seed `mseed_eq` of the packed MQ equations $\{\hat{A}_i\}, \{\hat{b}_i\}$, and $\{\hat{y}_i\}$
Output: coefficient array α_0

if batching **then** ▷ batching = True ⇒ 5-round variant
  $\Gamma \in \mathbb{K}^{\eta \times \hat{m}} \leftarrow$ Parse(XOF$_8$(`com`, `len` $:= \eta \cdot \hat{m} \cdot \log_2 |\mathbb{K}|$))
else ▷ batching = False ⇒ 3-round variant
  $\Gamma \leftarrow I_\eta$ ▷ Identity matrix $I_\eta \in \mathbb{K}^{\eta \times \eta}$ with $\eta = \hat{m}$
$(\{\hat{A}_i\}, \{\hat{b}_i\}) \leftarrow$ ExpandEquations(`mseed_eq`)
for $e = 0$ **to** $\tau - 1$ **do**
  Let $r = \omega_{i^*[e]}$ ▷ $r \in \mathbb{K}$
  Let $v_x = \mathsf{x\_eval}[e]$ ▷ $v_x = P_x(r) \in \mathbb{K}^n$
  Let $v_u = \mathsf{u\_eval}[e]$ ▷ $v_u = P_u(r) \in \mathbb{K}^\eta$
  $v_z \leftarrow$ ComputePzEval$(r, v_x, \{\hat{A}_i\}, \{\hat{b}_i\}, \{\hat{y}_i\})$ ▷ $v_z = P_z(r) \in \mathbb{K}^{\hat{m}}$
  $v_\alpha \leftarrow v_u + \Gamma \cdot v_z$ ▷ $v_\alpha = P_\alpha(r) = \alpha_0[e] + \alpha_1[e] \cdot r$
  $\alpha_0[e] \leftarrow v_\alpha - \alpha_1[e] \cdot r$ ▷ $\alpha_0[e] \in \mathbb{K}^\eta$
return α_0

Algorithm 9 ComputePzEval$(r, v_x, \{\hat{A}_i\}, \{\hat{b}_i\}, \{\hat{y}_i\})$

Input: evaluation point $r \in \Omega$, evaluation $v_x \in \mathbb{K}$, MQ equations $\{\hat{A}_i\}, \{\hat{b}_i\}, \{\hat{y}_i\}$
Output: evaluation $v_z \in \mathbb{K}^{\hat{m}}$

▷ Compute $v_{z,i} = v_x^\intercal \hat{A}_i v_x + \hat{b}_i^\intercal v_x \cdot r - y_i \cdot r^2$ for all $i \in [1, \hat{m}]$
for $i = 1$ **to** $\hat{m}$ **do**
  ▷ Compute $v_t = P_t(r) = \hat{A}_i \cdot P_x(r) + \hat{b}_i \cdot r$
  $v_t \leftarrow \hat{A}_i \cdot v_x + \hat{b}_i \cdot r$ ▷ $v_t \in \mathbb{K}^n$
  ▷ Compute $v_{z,i} = P_{z,i}(r) = v_t^\intercal v_x - \hat{y}_i \cdot r^2$
  $v_{z,i} \leftarrow v_t^\intercal \cdot v_x - \hat{y}_i \cdot r^2$ ▷ $v_{z,i} \in \mathbb{K}$
$v_z \leftarrow (v_{z,1}, \ldots, v_{z,\hat{m}})$ ▷ $v_z \in \mathbb{K}^{\hat{m}}$
return v_z

2.5.2 Batch line commitment routines

The BLC.Commit routine computes the BLC commitment $\texttt{com}_1$, the associated opening key (the nodes of the GGM trees), and the associated polynomials P_x, P_u returned as array of coefficients.

Algorithm 10 BLC.Commit($\texttt{mseed}, \texttt{salt}, x$)

Input: a master seed $\texttt{mseed} \in \{0,1\}^\lambda$, a salt $\texttt{salt} \in \{0,1\}^\lambda$, an MQ secret solution x
Output: a BLC commitment $\texttt{com}_1$, an opening key $\texttt{key}$, coefficient arrays x_0, u_0, u_1

$(\texttt{rseed}[0], \ldots, \texttt{rseed}[\tau-1]) \leftarrow \mathsf{Parse}(\mathsf{PRG}(0^\lambda, 0, \texttt{mseed}, \tau \cdot \lambda))$
$\delta \leftarrow \mathsf{FirstBits}_\lambda(x)$ ▷ $\delta \in \{0,1\}^\lambda$
for $e = 0$ **to** $\tau - 1$ **do**
  $(\texttt{node}[e], \texttt{lseed}[e]) \leftarrow \mathsf{GGMTree.Expand}(\texttt{salt}, \texttt{rseed}[e], e, \delta)$
  $\texttt{tweaked\_salt} \leftarrow \mathsf{TweakSalt}(\texttt{salt}, 0, e, 0)$
  for $i = 0$ **to** $N - 1$ **do**
    $\texttt{ls\_com}[e][i] \leftarrow \mathsf{SeedCommit}(\texttt{tweaked\_salt}, \texttt{lseed}[e][i])$
    $\texttt{exp}[e][i] \leftarrow \mathsf{PRG}(\texttt{salt}, e, \texttt{lseed}[e][i], |x|_8 + |u|_8 - \lambda/8)$
    $(\bar{x}_i, \bar{u}_i) \leftarrow \mathsf{Parse}(\texttt{lseed}[e][i] \,\|\, \texttt{exp}[e][i])$ ▷ $\bar{x}_i \in \mathbb{F}^n$, $\bar{u}_i \in \mathbb{K}^\eta$
  $\texttt{hash\_ls\_com}[e] \leftarrow \mathsf{Hash}_6(\texttt{ls\_com}[e])$
  ▷ Compute $P_u = u_0[e] + u_1[e] \cdot X = \sum_{i=0}^{N-1} \bar{u}_i \cdot (X - \omega_i)$
  $u_0[e] \leftarrow -\sum_{i=0}^{N-1} \omega_i \cdot \bar{u}_i$ ▷ $u_0[e] \in \mathbb{K}^\eta$
  $u_1[e] \leftarrow \sum_{i=0}^{N-1} \bar{u}_i$ ▷ $u_1[e] \in \mathbb{K}^\eta$
  ▷ Compute $P_x = x_0[e] + x \cdot X = \Delta_x[e] \cdot X + \sum_{i=0}^{N-1} \bar{x}_i \cdot (X - \omega_i)$
  $x_0[e] \leftarrow -\sum_{i=0}^{N-1} \omega_i \cdot \bar{x}_i$ ▷ $x_0[e] \in \mathbb{K}^n$
  $\Delta_x[e] \leftarrow x - \sum_{i=0}^{N-1} \bar{x}_i$ ▷ $\Delta_x[e] \in \mathbb{F}^n$
  $\Delta_x^{(1)}[e] \leftarrow \mathsf{NextBits}_\lambda(\Delta_x[e])$ ▷ $\Delta_x^{(1)}[e] \in \{0,1\}^{|x|_2 - \lambda}$
$\texttt{com}_1 \leftarrow \mathsf{Hash}_7(\texttt{hash\_ls\_com}, \Delta_x^{(1)})$
$\texttt{key} \leftarrow \mathsf{Serialize}(\texttt{node}, \texttt{ls\_com}, \Delta_x^{(1)})$
return $(\texttt{com}_1, \texttt{key}, x_0, u_0, u_1)$

From an opening key and an index array i^*, the BLC.Open routine returns the opening tuple made of the sibling paths ($\texttt{path}$), the hidden leaf commitments ($\texttt{out\_ls\_com}$) and the correction values ($\Delta_x^{(1)}$).

Algorithm 11 BLC.Open($\texttt{key}, i^*$)

Input: a commitment key $\texttt{key}$, an index array i^*
Output: a BLC opening $\texttt{opening} \in \{0,1\}^{\lambda \cdot \tau \cdot (\log_2(N)+2)}$

$(\texttt{node}, \texttt{ls\_com}, \Delta_x^{(1)}) \leftarrow \mathsf{Parse}(\texttt{key})$
for $e = 0$ **to** $\tau - 1$ **do**
  $\texttt{path}[e] \leftarrow \mathsf{GGMTree.Open}(\texttt{node}[e], i^*[e])$
  $\texttt{out\_ls\_com}[e] \leftarrow \texttt{ls\_com}[e][i^*[e]]$
$\texttt{opening} \leftarrow \mathsf{Serialize}(\texttt{path}, \texttt{out\_ls\_com}, \Delta_x^{(1)})$
return $\texttt{opening}$

The BLC.Eval routine is called by the verification algorithm to check the opening validity and derive the underlying evaluations $P_x(r)$, $P_u(r)$ for all the executions $e \in [0, \tau - 1]$.

Algorithm 12 BLC.Eval($\texttt{salt}, \texttt{com}, \texttt{opening}, i^*$)

Input: a salt `salt`, a BLC commitment `com`, a BLC opening `opening`, index array i^*
Output: `ret` $\in \{\mathsf{True}, \mathsf{False}\}$, evaluation arrays `x_eval`, `u_eval`

1: $(\texttt{path}, \texttt{out\_ls\_com}, \Delta_x^{(1)}) \leftarrow \mathsf{Parse}(\texttt{opening})$
2: **for** $e = 0$ **to** $\tau - 1$ **do**
▷ Compute partial GGM trees
3: $\texttt{lseed}[e] \leftarrow \mathsf{GGMTree.PartiallyExpand}(\texttt{salt}, \texttt{path}[e], i^*[e])$
▷ Compute evaluations
4: $\texttt{tweaked\_salt} \leftarrow \mathsf{TweakSalt}(\texttt{salt}, 0, e, 0)$
5: **for** $i = 0$ **to** $N - 1$ **do**
6: **if** $i \neq i^*[e]$ **then**
7: $\texttt{ls\_com}[e][i] \leftarrow \mathsf{SeedCommit}(\texttt{tweaked\_salt}, \texttt{lseed}[e][i])$
8: $\texttt{exp}[e][i] \leftarrow \mathsf{PRG}(\texttt{salt}, e, \texttt{lseed}[e][i], |x|_8 + |u|_8 - \lambda/8)$
9: $(\bar{x}_i, \bar{u}_i) \leftarrow \mathsf{Parse}(\texttt{lseed}[e][i] \parallel \texttt{exp}[e][i])$ ▷ $\bar{x}_i \in \mathbb{F}^n$, $\bar{u}_i \in \mathbb{K}^\eta$
10: $\texttt{ls\_com}[e][i^*[e]] \leftarrow \texttt{out\_ls\_com}[e]$
11: $\texttt{hash\_ls\_com}[e] \leftarrow \mathsf{Hash}_6(\texttt{ls\_com}[e])$
12: Let $r = \omega_{i^*[e]}$ ▷ $r \in \mathbb{K}$
13: $\Delta_x[e] \leftarrow \mathsf{PadLeft}_\lambda(\Delta_x^{(1)}[e])$ ▷ $\Delta_x[e] \in \mathbb{F}^n$
14: $v_x \leftarrow \Delta_x[e] \cdot r + \sum_{i \neq i^*[e]} \bar{x}_i \cdot (r - \omega_i)$ ▷ $v_x = P_x(r) \in \mathbb{K}^n$
15: $v_u \leftarrow \sum_{i \neq i^*[e]} \bar{u}_i \cdot (r - \omega_i)$ ▷ $v_u = P_u(r) \in \mathbb{K}^\eta$
16: $\texttt{x\_eval}[e] \leftarrow v_x$
17: $\texttt{u\_eval}[e] \leftarrow v_u$
▷ *Verify opening*
18: $\texttt{com}' \leftarrow \mathsf{Hash}_7(\texttt{hash\_ls\_com}, \Delta_x^{(1)})$
19: **if** $\texttt{com}' \neq \texttt{com}$ **then**
20: **return** $(\mathsf{False}, \perp, \perp)$
21: **return** $(\mathsf{True}, \texttt{x\_eval}, \texttt{u\_eval})$

Optimized folding based on Gray Code. While $u_0[e]$, $u_1[e]$, $x_0[e]$ and $\Delta_x[e]$ in BLC.Commit can be computed using generic field operations over $\mathbb{K}$, the *order* of the public evaluation points $\omega_0, \ldots, \omega_{N-1}$ from Ω has been chosen to enable optimization. Using the classical lexicographic order yields:

- computational complexity $O(N \cdot \log_2 N)$ with a memory complexity $O(1)$ when using direct computation;
- computational complexity $O(N + \log_2 N)$ with a memory complexity $O(N)$ when using the divide-and-conquer method [Roy22].

Although memory scaling in $O(N)$ is acceptable on laptops or servers, it can be problematic for embedded devices with limited memory. In MQOM, as in the round-2 SDitH candidate [AFG+24], we use a Gray-code ordering that achieves the best of both worlds with a

computational complexity of $O(N + \log_2 N)$ and memory usage of $O(1)$. By definition, the Gray-code ordering ensures that two consecutive values differ in exactly one bit (see Section 3.1 for the precise definition of $\omega_1, \ldots, \omega_{N-1}$).

For a fixed loop iteration $e \in \{0, \ldots, \tau - 1\}$, we define:

$$\mathtt{raw}_i := \mathtt{lseed}[e][i] \parallel \mathtt{exp}[e][i]$$

so that $(\bar{x}_i, \bar{u}_i) = \mathsf{Parse}(\mathtt{raw}_i)$. The procedure BLC.ComputeFolding, depicted below, takes as input the raw random tapes $\mathtt{raw}_0, \ldots, \mathtt{raw}_{N-1}$ and efficiently computes the following values:

$$\bar{x}_{\mathrm{ACC}} := \sum_i \bar{x}_i, \quad \bar{u}_{\mathrm{ACC}} := \sum_i \bar{u}_i, \quad \bar{x}_{\mathrm{FOLD}} := \sum_i \omega_i \cdot \bar{x}_i, \quad \bar{u}_{\mathrm{FOLD}} := \sum_i \omega_i \cdot \bar{u}_i \ .$$

This procedure is invoked in BLC.Commit (within the signing algorithm) and in BLC.Eval (within the verification algorithm). In the latter case, the random tape of the hidden leaf $i^*[e]$ is unknown, so the procedure is called with $\mathtt{raw}_{i^*[e]} := 0$. This amounts to computing the above values as sums over all indices $i \neq i^*[e]$.

In BLC.Commit (signing algorithm), these values directly yield the line coefficients and correction value as:

$$u_0[e] = -\bar{u}_{\mathrm{FOLD}} \ , \quad u_1[e] = \bar{u}_{\mathrm{ACC}} \ , \quad x_0[e] = -\bar{x}_{\mathrm{FOLD}} \ , \quad \Delta_x[e] = x - \bar{x}_{\mathrm{ACC}} \ .$$

In BLC.Eval (verification algorithm), these values are used to compute the evaluations v_x and v_u as:

$$\begin{aligned} v_x &= (\Delta_x[e] + \bar{x}_{\mathrm{ACC}}) \cdot r - \bar{x}_{\mathrm{FOLD}} \\ v_u &= \bar{u}_{\mathrm{ACC}} \cdot r - \bar{u}_{\mathrm{FOLD}} \ . \end{aligned}$$

From these equations, one can observe that the contributions of $\bar{x}_{i^*[e]}$ (resp. $\bar{u}_{i^*[e]}$) cancel out in the computation of v_x (resp. v_u). Hence, setting $\mathtt{raw}_{i^*[e]} = 0$ does not affect the final result.

The procedure BLC.ComputeFolding works as follows. After i iterations of the main loop:

- the variable $\mathtt{acc}$ stores the partial sum $\sum_{k=0}^{i} \mathtt{raw}_k$;
- the variables $\{\mathtt{fd}_0, \ldots, \mathtt{fd}_{\log_2 N - 1}\}$ represent the value

$$\sum_{j=0}^{i} (w_j - w_{j+1}) \cdot \sum_{k=0}^{i} \mathtt{raw}_k = \sum_{k=0}^{i} w_k \cdot \mathtt{raw}_k - w_{i+1} \cdot \sum_{k=0}^{i} \mathtt{raw}_k \ ,$$

  where $\mathtt{fd}_j$ corresponds to the j^{th} coordinate of this value in the canonical $\mathbb{F}_2$-basis of $\mathbb{K}$.

At the end of the loop, we have $\mathtt{acc} = \sum_{k=0}^{N-1} \mathtt{raw}_k$ and $\{\mathtt{fd}_j\}_j$ encoding $\sum_{k=0}^{N-1} w_k \cdot \mathtt{raw}_k$, with the convention $w_N := 0$. The final desired values are then obtained through parsing and scaling.

Note that, in memory-constrained contexts, BLC.ComputeFolding should be implemented incrementally to avoid large memory overhead.

Algorithm 13 BLC.ComputeFolding($\mathtt{raw}_0, \ldots, \mathtt{raw}_{N-1}$)

Input: $\mathtt{raw}_0, \ldots, \mathtt{raw}_{N-1} \in \{0,1\}^{n+\mu\cdot\eta}$

$\mathtt{acc} = 0$ ▷ $\mathtt{acc} \in \{0,1\}^{n+\mu\cdot\eta}$
$\mathtt{fd}_0 = 0, \ldots, \mathtt{fd}_{\log_2 N-1} = 0$ ▷ $\mathtt{fd}_j \in \{0,1\}^{n+\mu\cdot\eta}$
for $i = 0$ **to** $N-1$ **do**
  $\mathtt{acc} \leftarrow \mathtt{acc} \oplus \mathtt{raw}_i$
  $\mathtt{fd}_{p_i} \leftarrow \mathtt{fd}_{p_i} \oplus \mathtt{acc}$ ▷ p_i is the position of the only bit set in $\omega_i \oplus \omega_{i+1}$
$(\bar{x}_{\text{ACC}}, \bar{u}_{\text{ACC}}) \leftarrow$ Parse($\mathtt{acc}$) ▷ $\bar{x}_{\text{ACC}} \in \mathbb{F}^n$, $\bar{u}_{\text{ACC}} \in \mathbb{K}^\eta$
$\bar{x}_{\text{FOLD}} = 0, \bar{u}_{\text{FOLD}} = 0$ ▷ $\bar{x}_{\text{FOLD}} \in \mathbb{K}^n$, $\bar{u}_{\text{FOLD}} \in \mathbb{K}^\eta$
for $j = 0$ **to** $\log_2 N - 1$ **do**
  $(\mathtt{fd}_j^x, \mathtt{fd}_j^u) \leftarrow$ Parse($\mathtt{fd}_j$) ▷ $\mathtt{fd}_j^x \in \mathbb{F}^n$, $\mathtt{fd}_j^u \in \mathbb{K}^\eta$
  $\bar{x}_{\text{FOLD}} \leftarrow \bar{x}_{\text{FOLD}} + e_j \cdot \mathtt{fd}_j^x$ ▷ $\{e_0, \ldots, e_{\log_2 |\mathbb{K}|-1}\}$ is the canonical $\mathbb{F}_2$-basis of $\mathbb{K}$
  $\bar{u}_{\text{FOLD}} \leftarrow \bar{u}_{\text{FOLD}} + e_j \cdot \mathtt{fd}_j^u$
return $(\bar{x}_{\text{ACC}}, \bar{u}_{\text{ACC}}), (\bar{x}_{\text{FOLD}}, \bar{u}_{\text{FOLD}})$

2.5.3 GGM tree routines

The GGM tree subroutines are depicted hereafter. The routine GGMTree.Expand (which is called in BLC.Commit) expands a GGM tree from a root seed with a salt, an execution index e (for domain separation) and the offset δ (for correlated tree optimization). It returns the derived list of nodes and leaf seeds. The routine GGMTree.Open (which is called in BLC.Open) extracts the sibling path from the nodes for a given hidden index. The routine GGMTree.PartiallyExpand (which is called in BLC.Eval) expands a GGM tree partially from a sibling path with a salt, an execution index e (for domain separation) and the underlying hidden index. The reader is referred to Figure 3 for an illustration of the tree structure and numbering of nodes.

Algorithm 14 GGMTree.Expand($\mathtt{salt}, \mathtt{rseed}[e], e, \delta$)

Input: a salt $\mathtt{salt} \in \{0,1\}^\lambda$, a root seed $\mathtt{rseed}[e] \in \{0,1\}^\lambda$, an execution index $e \in [0, \tau-1]$, an offset $\delta \in \{0,1\}^\lambda$
Output: a tree node array $\mathtt{node}[e]$, a leaf seed array $\mathtt{lseed}[e]$

$\mathtt{node}[e][2] \leftarrow \mathtt{rseed}[e]$
$\mathtt{node}[e][3] \leftarrow \mathtt{rseed}[e] \oplus \delta$
for $j = 1$ **to** $\log_2(N) - 1$ **do**
    $\mathtt{tweaked\_salt} = \mathsf{TweakSalt}(\mathtt{salt}, 2, e, j)$
    for $k = 2^j$ **to** $2^{j+1} - 1$ **do**
        $\mathtt{node}[e][2k] \leftarrow \mathsf{SeedDerive}(\mathtt{tweaked\_salt}, \mathtt{node}[e][k])$
        $\mathtt{node}[e][2k+1] \leftarrow \mathtt{node}[e][2k] \oplus \mathtt{node}[e][k]$
for $i = 0$ **to** $N - 1$ **do**
    $\mathtt{lseed}[e][i] \leftarrow \mathtt{node}[e][N+i]$
return $(\mathtt{node}[e], \mathtt{lseed}[e])$

Algorithm 15 GGMTree.Open($\mathtt{node}[e], i^*[e]$)

Input: a tree node array $\mathtt{node}[e]$, a hidden leaf index $i^*[e]$
Output: sibling path $\mathtt{path}[e]$

$i \leftarrow N + i^*[e]$ ▷ i: index of the hidden node at layer j
for $j = 0$ **to** $\log_2(N) - 1$ **do**
    $\mathtt{path}[e][j] \leftarrow \mathtt{node}[e][i \oplus 1]$
    $i \leftarrow \lfloor i/2 \rfloor$
return path

Algorithm 16 GGMTree.PartiallyExpand($\mathtt{salt}, \mathtt{path}[e], e, i^*[e]$)

Input: a salt $\mathtt{salt} \in \{0,1\}^\lambda$, a sibling path $\mathtt{path}[e]$, an execution index $e \in [0, \tau-1]$, a hidden leaf index $i^*[e] \in [0, N-1]$
Output: a partial leaf seed array $\mathtt{lseed}[e]$

▷ Initialize nodes to $\perp$
$(\mathsf{nodes}[e][1], \ldots, \mathsf{nodes}[e][2N-1]) = (\perp, \ldots, \perp)$
▷ Assign nodes with sibling path
$i \leftarrow N + i^*[e]$ ▷ i: index of the hidden node at layer j
for $j = 0$ **to** $\log_2(N) - 1$ **do**
  $\mathtt{node}[e][i \oplus 1] \leftarrow \mathtt{path}[e][j]$
  $i \leftarrow \lfloor i/2 \rfloor$
▷ Derive nodes from sibling path
for $j = 1$ **to** $\log_2(N) - 1$ **do**
  $\mathtt{tweaked\_salt} = \mathsf{TweakSalt}(\mathtt{salt}, 2, e, j)$
  for $k = 2^j$ **to** $2^{j+1} - 1$ **do**
    if $\mathtt{node}[e][k] \neq \perp$ **then**
      $\mathtt{node}[e][2k] \leftarrow \mathsf{SeedDerive}(\mathtt{tweaked\_salt}, \mathtt{node}[e][k])$
      $\mathtt{node}[e][2k+1] \leftarrow \mathtt{node}[e][2k] \oplus \mathtt{node}[e][k]$
for $i = 0$ **to** $N - 1$ **do**
  $\mathtt{lseed}[e][i] \leftarrow \mathtt{node}[e][N+i]$
return $\mathtt{lseed}[e]$

2.5.4 Seed processing routines

The following algorithms depict the subroutines of the GGM trees that are used to derive, commit and expand the seeds.

Algorithm 17 TweakSalt($\texttt{salt}, \texttt{sel}, e, j$)

Input: a salt $\texttt{salt} \in \{0,1\}^\lambda$, a selector $\texttt{sel} \in \{0,1,2\}$, an execution index $e \in [0, \tau - 1]$, a tree layer $j \in [0, \log_2(N) - 1]$
Output: a tweaked salt $\texttt{tweaked\_salt} \in \{0,1\}^\lambda$

▷ $\texttt{sel} = 0$ for seed commitment (first part)
▷ $\texttt{sel} = 1$ for seed commitment (second part)
▷ $\texttt{sel} = 2$ for seed derivation
▷ $\texttt{sel} = 3$ for PRG

1: $\texttt{tweak} \leftarrow \texttt{sel} + 4 \cdot e + 256 \cdot j$
2: $\texttt{tweaked\_salt} \leftarrow \texttt{salt} \oplus \mathsf{Bits}_\lambda(\texttt{tweak})$
3: **return** $\texttt{tweaked\_salt}$

Algorithm 18 SeedDerive($\texttt{tweaked\_salt}, \mathsf{seed}$)

Input: a tweaked salt $\texttt{tweaked\_salt} \in \{0,1\}^\lambda$, a seed $\mathsf{seed} \in \{0,1\}^\lambda$
Output: a derived seed $\texttt{new\_seed} \in \{0,1\}^\lambda$

1: $\texttt{new\_seed} \leftarrow \mathsf{Enc}(\texttt{key} := \texttt{tweaked\_salt}, \texttt{ptx} := \mathsf{seed}) \oplus \psi(\mathsf{seed})$
2: **return** $\texttt{new\_seed}$

Algorithm 19 SeedCommit($\texttt{tweaked\_salt}, \mathsf{seed}$)

Input: a tweaked salt $\texttt{tweaked\_salt} \in \{0,1\}^\lambda$, a seed $\mathsf{seed} \in \{0,1\}^\lambda$
Output: a seed commitment $\texttt{seed\_com} \in \{0,1\}^{2\lambda}$

1: $\texttt{com}_1 \leftarrow \mathsf{Enc}(\texttt{key} := \texttt{tweaked\_salt}, \texttt{ptx} := \mathsf{seed}) \oplus \psi(\mathsf{seed})$
2: $\texttt{com}_2 \leftarrow \mathsf{Enc}(\texttt{key} := \texttt{tweaked\_salt} \oplus \mathsf{Bits}_\lambda(1), \texttt{ptx} := \mathsf{seed}) \oplus \psi(\mathsf{seed})$
3: $\texttt{seed\_com} \leftarrow \texttt{com}_1 \,\|\, \texttt{com}_2$
4: **return** $\texttt{seed\_com}$

Algorithm 20 PRG($\texttt{salt}, e, \mathsf{seed}, n_{\text{bytes}}$)

Input: a seed $\mathsf{seed} \in \{0,1\}^\lambda$, an execution index $e \in [0, \tau - 1]$, a salt $\texttt{salt} \in \{0,1\}^\lambda$, a number of bytes $n_{\text{bytes}} \in \mathbb{N}$
Output: a pseudorandom byte string $\texttt{out} \in \{0,1\}^{8 \cdot n_{\text{bytes}}}$

1: $n_{\text{blocks}} \leftarrow \lceil 8 \cdot n_{\text{bytes}} / \lambda \rceil$
2: **for** $i = 0$ **to** $n_{\text{blocks}} - 1$ **do**
3: $\quad \texttt{tweaked\_salt} \leftarrow \mathsf{TweakSalt}(\texttt{salt}, 3, e, i)$
4: $\quad \texttt{block}[i] \leftarrow \mathsf{Enc}(\texttt{key} := \texttt{tweaked\_salt}, \texttt{ptx} := \mathsf{seed}) \oplus \psi(\mathsf{seed})$
5: $(\texttt{byte}[0] \,\|\, \ldots \,\|\, \texttt{byte}[n_{\text{blocks}} \cdot \lambda/8 - 1]) \leftarrow \mathsf{Parse}(\texttt{block}[0] \,\|\, \ldots \,\|\, \texttt{block}[n_{\text{blocks}} - 1])$
6: $\texttt{out} \leftarrow \texttt{byte}[0] \,\|\, \ldots \,\|\, \texttt{byte}[n_{\text{bytes}} - 1]$
7: **return** $\texttt{out}$

2.5.5 Symmetric primitives

MQOM relies on two symmetric primitives:

1. A block cipher:
$$\mathsf{Enc} : (\mathtt{key}, \mathtt{ptx}) \in \{0,1\}^\lambda \times \{0,1\}^\lambda \mapsto \mathtt{ctx} \in \{0,1\}^\lambda \ ;$$
2. An extendable-output hash function:
$$\mathsf{XOF} : (\mathtt{in}, \mathtt{len}) \in \{0,1\}^* \times \mathbb{N} \mapsto \mathtt{out} \in \{0,1\}^{\mathtt{len}} \ .$$

We further define a (fixed-length output) hash function as:
$$\mathsf{Hash} : \mathtt{in} \in \{0,1\}^* \mapsto \mathsf{XOF}(\mathtt{in}, 2\lambda) \in \{0,1\}^{2\lambda} \ .$$

Table 4 summarizes the instantiations of these two primitives for the NIST Categories I, III and V (corresponding to a parameter $\lambda = 128$, $\lambda = 192$, $\lambda = 256$ respectively). For Category III ($\lambda = 192$), Enc is defined as a truncated version of Rijndael-256-256 (hence the asterisk), which is formally defined as:
$$\mathsf{Enc}^{(192)} : (\mathtt{key}, \mathtt{ptx}) \in \{0,1\}^{192} \times \{0,1\}^{192} \mapsto \mathsf{Truncate}_{192}(\mathsf{Enc}^{(256)}(\mathtt{key} \parallel 0^{64}, \mathtt{ptx} \parallel 0^{64})) \ .$$

Table 4: Symmetric primitives in MQOM.

	Category I ($\lambda = 128$)	Category III ($\lambda = 192$)	Category V ($\lambda = 256$)
Enc	AES-128	Rijndael-256-256*	Rijndael-256-256
XOF	SHAKE-128	SHAKE-256	SHAKE-256

Domain separation. We enforce domain separation for different calls to the XOF (or Hash) functions by prepending a byte representing the call index i to the data being hashed. Specifically, for $i \in \mathbb{N}$, with $i < 256$, we define:
$$\mathsf{XOF}_i(\mathtt{in}, \mathtt{len}) := \mathsf{XOF}(\mathsf{Bits}_8(i) \parallel \mathtt{in}, \mathtt{len}) \ ,$$
and consequently $\mathsf{Hash}_i(\mathtt{in}) = \mathsf{Hash}(\mathsf{Bits}_8(i) \parallel \mathtt{in})$.

Here is a summary of the invocations to the (extendable output) hash function with associated purposes:

- XOF_0: expansion of `seed_key` (secret key),
- XOF_1: expansion of `seed_eq` (MQ equations),
- Hash_2: message hash,
- Hash_3: hash commitment of α_0, α_1,
- Hash_4: Fiat-Shamir hash,
- XOF_5: challenge sampling (with grinding),
- Hash_6: hash commitment of leaf seed commitments,
- Hash_7: BLC commitment,
- XOF_8: generation of Γ (batching variant).

2.5.6 Bit manipulation

We define hereafter the bit manipulation functions. The function

$$\mathsf{Bits}_\ell : [0, 2^\ell - 1] \to \{0,1\}^\ell$$

takes as input an integer and returns its binary representation. The functions $\mathsf{FirstBits}_\lambda$ and $\mathsf{NextBits}_\lambda$ provide the λ first bits and $|x|_2 - \lambda$ next bits of a $|x|_2$-bit string. Formally, we define:

$$\mathsf{FirstBits}_\lambda : \Delta_x \in \mathbb{F}^n \mapsto \Delta_x^{(0)} \in \{0,1\}^\lambda$$

and

$$\mathsf{NextBits}_\lambda : \Delta_x \in \mathbb{F}^n \mapsto \Delta_x^{(1)} \in \{0,1\}^{|x|_2 - \lambda} \ .$$

where

$$(\Delta_x^{(0)} \parallel \Delta_x^{(1)}) = \mathsf{Serialize}(\Delta_x) \in \{0,1\}^{|x|_2} \ .$$

We further define the function $\mathsf{PadLeft}_\lambda$ as

$$\mathsf{PadLeft}_\lambda : \Delta_x^{(1)} \in \{0,1\}^{|x|_2 - \lambda} \mapsto \mathsf{Parse}(0^\lambda \parallel \Delta_x^{(1)}) \in \mathbb{F}^n \ .$$

Finally, the function

$$\mathsf{Truncate}_\ell : \{0,1\}^* \to \{0,1\}^\ell$$

returns the ℓ first bits of its input bit string.

3 MQOM instances

In this section, we propose several parameter sets for the MQOM signature scheme. As explained hereafter, those parameters have been selected to meet the categories I, III and V defined by the NIST while targeting good performances (in terms of signature size and running times).

3.1 Parameter selection

MQ parameters. Instead of considering prime field as in the first version, MQOM v2 relies on the binary fields. The main motivation for this update is to avoid rejection sampling and arithmetic-Boolean conversions. As first option, we chose $|\mathbb{F}| = 2$ for the base field, which leads to the shortest signatures. As second option, we chose $|\mathbb{F}| = 256$ which enjoys easier and faster implementation (with a field element matching a byte). As third option, we chose $|\mathbb{F}| = 16$ which enjoys fast implementation and short signature. For those three fields, we took the number of equations m to be equal the number of unknowns n and selected the minimal $m = n$ to achieve a target security level (for categories I, III and V) according to the state of the art of MQ cryptanalysis (see Section 4.2).

Looking ahead, the extension field $\mathbb{K}$ is either defined as $\mathbb{F}_{256}$ or $\mathbb{F}_{2^{16}}$ (see explanations below). In order to ensure that m is always divisible by $\mu = [\mathbb{K} : \mathbb{F}]$ (which simplifies the packing strategy – see Section 2.1.2), we restricted the selection to values of m that are multiples of 16 for $\mathbb{F} = \mathbb{F}_2$, multiples of 4 for $\mathbb{F} = \mathbb{F}_{16}$, and multiples of 2 for $\mathbb{F} = \mathbb{F}_{256}$.

Proof system parameters. The MQOM proof system relies on the parameters summarized in Table 2: the size N of the evaluation set $\Omega := \{\omega_0, \ldots, \omega_{N-1}\}$, the extension field $\mathbb{K}$ of degree μ, the number η of internal repetitions, the number τ of external repetitions and the grinding proof-of-work parameter w.

We chose N as a power of two to manipulate complete binary GGM trees. A larger N leads to a shorter signature at the cost of slower signing and verification algorithms. We chose to consider two values for N, namely $N = 2048$ (short variant) and $N = 256$ (fast variant), to obtain two different trade-offs between communication and computation. Then, the extension field $\mathbb{K}$ is chosen such that $|\mathbb{K}| \geq N$. To ease the implementation, we chose to consider a common $\mathbb{K}$ for the three base fields ($\mathbb{F}_2$, $\mathbb{F}_{16}$ and $\mathbb{F}_{256}$) and thus define $\mathbb{K}$ as their common extension such that $|\mathbb{K}| \leq N$. This way, we get $\mathbb{K} = \mathbb{F}_{2^{16}}$ for $N = 2048$ and $\mathbb{K} = \mathbb{F}_{256}$ for $N = 256$.

Given the pair $(N, \mathbb{K})$, we selected the remaining parameters to achieve λ bits of soundness, with λ equal to 128, 192 and 256 for Categories I, III and V, respectively. On the one hand, we took $\eta = \lambda / \log_2 |\mathbb{K}|$ for the batching (5-round) variant to ensure a soundness error of $1/|\mathbb{K}|^\eta = 2^{-\lambda}$ (while η is fixed to as m/μ by design for the 3-round variant). On the other hand, we chose the parameters τ and w such that $\left(\frac{2}{N}\right)^\tau \cdot 2^{-w} \leq 2^{-\lambda}$ (see Section 2.1.4).

Field extension. As explained previously, the MQOM signature scheme relies on four different fields for $\mathbb{F}$ and $\mathbb{K}$: $\mathbb{F}_2$, $\mathbb{F}_{2^4}$, $\mathbb{F}_{2^8}$ and $\mathbb{F}_{2^{16}}$. Table 5 summarizes the field extensions that we use in our instances.

Table 5: Definition of field extensions.

Field ($\mathbb{F}$ or $\mathbb{K}$)	Field extension
$\mathbb{F}_{2^4}$	$\mathbb{F}_2[\rho]/\langle \rho^4 + \rho + 1\rangle$
$\mathbb{F}_{2^8}$	$\mathbb{F}_2[\xi]/\langle \xi^8 + \xi^4 + \xi^3 + \xi + 1\rangle$
$\mathbb{F}_{2^{16}}$	$\mathbb{F}_{2^8}[\nu]/\langle \nu^2 + \nu + \xi^5\rangle$

At some stage, the MQOM signature requires lifting field elements into an extension field. This lifting is straightforward by construction in the cases $\mathbb{F}_2 \hookrightarrow \mathbb{F}_{2^4}$ and $\mathbb{F}_{2^8} \hookrightarrow \mathbb{F}_{2^{16}}$, thanks to the tower field structure. However, the situation is different when lifting elements from $\mathbb{F}_{2^4}$ to $\mathbb{F}_{2^8}$. In this case, we rely on a field morphism between $\mathbb{F}_{2^4}$ and $\mathbb{F}_{2^8}$, defined such that the element $\rho \in \mathbb{F}_{2^4}$ is mapped to $\xi^7 + \xi^6 + \xi^5 \in \mathbb{F}_{2^8}$.

Evaluation domain. The PIOP evaluation query is sampled from the evaluation domain $\Omega := \{\omega_0, \ldots, \omega_{N-1}\}$ of size N. In our instances, as explained in Section 2.5.2, we use the Gray-code ordering, namely

$$\omega_i := \nu \cdot \sum_{j=0}^{7} (\theta_{8+j}^{(i)} \cdot \xi^j) + \sum_{j=0}^{7} (\theta_j^{(i)} \cdot \xi^j) \in \mathbb{K}$$

for all $i \in \{0, N-1\}$, where $\theta_j^{(i)} = \mathsf{i}_j \oplus \mathsf{i}_{j+1}$ for all j, with $(\mathsf{i}_0, \ldots, \mathsf{i}_{16})$ the binary decomposition of $i := \sum_{j=0}^{16} \mathsf{i}_j \cdot 2^j$.

3.2 Key and signature sizes

Public key. The public key consists of a 2λ-bit seed `mseed_eq` for the generation of the MQ equations, and a serialized vector $\hat{y} \in \mathbb{K}^{\hat{m}}$ corresponding to the outputs of the equations. For $|\mathbb{K}| = 256$, we store one field element on one byte. For $|\mathbb{K}| = 256^2$, we store one field element on two bytes. Thus, the size of the public key is given by:

$$|\mathtt{pk}| = \begin{cases} \frac{2\lambda}{8} + \frac{m}{8} \text{ bytes} & \text{for } \mathbb{F} := \mathbb{F}_2 \\ \frac{2\lambda}{8} + \frac{m}{2} \text{ bytes} & \text{for } \mathbb{F} := \mathbb{F}_{16} \\ \frac{2\lambda}{8} + m \text{ bytes} & \text{for } \mathbb{F} := \mathbb{F}_{256}. \end{cases}$$

Secret key. The secret key consists of the same elements as the public key, plus a serialized vector $x \in \mathbb{F}^n$ corresponding to the secret solution of the MQ system. For $|\mathbb{F}| = 2$, we store 8 field elements on one byte. For $|\mathbb{F}| = 16$, we store two field elements on one byte. For $|\mathbb{F}| = 256$, we store one field element on one byte. Thus, the size of the secret key is given by:

$$|\mathtt{sk}| = \begin{cases} \frac{2\lambda}{8} + \frac{m}{8} + \frac{n}{8} \text{ bytes} & \text{for } \mathbb{F}_2 \\ \frac{2\lambda}{8} + \frac{m}{2} + \frac{n}{2} \text{ bytes} & \text{for } \mathbb{F}_{16} \\ \frac{2\lambda}{8} + m + n \text{ bytes} & \text{for } \mathbb{F}_{256} \end{cases}$$

As all the existing public-key schemes, let us remark that we have an alternative definition of the key generation in which the secret key would be `seed_key`, the seed from which $(\mathtt{mseed\_eq}, y, x)$ are derived. In that case, the size of the secret key would be of $2\lambda/8$ bytes, but the signer would need to recompute `mseed_eq`, y and x at each signature, increasing the running time of the signing process. Moreover, the signing algorithm would be more sensitive to

side-channel attacks. We hence recommend to use this alternative only if the size of the secret key is critical.

Signature size. The size (in bits) of a signature is given by:

$$
\begin{aligned}
|\sigma| &= 32 && \text{size of } \texttt{nonce} \\
&+ \lambda && \text{size of the } \texttt{salt} \\
&+ 4\lambda && \text{size of } \texttt{com}_1 \text{ and } \texttt{com}_2 \\
&+ \tau \cdot (\eta \cdot \mu \cdot \log_2 |\mathbb{F}|) && \text{size of } \alpha_1 \\
&+ \tau \cdot (n \cdot \log_2 |\mathbb{F}| - \lambda) && \text{size of } \Delta_{x'}\texttt{[}e\texttt{]} \text{ in } \texttt{opening} \\
&+ \tau \cdot \lambda \cdot \log_2 N && \text{size of } \texttt{path} \text{ in } \texttt{opening} \\
&+ \tau \cdot 2\lambda && \text{size of } \texttt{out\_ls\_com} \text{ in } \texttt{opening}
\end{aligned}
$$

Given our natural serialization of field elements, $\log_2 |\mathbb{F}|$ is 1 for $\mathbb{F}_2$, 4 for $\mathbb{F}_{16}$, and 8 for $\mathbb{F}_{256}$. We obtain the following sizes in bytes:

$$|\sigma| = 4 + \frac{\tau \cdot \big(n + \eta \cdot \mu\big)}{8} + \frac{5\lambda + \tau \cdot \lambda \cdot (\log_2 N + 1)}{8} \quad \text{for } \mathbb{F}_2,$$

$$|\sigma| = 4 + \frac{\tau \cdot \big(n + \eta \cdot \mu\big)}{2} + \frac{5\lambda + \tau \cdot \lambda \cdot (\log_2 N + 1)}{8} \quad \text{for } \mathbb{F}_{16},$$

and

$$|\sigma| = 4 + \tau \cdot \big(n + \eta \cdot \mu\big) + \frac{5\lambda + \tau \cdot \lambda \cdot (\log_2 N + 1)}{8} \quad \text{for } \mathbb{F}_{256}.$$

The only difference in terms of signature size between the 3-round and the 5-round variants, comes from the parameter η, which is a bit larger in the 3-round variant (i.e., $\eta = \hat{m} = m/\mu$).

3.3 Proposed instances

All the signature parameters are summarized in Table 6, while the corresponding key and signature sizes are given in Table 7.

Table 6: The MQ and proof system parameters of MQOM for NIST Security Categories I, III, and V.

Parameter Sets	**NIST Security**	**MQ Parameters**		**Proof System Parameters**				
		$\lvert\mathbb{F}\rvert$	$m = n$	τ	N	μ	η	w
MQOM2-L1-gf2-short-3r/5r	Cat. I	2	160	12	2048	16	10/8	8
MQOM2-L1-gf2-fast-3r/5r	Cat. I	2	160	17	256	8	20/16	9
MQOM2-L1-gf16-short-3r/5r	Cat. I	16	56	12	2048	4	14/8	8
MQOM2-L1-gf16-fast-3r/5r	Cat. I	16	56	17	256	2	28/16	9
MQOM2-L1-gf256-short-3r/5r	Cat. I	256	48	12	2048	2	24/8	8
MQOM2-L1-gf256-fast-3r/5r	Cat. I	256	48	17	256	1	48/16	9
MQOM2-L3-gf2-short-3r/5r	Cat. III	2	240	18	2048	16	15/12	12
MQOM2-L3-gf2-fast-3r/5r	Cat. III	2	240	27	256	8	30/24	3
MQOM2-L3-gf16-short-3r/5r	Cat. III	16	84	18	2048	4	21/12	12
MQOM2-L3-gf16-fast-3r/5r	Cat. III	16	84	27	256	2	42/24	3
MQOM2-L3-gf256-short-3r/5r	Cat. III	256	72	18	2048	2	36/12	12
MQOM2-L3-gf256-fast-3r/5r	Cat. III	256	72	27	256	1	72/24	3
MQOM2-L5-gf2-short-3r/5r	Cat. V	2	320	25	2048	16	20/16	6
MQOM2-L5-gf2-fast-3r/5r	Cat. V	2	320	36	256	8	40/32	4
MQOM2-L5-gf16-short-3r/5r	Cat. V	16	116	25	2048	4	29/16	6
MQOM2-L5-gf16-fast-3r/5r	Cat. V	16	116	36	256	2	58/32	4
MQOM2-L5-gf256-short-3r/5r	Cat. V	256	96	25	2048	2	48/16	6
MQOM2-L5-gf256-fast-3r/5r	Cat. V	256	96	36	256	1	96/32	4

Table 7: The key and signature sizes in bytes.

Parameter Set	**Sizes (in bytes)**		
	pk	sk	Sig.
MQOM2-L1-gf2-short-3r/5r	52	72	2 868 / 2 820
MQOM2-L1-gf16-short-3r/5r	60	88	3 060 / 2 916
MQOM2-L1-gf256-short-3r/5r	80	128	3 540 / 3 156
MQOM2-L1-gf2-fast-3r/5r	52	72	3 212 / 3 144
MQOM2-L1-gf16-fast-3r/5r	60	88	3 484 / 3 280
MQOM2-L1-gf256-fast-3r/5r	80	128	4 164 / 3 620
MQOM2-L3-gf2-short-3r/5r	78	108	6 388 / 6 280
MQOM2-L3-gf16-short-3r/5r	90	132	6 820 / 6 496
MQOM2-L3-gf256-short-3r/5r	120	192	7 900 / 7 036
MQOM2-L3-gf2-fast-3r/5r	78	108	7 576 / 7 414
MQOM2-L3-gf16-fast-3r/5r	90	132	8 224 / 7 738
MQOM2-L3-gf256-fast-3r/5r	120	192	9 844 / 8 548
MQOM2-L5-gf2-short-3r/5r	104	144	11 764 / 11 564
MQOM2-L5-gf16-short-3r/5r	122	180	12 664 / 12 014
MQOM2-L5-gf256-short-3r/5r	160	256	14 564 / 12 964
MQOM2-L5-gf2-fast-3r/5r	104	144	13 412 / 13 124
MQOM2-L5-gf16-fast-3r/5r	122	180	14 708 / 13 772
MQOM2-L5-gf256-fast-3r/5r	160	256	17 444 / 15 140

3.4 Benchmarks

3.4.1 Benchmarks on `x86` platforms

Benchmarking platforms and protocol: The following `x86` platforms profiles have been used for benchmarking:

- an AVX2 optimized implementation, whose results are given in Table 8;
- an AVX2+GFNI optimized implementation, whose results are given in Table 9;
- an AVX-512+GFNI optimized implementation, whose results are given in Table 10.

The benchmarks were more specifically conducted on:

- an Intel Core Ultra 7 265U, a laptop grade CPU which has AVX2+GFNI support;
- an AMD Ryzen Threadripper PRO 7995WX, a workstation grade CPU which has AVX-512+GFNI support.

The GFNI instruction set brings native $\mathbb{F}_{256}$ multiplication acceleration in the Rijndael field. Regarding AVX-512, the MQOM implementation leverages dedicated optimizations that specifically make use of the `avx512f`, `avx512vl`, `avx512bw`, `avx512vpopcntdq` and `avx512vbmi` extensions. The cycles measurements make use of performance counters of the machine for accurate values. The timing measurements have been made with the turbo boost mode (*i.e.* automatic frequency scaling of the CPU) deactivated. All the results have been gathered using the `gcc` toolchain in version `15.2.0` with the `-O3` compilation option.

About GFNI and AVX-512 support across `x86` platforms: As we can see on Table 9, GFNI brings an interesting performance boost for MQOM (up to 50% on some instances). AVX-512 also allows saving cycles on compatible platforms. This raises the question of how widespread these `x86` extensions are across modern Intel and AMD processors. Although the specific support of GFNI is usually not detailed on Intel's and AMD's product briefs, we have used an open benchmarking platform [Ope] that gathers a large CPU database (more than 1700 CPUs listed from the 10 last years) with the result of the Linux command "`cat /proc/cpuinfo`" allowing to check for specific extensions.

From this database, we can see that GFNI has been introduced by Intel around Q4 2020 with the Ice Lake microarchitecture: the oldest referenced CPU supporting it is the Intel Core i5-1038NG7. Since Q1 2022, most of Intel CPUs seem to support AVX2 with GFNI, from Core i3 laptop to Xeon server grade ones (even the low-end Intel Celeron N5095 embeds it). AVX-512 support (with its various sub-extensions) is more erratic, as some low-end processors such as Core i3-1115G4 from Q4 2020 seem to support them, but more recent high-end CPUs such as the Meteor Lake Intel Core Ultra 7 165U or the Arrow Lake Intel Core Ultra 7 265U (that we use for our benchmarks) do not support them anymore. This seems to be related to the fact that AVX-512 was not fuse-disabled on early consumer grade Alder Lake CPUs, leading to a bypass activating them in the BIOS [Wik]. In fact, Intel officially reserves AVX-512 support exclusively for its Xeon server-grade processors.

Regarding AMD, the situation appears more straightforward with GFNI and AVX-512 usually coming together. They have been introduced only on server grade CPUs in the Zen 4 microarchitecture in 2023 (this is the case for our AMD Ryzen Threadripper PRO 7995WX benchmarking CPU). With the introduction of Zen 5 in Q2 2024, all the AMD CPUs from

laptop grade to server grade support both GFNI and AVX-512. The only exceptions may be certain custom SoCs that AMD manufactures for specific customers, where these units are disabled to reduce silicon area or power consumption; however, this applies only to a marginal set of devices.

All in all, homogeneous GFNI support across `x86` has become a reality in 2025, which MQOM can take advantage of. AVX-512 has also been somewhat democratized with the advent of AMD Zen 5, although Intel continues to reserve it for its server-grade processors.

Table 8: Benchmark of **AVX2-optimized implementation** of the MQOM on an AVX2 machine. Timings were run on an Intel Core Ultra 7 265U (with compilation for the AVX2 restricted instructions set using the `'-maes -mavx2'` compilation flags).

Instance	KeyGen		Sign		Verify	
	ms	cycles	ms	cycles	ms	cycles
MQOM2-L1-gf2-fast-r3	0.96	1.22M	3.36	6.75M	3.24	6.33M
MQOM2-L1-gf2-fast-r5	0.76	1.21M	3.48	6.79M	3.28	6.27M
MQOM2-L1-gf2-short-r3	0.48	1.11M	5.92	11.94M	5.68	11.70M
MQOM2-L1-gf2-short-r5	0.60	1.15M	5.56	11.86M	5.68	11.62M
MQOM2-L1-gf16-fast-r3	0.08	0.28M	1.32	2.80M	1.28	2.35M
MQOM2-L1-gf16-fast-r5	0.12	0.28M	1.32	2.77M	1.16	2.29M
MQOM2-L1-gf16-short-r3	0.08	0.35M	3.24	6.56M	3.16	6.31M
MQOM2-L1-gf16-short-r5	0.24	0.34M	3.00	6.33M	2.96	6.03M
MQOM2-L1-gf256-fast-r3	0.12	0.30M	1.64	3.45M	1.52	3.01M
MQOM2-L1-gf256-fast-r5	0.28	0.28M	1.60	3.36M	1.36	2.89M
MQOM2-L1-gf256-short-r3	0.32	0.33M	3.68	7.51M	3.36	7.26M
MQOM2-L1-gf256-short-r5	0.40	0.33M	3.20	6.89M	3.12	6.60M
MQOM2-L3-gf2-fast-r3	2.40	5.03M	14.36	30.01M	14.04	29.41M
MQOM2-L3-gf2-fast-r5	2.36	4.98M	14.68	30.41M	14.16	29.69M
MQOM2-L3-gf2-short-r3	2.84	5.29M	29.16	61.33M	27.72	58.27M
MQOM2-L3-gf2-short-r5	2.44	5.24M	29.00	60.71M	27.72	57.81M
MQOM2-L3-gf16-fast-r3	0.68	1.33M	5.48	11.77M	5.56	11.36M
MQOM2-L3-gf16-fast-r5	0.64	1.31M	5.24	11.35M	5.32	10.61M
MQOM2-L3-gf16-short-r3	0.72	1.30M	17.16	35.84M	15.12	31.80M
MQOM2-L3-gf16-short-r5	0.48	1.32M	15.84	33.02M	14.36	29.48M
MQOM2-L3-gf256-fast-r3	0.72	1.51M	7.68	16.01M	7.08	14.82M
MQOM2-L3-gf256-fast-r5	0.72	1.49M	6.68	14.04M	6.48	13.42M
MQOM2-L3-gf256-short-r3	0.64	1.27M	20.28	42.55M	18.60	38.49M
MQOM2-L3-gf256-short-r5	0.76	1.27M	17.68	37.36M	15.92	33.20M
MQOM2-L5-gf2-fast-r3	4.00	8.26M	35.64	74.39M	35.76	75.00M
MQOM2-L5-gf2-fast-r5	3.92	8.15M	35.56	74.53M	34.96	72.95M
MQOM2-L5-gf2-short-r3	3.80	8.05M	64.72	135.01M	63.84	133.62M
MQOM2-L5-gf2-short-r5	3.80	8.01M	65.44	136.32M	63.88	133.36M
MQOM2-L5-gf16-fast-r3	1.28	2.53M	11.84	24.95M	11.84	24.62M
MQOM2-L5-gf16-fast-r5	0.56	2.52M	11.76	24.50M	11.80	23.31M
MQOM2-L5-gf16-short-r3	1.12	2.54M	27.36	56.83M	26.16	54.62M
MQOM2-L5-gf16-short-r5	1.32	2.52M	25.64	53.79M	25.12	52.26M
MQOM2-L5-gf256-fast-r3	1.24	2.56M	14.04	29.21M	14.04	29.51M
MQOM2-L5-gf256-fast-r5	1.16	2.57M	13.56	28.14M	13.28	27.52M
MQOM2-L5-gf256-short-r3	1.08	2.29M	30.68	64.02M	30.44	63.70M
MQOM2-L5-gf256-short-r5	2.16	2.29M	27.28	58.08M	26.60	56.81M

Table 9: Benchmark of **optimized implementation** of the MQOM on an AVX2+GFNI machine. Timings were run on an Intel Core Ultra 7 265U with the `'-march=native -mtune=native'` compilation flags.

Instance	KeyGen		Sign		Verify	
	ms	cycles	ms	cycles	ms	cycles
MQOM2-L1-gf2-fast-r3	0.68	0.99M	1.96	3.44M	1.68	3.14M
MQOM2-L1-gf2-fast-r5	0.80	0.98M	1.80	3.55M	1.76	3.04M
MQOM2-L1-gf2-short-r3	0.56	0.96M	3.04	6.24M	2.92	6.02M
MQOM2-L1-gf2-short-r5	0.52	0.94M	2.88	6.32M	3.04	6.01M
MQOM2-L1-gf16-fast-r3	0.08	0.24M	1.16	1.95M	0.64	1.56M
MQOM2-L1-gf16-fast-r5	0.20	0.24M	1.12	1.91M	0.52	1.54M
MQOM2-L1-gf16-short-r3	0.16	0.25M	2.52	5.29M	2.48	5.04M
MQOM2-L1-gf16-short-r5	0.12	0.25M	2.40	4.98M	2.36	4.77M
MQOM2-L1-gf256-fast-r3	0.16	0.21M	1.04	2.29M	0.96	1.91M
MQOM2-L1-gf256-fast-r5	0.12	0.22M	1.36	2.27M	0.64	1.81M
MQOM2-L1-gf256-short-r3	0.12	0.21M	2.76	5.91M	2.92	5.74M
MQOM2-L1-gf256-short-r5	0.08	0.21M	2.40	5.29M	2.72	5.14M
MQOM2-L3-gf2-fast-r3	1.92	4.25M	6.96	14.51M	6.64	13.59M
MQOM2-L3-gf2-fast-r5	2.20	4.33M	7.32	15.21M	6.32	13.50M
MQOM2-L3-gf2-short-r3	1.96	4.83M	16.44	34.07M	14.80	30.36M
MQOM2-L3-gf2-short-r5	1.92	4.77M	16.20	33.60M	14.64	30.01M
MQOM2-L3-gf16-fast-r3	0.44	0.95M	3.76	7.69M	3.48	7.31M
MQOM2-L3-gf16-fast-r5	0.48	0.91M	3.52	7.29M	3.20	6.78M
MQOM2-L3-gf16-short-r3	0.48	1.03M	14.08	29.39M	12.56	26.20M
MQOM2-L3-gf16-short-r5	0.64	1.01M	12.96	27.13M	11.20	23.58M
MQOM2-L3-gf256-fast-r3	0.44	0.96M	4.72	9.86M	4.60	9.52M
MQOM2-L3-gf256-fast-r5	0.56	0.96M	4.04	8.41M	4.00	8.35M
MQOM2-L3-gf256-short-r3	0.44	0.99M	16.56	34.60M	15.36	31.41M
MQOM2-L3-gf256-short-r5	0.40	0.99M	13.88	29.32M	12.80	26.32M
MQOM2-L5-gf2-fast-r3	3.24	6.88M	13.32	27.92M	14.00	28.92M
MQOM2-L5-gf2-fast-r5	3.28	6.77M	12.84	26.95M	12.52	26.03M
MQOM2-L5-gf2-short-r3	3.56	7.39M	24.12	50.33M	23.32	48.78M
MQOM2-L5-gf2-short-r5	3.52	7.49M	24.48	50.93M	23.08	48.23M
MQOM2-L5-gf16-fast-r3	0.84	1.66M	6.40	13.18M	6.00	12.52M
MQOM2-L5-gf16-fast-r5	0.84	1.66M	6.00	12.60M	5.88	12.21M
MQOM2-L5-gf16-short-r3	0.92	1.88M	18.36	37.79M	17.52	36.85M
MQOM2-L5-gf16-short-r5	0.96	1.89M	16.64	34.86M	16.24	33.89M
MQOM2-L5-gf256-fast-r3	0.60	1.57M	7.76	16.11M	7.60	15.60M
MQOM2-L5-gf256-fast-r5	0.68	1.57M	7.32	15.14M	6.96	14.48M
MQOM2-L5-gf256-short-r3	0.84	1.57M	20.20	42.36M	20.24	42.27M
MQOM2-L5-gf256-short-r5	0.72	1.56M	17.40	36.27M	17.36	36.28M

Table 10: Benchmark of **optimized implementation** of the MQOM on an AVX-512+GFNI machine. Timings were run on an AMD Ryzen Threadripper PRO 7995WX with the `'-march=native -mtune=native'` compilation flags.

Instance	KeyGen		Sign		Verify	
	ms	cycles	ms	cycles	ms	cycles
MQOM2-L1-gf2-fast-r3	0.84	0.86M	1.52	2.50M	1.20	2.11M
MQOM2-L1-gf2-fast-r5	0.72	0.93M	1.40	2.35M	1.40	2.11M
MQOM2-L1-gf2-short-r3	0.32	0.86M	2.04	5.09M	2.08	4.93M
MQOM2-L1-gf2-short-r5	0.36	0.87M	2.08	5.11M	2.00	4.95M
MQOM2-L1-gf16-fast-r3	0.00	0.24M	0.64	1.59M	0.64	1.24M
MQOM2-L1-gf16-fast-r5	0.16	0.25M	0.64	1.53M	0.48	1.18M
MQOM2-L1-gf16-short-r3	0.12	0.23M	1.84	4.35M	1.80	4.25M
MQOM2-L1-gf16-short-r5	0.08	0.21M	1.88	4.11M	1.56	3.96M
MQOM2-L1-gf256-fast-r3	0.00	0.24M	0.76	1.77M	0.76	1.52M
MQOM2-L1-gf256-fast-r5	0.16	0.23M	0.64	1.62M	0.60	1.40M
MQOM2-L1-gf256-short-r3	0.16	0.20M	2.08	5.04M	2.12	4.99M
MQOM2-L1-gf256-short-r5	0.16	0.19M	1.76	4.42M	1.88	4.30M
MQOM2-L3-gf2-fast-r3	1.08	2.94M	3.52	8.39M	3.24	8.04M
MQOM2-L3-gf2-fast-r5	1.16	2.86M	3.44	8.55M	3.32	8.05M
MQOM2-L3-gf2-short-r3	1.56	3.65M	9.36	23.69M	8.56	20.63M
MQOM2-L3-gf2-short-r5	1.44	3.45M	9.80	24.26M	8.64	21.12M
MQOM2-L3-gf16-fast-r3	0.32	0.74M	2.16	5.20M	1.88	4.77M
MQOM2-L3-gf16-fast-r5	0.32	0.73M	2.04	4.96M	1.76	4.48M
MQOM2-L3-gf16-short-r3	0.44	0.71M	8.36	20.58M	7.16	18.02M
MQOM2-L3-gf16-short-r5	0.56	0.74M	7.44	19.23M	6.64	16.10M
MQOM2-L3-gf256-fast-r3	0.04	0.66M	2.44	6.16M	2.68	5.85M
MQOM2-L3-gf256-fast-r5	0.28	0.66M	2.20	5.49M	2.16	5.20M
MQOM2-L3-gf256-short-r3	0.20	0.67M	9.60	23.99M	8.92	21.35M
MQOM2-L3-gf256-short-r5	0.28	0.66M	8.48	20.99M	7.24	17.80M
MQOM2-L5-gf2-fast-r3	1.80	4.54M	6.08	14.80M	5.68	13.96M
MQOM2-L5-gf2-fast-r5	1.96	4.64M	5.96	14.73M	5.84	14.35M
MQOM2-L5-gf2-short-r3	1.84	4.86M	13.52	32.45M	12.60	31.46M
MQOM2-L5-gf2-short-r5	2.00	4.94M	13.16	32.33M	12.76	31.31M
MQOM2-L5-gf16-fast-r3	0.48	1.29M	3.36	8.13M	3.08	7.64M
MQOM2-L5-gf16-fast-r5	0.56	1.26M	3.00	7.48M	2.80	6.93M
MQOM2-L5-gf16-short-r3	0.48	1.25M	10.76	26.64M	10.60	25.97M
MQOM2-L5-gf16-short-r5	0.16	1.27M	9.36	22.69M	9.16	22.05M
MQOM2-L5-gf256-fast-r3	0.40	1.06M	3.68	8.95M	3.64	8.96M
MQOM2-L5-gf256-fast-r5	0.48	1.10M	3.40	8.24M	3.28	8.21M
MQOM2-L5-gf256-short-r3	0.44	1.17M	11.36	27.85M	11.28	27.84M
MQOM2-L5-gf256-short-r5	0.36	1.06M	9.92	23.82M	9.52	23.86M

3.4.2 Benchmarks on embedded platforms

The MQOM implementation has been adapted[1] to fit embedded platforms with low-memory profiles, using dedicated memory optimizations for the PRG, PIOP and BLC primitives. We present hereafter some benchmarks on Cortex-M4 MCUs. We use a Nucleo-L4R5ZI board featuring a STM32 MCU with embedded 2MB of flash and 640KB of SRAM. All the results have been obtained with the `arm-none-eabi-gcc` toolchain in version `14.2.1` using the compilation flags `-O3` and `-march=armv7e-m -mtune=cortex-m4 -mfloat-abi=hard -mfpu=fpv4-sp-d16`.

Our benchmarking setup closely follows that of the PQM4 framework [KPR+]: we configure the MCU at 16MHz with a zero wait-state flash to remove effects of the prefetchers and have proper cycles measurements. Beyond cycle counts, we also measure SRAM usage through:

- stack usage: measured via stack spraying, and corresponding to the most consuming usage of a calling sequence;
- global variables usage: measured at link time using the compiling toolchain, by dedicating a specific ELF section of the firmware to these variables;
- dynamic allocation usage: measured by tracking `malloc` and `free` calls through dedicated wrappers.

The memory consumption reported in the following benchmarks corresponds to the sum of these three components. This figure typically represents an overestimation, since the program does not necessarily use all global variables or allocated variables along its most stack-consuming call path. Note that this memory consumption does not include signature or key-pair sizes, as our goal is solely to assess the internal memory usage of the primitives.

We provide three variants of our MQOM implementation (using only stack and global variables, no dynamic allocation), tailored to different usage contexts:

- An implementation with table-based AES/Rijndael and with $\mathbb{F}_{256}$ multiplication based on small log/exp lookup tables. For the L1 security level, optimized ARM Cortex-M assembly is used for AES, taken from [SS16]. The results are provided on Table 11.
- An implementation with table-based AES/Rijndael and with $\mathbb{F}_{256}$ multiplication based on a large lookup table of 2^{16} bytes. Compared to log/exp tables, the performance in cycles are slightly better at the expense of a much larger memory usage. The results are provided on Table 12.
- An implementation avoiding any table lookup on sensitive data. AES/Rijndael uses the ARM Cortex-M assembly "fixsliced" implementation from [AP21].[2] For the $\mathbb{F}_{256}$ multiplication, the SWAR technique (SIMD Within a Register) is used to vectorize 4-ways operations within 32-bit registers. The results are provided on Table 13 (only the L1 security level is provided for this variant). As we can see, this variant runs slower but uses less memory.

The rationale of providing the third variant is to have an implementation whose constant time property is ensured whatever the underlying Cortex-M4 platform is. Using lookup tables in SRAM is constant time when there is no prefetching or caching technology between the

[1] https://github.com/mqom/mqom-embedded/

[2] For the key schedule, which does not manipulate secrets in MQOM, we kept table-based implementation from [SS16] instead of the "fixsliced" implementation.

ARM core and the peripherals (SRAM in this case). In the STM32 Cortex-M4 MCU line, this is usually the case and the two first implementation variants should be safe.[3] However, in the general case for Cortex-M4 hardware instantiations, a constant-time access to SRAM is not guaranteed. It is noticeable that all constant-time MQOM L1-gf16 variants fit in **less than 10kB** of SRAM.

We have also ported MQOM on a custom board featuring a STM32F437 MCU that embeds a dedicated coprocessor accelerating AES-128, allowing to improve the BLC computation performance. The results for the constant time implementation are provided on Table 14 (to be directly compared with the results from Table 13): we can see a speedup by a factor up to 4, as well as a slightly improved SRAM usage.

[3] This is not the case for the flash peripheral whose access latency depends on the MCU configuration, and for which prefetchers are used to accelerate the accesses.

Table 11: Benchmark of **optimized implementation** of the MQOM on Nucleo-L4R5ZI board with a Cortex-M4 MCU. The Rijndael implementation is table based with optimized assembly for L1, and the $\mathbb{F}_{256}$ field multiplication uses small log/exp tables.

Instance	KeyGen		Sign		Verify	
	memory	cycles	memory	cycles	memory	cycles
MQOM2-L1-gf2-fast-r3	8.06kB	24.18M	16.19kB	150.36M	15.22kB	139.81M
MQOM2-L1-gf2-fast-r5	8.06kB	24.18M	16.26kB	149.84M	15.58kB	139.81M
MQOM2-L1-gf2-short-r3	8.38kB	21.16M	18.05kB	311.21M	17.46kB	311.66M
MQOM2-L1-gf2-short-r5	8.38kB	21.16M	18.10kB	312.19M	17.62kB	311.43M
MQOM2-L1-gf16-fast-r3	7.90kB	6.15M	14.85kB	71.18M	13.98kB	59.04M
MQOM2-L1-gf16-fast-r5	7.90kB	6.15M	13.82kB	73.04M	13.18kB	54.02M
MQOM2-L1-gf16-short-r3	8.02kB	4.88M	14.76kB	243.32M	14.25kB	240.42M
MQOM2-L1-gf16-short-r5	8.02kB	4.88M	14.06kB	220.97M	13.69kB	211.73M
MQOM2-L1-gf256-fast-r3	7.94kB	7.09M	16.94kB	83.25M	15.38kB	76.77M
MQOM2-L1-gf256-fast-r5	7.94kB	7.09M	14.32kB	77.25M	13.30kB	65.37M
MQOM2-L1-gf256-short-r3	8.04kB	5.74M	16.51kB	315.55M	15.50kB	313.24M
MQOM2-L1-gf256-short-r5	8.04kB	5.74M	14.46kB	250.10M	13.85kB	248.93M
MQOM2-L3-gf2-fast-r3	7.80kB	226.99M	26.83kB	892.71M	24.47kB	871.85M
MQOM2-L3-gf2-fast-r5	7.80kB	226.99M	26.93kB	893.34M	24.93kB	872.15M
MQOM2-L3-gf2-short-r3	8.28kB	216.68M	29.78kB	1830.54M	28.24kB	1792.01M
MQOM2-L3-gf2-short-r5	8.28kB	216.58M	29.71kB	1872.01M	28.47kB	1792.38M
MQOM2-L3-gf16-fast-r3	7.55kB	46.67M	23.13kB	379.34M	20.97kB	370.98M
MQOM2-L3-gf16-fast-r5	7.55kB	46.67M	20.94kB	340.04M	19.26kB	331.13M
MQOM2-L3-gf16-short-r3	7.72kB	41.56M	22.47kB	1556.62M	21.15kB	1433.39M
MQOM2-L3-gf16-short-r5	7.72kB	41.57M	20.86kB	1312.58M	19.86kB	1218.38M
MQOM2-L3-gf256-fast-r3	7.60kB	57.04M	27.94kB	492.33M	24.17kB	487.03M
MQOM2-L3-gf256-fast-r5	7.60kB	57.04M	21.96kB	413.57M	19.40kB	407.01M
MQOM2-L3-gf256-short-r3	7.75kB	51.23M	25.99kB	2025.81M	23.57kB	1897.36M
MQOM2-L3-gf256-short-r5	7.75kB	51.22M	21.54kB	1632.67M	19.98kB	1466.92M
MQOM2-L5-gf2-fast-r3	8.04kB	398.89M	41.61kB	2121.29M	37.40kB	2075.26M
MQOM2-L5-gf2-fast-r5	8.04kB	398.91M	41.77kB	2122.64M	38.03kB	2076.16M
MQOM2-L5-gf2-short-r3	8.68kB	375.60M	48.17kB	3550.74M	45.28kB	3528.78M
MQOM2-L5-gf2-short-r5	8.68kB	375.60M	48.05kB	3550.24M	45.50kB	3527.75M
MQOM2-L5-gf16-fast-r3	7.72kB	92.53M	31.10kB	733.98M	26.14kB	691.72M
MQOM2-L5-gf16-fast-r5	7.72kB	92.54M	29.22kB	684.47M	24.21kB	641.13M
MQOM2-L5-gf16-short-r3	7.95kB	81.39M	30.14kB	2257.34M	26.62kB	2238.70M
MQOM2-L5-gf16-short-r5	7.95kB	81.39M	28.49kB	1971.16M	25.07kB	1949.75M
MQOM2-L5-gf256-fast-r3	7.78kB	100.70M	39.27kB	886.91M	30.46kB	866.26M
MQOM2-L5-gf256-fast-r5	7.78kB	100.70M	33.08kB	785.51M	25.36kB	763.30M
MQOM2-L5-gf256-short-r3	7.98kB	89.54M	34.79kB	2890.61M	29.59kB	2878.14M
MQOM2-L5-gf256-short-r5	7.98kB	89.53M	29.90kB	2309.75M	24.62kB	2295.63M

Table 12: Benchmark of **optimized implementation** of the MQOM on Nucleo-L4R5ZI board with a Cortex-M4 MCU. The Rijndael implementation is table based with optimized assembly for L1, and the $\mathbb{F}_{256}$ field multiplication uses a large table of 65kB.

Instance	KeyGen		Sign		Verify	
	memory	cycles	memory	cycles	memory	cycles
MQOM2-L1-gf2-fast-r3	72.58kB	24.18M	80.70kB	118.67M	79.73kB	112.50M
MQOM2-L1-gf2-fast-r5	72.58kB	24.18M	80.74kB	118.06M	80.06kB	112.46M
MQOM2-L1-gf2-short-r3	72.90kB	21.16M	82.54kB	253.96M	81.96kB	254.62M
MQOM2-L1-gf2-short-r5	72.90kB	21.16M	82.72kB	255.03M	82.26kB	254.21M
MQOM2-L1-gf16-fast-r3	72.40kB	5.90M	79.34kB	64.96M	78.48kB	53.29M
MQOM2-L1-gf16-fast-r5	72.40kB	5.90M	78.32kB	66.76M	77.68kB	48.24M
MQOM2-L1-gf16-short-r3	72.52kB	4.56M	79.36kB	233.10M	78.86kB	230.51M
MQOM2-L1-gf16-short-r5	72.52kB	4.56M	78.50kB	210.82M	78.10kB	201.72M
MQOM2-L1-gf256-fast-r3	72.44kB	6.66M	81.46kB	75.91M	79.90kB	69.34M
MQOM2-L1-gf256-fast-r5	72.44kB	6.66M	78.82kB	69.77M	77.80kB	57.99M
MQOM2-L1-gf256-short-r3	72.53kB	5.40M	81.00kB	301.93M	79.98kB	300.23M
MQOM2-L1-gf256-short-r5	72.53kB	5.40M	78.90kB	236.57M	78.26kB	235.87M
MQOM2-L3-gf2-fast-r3	72.31kB	226.99M	91.33kB	748.20M	88.96kB	704.34M
MQOM2-L3-gf2-fast-r5	72.31kB	227.03M	91.41kB	748.72M	89.42kB	704.56M
MQOM2-L3-gf2-short-r3	72.79kB	216.58M	94.26kB	1567.44M	92.82kB	1536.77M
MQOM2-L3-gf2-short-r5	72.79kB	216.68M	94.18kB	1609.13M	93.06kB	1537.54M
MQOM2-L3-gf16-fast-r3	72.05kB	45.87M	87.66kB	347.56M	85.48kB	336.83M
MQOM2-L3-gf16-fast-r5	72.05kB	45.88M	85.47kB	307.91M	83.77kB	296.90M
MQOM2-L3-gf16-short-r3	72.22kB	40.54M	86.96kB	1506.91M	85.63kB	1383.60M
MQOM2-L3-gf16-short-r5	72.22kB	40.55M	85.41kB	1262.70M	84.46kB	1168.47M
MQOM2-L3-gf256-fast-r3	72.11kB	55.84M	92.45kB	456.77M	88.68kB	449.42M
MQOM2-L3-gf256-fast-r5	72.11kB	55.83M	86.44kB	376.91M	83.90kB	369.35M
MQOM2-L3-gf256-short-r3	72.25kB	50.03M	90.49kB	1961.75M	88.04kB	1835.69M
MQOM2-L3-gf256-short-r5	72.25kB	50.03M	86.07kB	1567.93M	84.53kB	1405.06M
MQOM2-L5-gf2-fast-r3	72.55kB	398.87M	106.10kB	1668.46M	101.90kB	1622.96M
MQOM2-L5-gf2-fast-r5	72.55kB	398.90M	106.25kB	1669.16M	102.52kB	1623.31M
MQOM2-L5-gf2-short-r3	73.19kB	375.60M	112.65kB	2640.97M	109.73kB	2670.83M
MQOM2-L5-gf2-short-r5	73.19kB	375.59M	112.50kB	2639.79M	109.97kB	2669.15M
MQOM2-L5-gf16-fast-r3	72.22kB	90.08M	95.59kB	626.04M	90.64kB	588.02M
MQOM2-L5-gf16-fast-r5	72.22kB	90.07M	93.70kB	575.54M	88.69kB	536.94M
MQOM2-L5-gf16-short-r3	72.46kB	78.75M	94.62kB	2068.97M	91.08kB	2068.24M
MQOM2-L5-gf16-short-r5	72.46kB	78.74M	92.94kB	1783.21M	89.54kB	1780.28M
MQOM2-L5-gf256-fast-r3	72.29kB	97.88M	103.77kB	762.82M	94.97kB	748.92M
MQOM2-L5-gf256-fast-r5	72.29kB	97.87M	97.56kB	660.54M	89.86kB	646.10M
MQOM2-L5-gf256-short-r3	72.47kB	86.76M	99.27kB	2690.38M	94.07kB	2685.10M
MQOM2-L5-gf256-short-r5	72.47kB	86.76M	94.35kB	2105.61M	89.07kB	2100.60M

Table 13: Benchmark of **optimized constant time implementation** of the MQOM on Nucleo-L4R5ZI board with a Cortex-M4 MCU. The Rijndael implementation is bit-slice based with optimized assembly, and the $\mathbb{F}_{256}$ field multiplication uses 32-bit registers SIMD-like optimizations in C. Only L1 has been implemented for now for the purpose of the benchmark.

Instance	KeyGen		Sign		Verify	
	memory	cycles	memory	cycles	memory	cycles
MQOM2-L1-gf2-fast-r3	3.07kB	94.45M	11.22kB	317.84M	10.26kB	307.98M
MQOM2-L1-gf2-fast-r5	3.07kB	94.44M	11.29kB	317.36M	10.63kB	308.01M
MQOM2-L1-gf2-short-r3	3.39kB	90.89M	13.09kB	857.42M	12.62kB	853.27M
MQOM2-L1-gf2-short-r5	3.39kB	90.89M	13.16kB	858.64M	12.76kB	852.80M
MQOM2-L1-gf16-fast-r3	2.90kB	21.78M	9.88kB	162.86M	9.02kB	147.01M
MQOM2-L1-gf16-fast-r5	2.90kB	21.78M	8.87kB	167.84M	8.22kB	145.09M
MQOM2-L1-gf16-short-r3	3.02kB	19.88M	9.77kB	659.80M	9.31kB	652.39M
MQOM2-L1-gf16-short-r5	3.02kB	19.88M	8.99kB	655.00M	8.62kB	640.89M
MQOM2-L1-gf256-fast-r3	2.96kB	24.89M	12.00kB	194.52M	10.46kB	186.08M
MQOM2-L1-gf256-fast-r5	2.96kB	24.90M	9.37kB	172.81M	8.35kB	159.12M
MQOM2-L1-gf256-short-r3	3.03kB	24.79M	11.47kB	830.21M	10.46kB	821.49M
MQOM2-L1-gf256-short-r5	3.03kB	24.79M	9.39kB	675.31M	8.80kB	668.62M

Table 14: Benchmark of **optimized constant time implementation** of the MQOM on a board with a Cortex-M4 STM32F437 MCU featuring **hardware accelerated AES-128**. The Rijndael implementation for L1 is hence using the hardware accelerator, and the $\mathbb{F}_{256}$ field multiplication uses 32-bit registers SIMD-like optimizations in C.

Instance	KeyGen		Sign		Verify	
	memory	cycles	memory	cycles	memory	cycles
MQOM2-L1-gf2-fast-r3	1.81kB	14.38M	9.74kB	155.73M	8.79kB	147.42M
MQOM2-L1-gf2-fast-r5	1.81kB	14.38M	9.82kB	155.23M	9.16kB	147.45M
MQOM2-L1-gf2-short-r3	1.92kB	11.41M	11.62kB	317.97M	11.15kB	315.36M
MQOM2-L1-gf2-short-r5	1.92kB	11.41M	11.69kB	319.16M	11.29kB	314.82M
MQOM2-L1-gf16-fast-r3	1.67kB	6.64M	8.38kB	66.00M	7.51kB	51.64M
MQOM2-L1-gf16-fast-r5	1.67kB	6.64M	7.38kB	70.74M	6.74kB	49.44M
MQOM2-L1-gf16-short-r3	1.81kB	5.57M	8.26kB	186.48M	7.81kB	180.50M
MQOM2-L1-gf16-short-r5	1.81kB	5.57M	7.50kB	180.27M	7.14kB	167.50M
MQOM2-L1-gf256-fast-r3	1.81kB	5.26M	10.48kB	71.82M	8.94kB	64.98M
MQOM2-L1-gf256-fast-r5	1.81kB	5.26M	7.87kB	71.50M	6.86kB	59.31M
MQOM2-L1-gf256-short-r3	1.81kB	6.56M	9.95kB	232.24M	8.94kB	225.10M
MQOM2-L1-gf256-short-r5	1.81kB	6.56M	7.90kB	198.10M	7.30kB	192.87M

4 Security

4.1 Unforgeability

The MQOM signature scheme aims at providing *unforgeability against chosen message attacks* (EUF-CMA). In this setting, the adversary is given a public key `pk` and they can ask an oracle (called the *signature oracle*) to sign messages $(\texttt{msg}_1, \ldots, \texttt{msg}_r)$ that they can select at will. The goal of the adversary is to generate a pair $(\texttt{msg}, \sigma)$ such that `msg` is not one of requests to the signature oracle and such that σ is a valid signature of `msg` with respect to `pk`.

Our security statement is based on the following assumptions:

- **MQ hardness.** Solving the considered MQ instance is $(\epsilon_{\text{MQ}}, t)$-*hard* for some $(\epsilon_{\text{MQ}}, t)$ which are implicit functions of the security parameter λ. Formally, any adversary $\mathcal{A}$ on input a random MQ instance $\big(\{A_i\}, \{b_i\}, y\big)$ and running in time at most t has probability at most ϵ_{MQ} to output the solution x of the input instance.
- **Random Oracle Modem (ROM).** Our security statement holds in the ROM where the (extendable-output) hash function XOF is modelled as a random oracle.
- **Ideal Cipher Model (ICM).** Our security statement holds in the ICM where the block cipher Enc is modelled as an ideal cipher.

Based on the ROM and the ICM, the EUF-CMA security of MQOM holds from the soundness and zero-knowledge properties of the underlying ZK-PoK (which are overviewed in Section 2.1). The formal EUF-CMA security proof of MQOM will be added to a future version of the specification. It will heavily rely on usual techniques for MPC-in-the-Head signature schemes with GGM trees such as, e.g., the security proof of MQOM v1 [FR23a; BFR24] with specificities related to correlated GGM trees as in [KLS24].

4.2 Attacks against MQ instances

The security of the MQOM signature scheme relies on the hardness to solve an instance of the multivariate quadratic problem, since the secret key is a solution of the MQ instance represented by the public key. There exists many algorithms to solve the MQ problem. Their complexity depends on several parameters: the number n of unknowns, the number m of quadratic equations, the size q of the field, the characteristic of the field, and the number of solutions. The optimal algorithm might vary depending on the values of these parameters.

The best algorithms to solve polynomial systems are quite different over $\mathbb{F}_2$ and over larger finite fields. While the global asymptotic complexity of most algorithms is well-understood, estimating the concrete number of operations that is required to invert a given quadratic function is more an art than a science.

Several software tools provide estimates of the number of operations required to execute polynomial system solving algorithms, notably the `MQEstimator` [BMS+22] that is available in the `CryptographicEstimators` software library [EVZ+24].

The estimates provided by such tools should always be taken with a grain of salt. When estimating the number of bit operations required to run the F_5 algorithm, we observed a noticeable difference between the values given by version 1.1.1 (released on September 5th, 2023) and version 1.2.0 (released on November 24th, 2023) of the `MQEstimator` library. This in turn modifies the cost estimates for the hybrid-F_5 algorithm. The results are shown in Table 15.

n	m	q	v1.1.1		v1.2.0 and v2.0.0	
			F_5	hybrid-F_5 (k)	F_5	hybrid-F_5 (k)
36	36	256	150.3	111.5 (2)	203.8	143.2 (4)

Table 15: Cost estimates for solving quadratic systems with different versions of the `CryptographicEstimators` library. v1.1.1 was released on September 5th, 2023 (git commit `17924f39`) and v1.2.0 was released on November 24th, 2023 (git commit `35bc27a1`). The "F_5" (resp. hybrid-F_5) columns shows the log in base 2 of the number of "bit operations" required by the corresponding algorithm. For hybrid-F_5, the optimal number of "guessed" variables is given in parentheses.

The two versions also differ in the number of variables to "guess" in the hybrid-F_5 algorithm. These numbers can be obtained by the following bit of code (adjust with the required sizes):

```
q = 256
n = 36
m = 36
from cryptographic_estimators import MQEstimator
MQEstimator.MQEstimator(n, m, q).f5.time_complexity()
e = MQEstimator.MQEstimator(n, m, q).hybrid_f5
e.time_complexity(), e.k()
```

We traced down the difference between the two versions to a change in the default value of the linear algebra constant, namely the value of ω such that matrix multiplications requires $\mathcal{O}(n^\omega)$ arithmetic operations. The best algorithms to solve polynomial systems heavily rely on either sparse or dense linear algebra with exponentially large matrices. The best known value of the linear algebra constant is $\omega = 2.3728596$ [AW21] but it is well-known that the corresponding algorithms are so impractical that they have never been implemented (they are "galactic"). The CryptographicEstimators library switched from using $w = 2$ by default in version `1.1.1` to using $w = 2.81$ in version `1.2.0`, which corresponds to the use of the Strassen algorithm. This modification alone may explain the observed differences in cost estimates between the two versions. We agree that the use of the Strassen algorith for dense linear algebra is practical: it is implemented in M4RI and M4RIE [AB24] for binary matrices and in FFLAS/FFPACK [DGP08] for matrices over larger finite fields.

In any case, we discuss below a number of shortcomings of the CryptographicEstimators library, and discuss our own estimates.

4.2.1 Tools and building blocks

Arithmetic over $\mathbb{F}_{256}$. We consider that addition over $\mathbb{F}_{256}$ costs 8 bit operations (to XOR the two operands). Bernstein proposed in 2000 an algorithm to multiply two degree-7 polynomials over $\mathbb{F}_2[X]$ in 100 bit operations. Once their degree-14 product has been computed, it must be reduced modulo the irreducible polynomial that defines the finite field. Take $F = X^8 + X^4 + X^3 + X + 1$ (as given in Table 5). The remainder of a degree-14 polynomial modulo F can be computed with 28 bit operations. Therefore we consider that multiplication requires 128 bit operations.

Arithmetic over $\mathbb{F}_{16}$. Similarly, we consider that addition over $\mathbb{F}_{16}$ costs 4 bit operations. Two degree-3 polynomials over $\mathbb{F}_2[X]$ can be multiplied in 25 bit operations. Once their degree-6

product has been computed, it must be reduced modulo the irreducible polynomial that defines the finite field. Take $F = X^4 + X + 1$ (as given in Table 5). The remainder of a degree-6 polynomial modulo F can be computed with 6 bit operations. Therefore we consider that multiplication requires 31 bit operations.

Monomials. It is well-known that there are $\binom{n+d-1}{d}$ monomials of degree exactly d in n variables, and that there are $\binom{n+d}{d}$ monomials of degree at most d.

The situation is slightly different in the binary case, where considering the effect of the so-called "field equations" $x_i^2 = x_i$ is beneficial. In this case, we mostly work in the Boolean algebra

$$\mathcal{R}_2 = \mathbb{F}_2[x_1, \ldots, x_n] \,/\, \langle x_1^2 - x_1, \ldots, x_n^2 - x_n \rangle .$$

In the Boolean algebra, there are $\binom{n}{d}$ monomials of degree exactly d and there are $\sum_{i=0}^{d} \binom{n}{i}$ monomials of degree at most d. This last sum has no closed expression.

Lastly, in an arbitrary finite field $\mathbb{F}_q$, we work in the algebra

$$\mathcal{R}_q = \mathbb{F}_q[x_1, \ldots, x_n] \,/\, \langle x_1^q - x_1, \ldots, x_n^q - x_n \rangle .$$

The number of degree-d monomials is the degree-d coefficient of the series

$$\left(\frac{1 - z^q}{1 - z}\right)^n = \left(1 + z + \cdots + z^{q-1}\right)^n$$

while the number of monomials of degree at most d is the degree-d coefficient of the series

$$\frac{1}{1 - z}\left(\frac{1 - z^q}{1 - z}\right)^n$$

Note that the number of degree-d monomials is precisely $\binom{n+d-1}{d}$ when $d < q$.

Macaulay matrices. Consider a sequence of quadratic polynomials $f_1, \ldots, f_m$ in $\mathbb{F}_q[x_1, \ldots, x_n]$. Denote by I the ideal they span. I can be seen as an infinite-dimensional vector space spanned by the mf_j, where m ranges across all possible monomials. Let I_d (resp. $I_{\leq d}$) denote the subspace formed by the mf_j where m ranges across all monomials of degree d (resp. at most d). In general, I_d is not equal to the set of all degree-d polynomials of I, because of potential *degree falls*: some low-degree polynomials in I can only be obtained by taking a high-degree polynomial combination of the f_j. Both sets are equal only when the f_j are a Gröbner basis of I, a fact that was noted long ago by Lazard [Laz83].

Polynomials of I with a special shape can often be found effectively by means of linear algebra, by searching inside $I_{\leq d}$ for a sufficiently large d. The degree-d *Macaulay matrix* of $f_1, \ldots, f_m$ is the matrix whose rows are the $m_i f_j$ with $\deg m_i \leq d - 2$ and whose columns correspond to all possible monomials of degree at most d. It follows that the row span of the degree-d Macaulay matrix is exactly $I_{\leq d}$.

The degree-d Macaulay matrix of $f_1, \ldots, f_m$ has $\binom{n+d}{d}$ columns and $m\binom{n+d-2}{d-2}$ rows. In the Boolean case, it has $\sum_{i=0}^{d} \binom{n}{i}$ columns and $m \sum_{i=0}^{d-2} \binom{n}{i}$ rows.

Macaulay matrices are quite sparse, because each row has at most $(n+1)(n+2)/2$ non-zero coefficients. It is well-known that they are also rank-deficient: there are linear dependencies between rows, at least because of the trivial relations $f_i f_j = f_j f_i$. Under the assumption that the f_j form a (semi-)regular sequence, then the above "trivial relations" between the f_i's are

the only ones, and thanks to that information the rank of the degree-d Macaulay matrix can be determined precisely. The assumption implies that it only depends on n and m, and does not depend from the actual coefficients of the f_j's. The assumption essentially means that the polynomials are not bound by "unexpected" algebraic relations. It is usually well-verified in practice on unstructured systems, and is therefore standard in all the cryptographic literature. The interested reader is referred to [Bar04; BFS15] for more details. We now assume that the the f_j's are (semi-)regular.

Consider the series expansion:

$$\sum_j a_j z^j = (1-z^2)^m/(1-z)^{n+1}.$$

The smallest index j such that $a_j \leq 0$ is the *solving degre* of the semi-regular sequence (see [CG23] for more details). When d is strictly less than the solving degree, then the rank of the degree-d Macaulay matrix is $\binom{n+d}{d} - a_d$ (in the non-binary case). If d is equal or greater than the solving degree, then the rank is just $\binom{n+d}{d}$ (the number of columns). Instead of explicitly working with the series, which requires tools from computer algebra, we use a simple recurrence relations between the ranks of Macaulay matrices. Write $R_{d,j}$ the rank of the degree-d Macaulay matrix of $f_1, \ldots, f_j$. Then

$$\begin{aligned} R_{0,j} &= 0 \\ R_{1,j} &= 0 \\ R_{d,0} &= 0 \\ R_{d,j+1} &= R_{d,j} + \binom{n+d-2}{d-2} - R_{d-2,j} \end{aligned}$$

The last relation comes from observing the behavior of the matrix-F5 algorithm [Bar04; BFS15]. And finally $R_{d,m}$ is equal to $\binom{n+d}{d} - a_d$ and is the rank of the degree-d Macaulay matrix, under the assumption that the f_j are (semi-)regular and that d is less than their solving degree. The smallest d such that $R_{d,m}$ is greater than or equal to $\binom{n+d}{d}$, which is the number of monomials in n variables of degree at most d, is the solving degree of the f_j's.

However, this is only valid in characteristic zero. Over $\mathbb{F}_q$, there are other trivial relations, namely $f_i^q = f$ over $\mathbb{F}_q$. Note that this last category of "trivial relations" only appear in degree $2q$. Over the binary field, and taking into account the field equations, the same reasoning can be applied, but the series is different:

$$\sum_j a_j z^j = (1+z)^n/(1+z^2)^m/(1-z)$$

and the recurrence relation is also different:

$$R_{d,j+1} = R_{d,j} + \left(\sum_{i=0}^{d-2} \binom{n}{i}\right) - R_{d-2,j+1}$$

Finally, over $\mathbb{F}_q$, to the best of our knowledge, the ranks of the Macaulay matrices are not known in general. However, up to degree $2q$, they can be predicted by a slight modification of the "characteristic zero" case. The coefficients of the following series:

$$\sum_j a_j z^j = (1+z^2)^m(1-z^q)^n/(1-z)^{n+1}$$

predict the ranks of the Macaulay matrices of the corresponding degrees, as long as they are strictly positive and the recurrence relation is also different:

$$R_{d,j+1} = R_{d,j} + [\#\text{monomials of degree } d-2] - R_{d-2,j}.$$

We note that, in general, the *solving degree* is the *degree of regularity* of a homogeneous (semi-regular) system of the same number of polynomials with one more variable.

Solving sparse linear systems with the block Wiedemann algorithm. In order to solve $Ax = b$ with a sparse matrix A, the Block Wiedemann algorithm is usually the solution of choice. We refer the reader to [CCN+12; BGG+20] for details about the algorithm and practical results. It has two main parameters, the "blocking factors", that we denote by $\tilde{m}$ and $\tilde{n}$. Let N denote the size of the matrix and $|A|$ denote the number of non-zero entries in A.

The bulk of the workload consists in "matrix-vector products", that are in fact (sparse $N \times N$ matrix) $\times$ (dense vector) products. It follows that each matrix-vector product requires $2|A|$ field operations (half additions and half multiplications). The block Wiedemann algorithm has three phases:

BW1 Compute the Krylov sequence $(uA^iv)_i$. Split in $\tilde{n}$ independent jobs. Each job does $(1/\tilde{n} + 1/\tilde{m})N$ iterations in sequence. Each iteration does a "sparse matrix-dense vector" as described above, followed by a (dense $\tilde{m} \times N$ matrix) $\times$ vector product that requires $2N\tilde{m}$ operations (half additions, half multiplications). In total, there are $(1 + \tilde{n}/\tilde{m})N$ iterations aggregated over the $\tilde{n}$ independent jobs. After each iteration, a dense vector of size $\tilde{m}$ must be stored persistently. The total output size of the $\tilde{n}$ independent jobs is therefore $(\tilde{m}+\tilde{n})N$ field elements. This phase requires $(1/\tilde{n}+1/\tilde{m})N$ sequential steps, even if the matrix-vector product itself is perfectly parallel. The total number of arithmetic operations is $2(1 + \tilde{n}/\tilde{m})N(|A| + \tilde{m}N)$.

BW2 Compute the linear recurrence relation of the Krylov sequence. Its input consists in $(\tilde{m} + \tilde{n})N$ field elements, it has quasi-linear running time complexity, and parallelizes well. Its memory usage may not be negligible though.

BW3 Assemble the solution from the linear recurrence. Can be split in a very high number of independent jobs. Does $N/\tilde{n}$ "sparse matrix-dense vector" products in total.

Choosing the optimal values of $\tilde{n}$ and $\tilde{m}$ is somewhat of an art. It is usual to choose $\tilde{m}/\tilde{n} = 2$ or $\tilde{m}/\tilde{n} = 3$. This yields a total workload of $(1.5 + 1/n)N$ or $(1.333 + 1/\tilde{n})N$ iterations, respectively. Increasing $\tilde{n}$ reduces the total time spent in BW3, and if $\tilde{m}/\tilde{n}$ is fixed, it does not increase the running time of BW1. However, increasing $\tilde{n}$ will increase the running time and the memory footprint of BW2. Note that increasing $\tilde{n}$ has another practical advantage, by increasing the level of coarse-grained parallelism in BW1.

4.2.2 Solving polynomial systems over "large" finite fields

We discuss in particular the cases of $\mathbb{F}_{256}$ and $\mathbb{F}_{16}$.

The XL algorithm. The XL algorithm was proposed by Courtois, Klimov, Patarin and Shamir [CKP+00] in 2000. In fact, it turned out to be a reinvention of a technique due to Lazard in 1983 [Laz83], and is more-or-less equivalent to modern Gröbner basis algorithms. What we say below about algorithmic and practical aspects is mostly based on the existing implementation

of [CCN+12], that has been demonstrated to work and currently holds several computational records. It is capable of running a parallel computation using a cluster of machines. It was notably used in Beullens's practical cryptanalysis of Rainbow [Beu22]. This particular implementation works only over $\mathbb{F}_{16}$ and $\mathbb{F}_{31}$.

The underlying idea of the XL algorithm is simple. Pick a degree d such that the degree-d Macaulay matrix has full rank (this is typically the solving degree). Cut the column corresponding to the constant monomial. Call the resulting vector b and the truncated matrix A. Solve the linear system $Ax + b = 0$. If the original polynomial system had a single solution $\hat{x}$, then this linear system also has a single solution where the coordinates of x describe the values of all possible monomials of degree at most d, evaluated over $\hat{x}$. Note that this linear system is sparse, and can be solved using the block Wiedemann algorithm. Also, because we are only interested in the value of degree-1 monomials, it is sufficient to recover only a very small fraction of the solution vector. This allows the implementation of [CCN+12] to use an unpublished trick that bypasses the BW3 step almost completely.

The number of columns of A is the number of monomials of degree at most d in n variables over $\mathbb{F}_q$. It has much more rows than columns, and the rows have linear dependencies. The aforementioned implementation uses the following heuristic: a random subset of the rows is extracted to obtain a nearly square matrix, which is full-rank with high probability. Solving the input polynomial system is thus reduced to solving a sparse linear system of dimension N (the number of monomials at most d in n variables over $\mathbb{F}_q$) with $\binom{n+2}{2}$ non-zero coefficients per row, using the block Wiedemann algorithm. Denoting by $\tilde{n}$ and $\tilde{m}$ the two blocking factors of the block Wiedemann algorithm, it follows from the discussion above that the total number of arithmetic operations in the BW1 step is approximately:

$$2\left(1+\frac{\tilde{n}}{\tilde{m}}\right)N^2\left(\binom{n+2}{2}+\tilde{m}\right)$$

Over $\mathbb{F}_{256}$, we can safely assume that $N = \binom{n+d}{d}$, because the solving degree d is always going to be less than 512. However, over $\mathbb{F}_{16}$, this is no longer going to be the case if the solving degree is greater than 16.

To estimate the total number of operations, we ignore the costs of the BW2 and BW3 steps (the latter is almost zero), and assume that exactly N matrix-vector products take place. In other terms, we assume that $\tilde{n}/\tilde{m} \approx 0$ and that $\tilde{m} \ll n^2$. This gives a lower-bound on the number of operations.

The hybrid method. The "hybrid method" [BFP09; BFP12] is usually the best technique for solving polynomial systems over finite fields. Its principle is simple:

1. Choose $0 \leq k \leq n$.
2. "Guess" the value of k variables.
3. Solve the remaining system of m equations $n - k$ variables using the F_5 of the XL-Wiedemann algorithm.
4. If no solution has been found, return to step 2.

The point is that the sub-systems that are actually solved in step 3 are more overdetermined than the input system, and therefore have a much lower solving degree. The resulting Macaulay matrices are thus much smaller.

There is an optimal number k of variables to guess. The asymptotic complexity of this procedure is determined in [BFP12] when $n \to +\infty$ with q and the ratio m/n fixed, under the assumption that the input system is sufficiently generic. Concretely, the optimal number of variables to guess depends on n, m, q and on the secondary algorithm used to solve the resulting polynomial systems.

The "polynomial XL" algorithm of [FK24]. This algorithm can be seen as a (slight) generalization of Crossbred. In the end, it uses the hybrid method combined with the XL algorithm, but tries to perform a big precomputation to accelerate the subsequent resolution of polynomial systems.

It partitions the n input variables $x = (x_1, \ldots, x_n)$ in two categories. Say that they are relabeled as $x = (y_1, \ldots, y_k, z_1, \ldots, z_{n-k})$. The input polynomials are seen over the polynomial ring $\mathbb{F}_q[y][z]$, i.e. as polynomials in the z's whose coefficients are polynomials in the y's. The y's are the variable that will be "guessed", leading to a polynomial system in the z's.

The preprocessing step consists in finding at least α (linearly independent) degree-d polynomials in the ideal spanned by the f_i such that the total number of distinct monomials in the z's that appear in these new polynomials is at most α.

Once this is done, the y's are fixed to a random value, and the resulting system of α polynomial equations in the z's can be solved by linearization, by considering each of the possible α monomials as an independent variable.

The authors of Polynomial-XL (PXL) described a specific echelonization procedure to produce these α polynomials. Hence, this uses dense linear algebra on Macaulay matrices.

There is an effective way to predict the value of α, as well as the total number of field coefficients of the matrix after the end of the preprocessing. In [FK24], the authors estimate the number of operation of their algorithm using either $\omega = 2.37$ or $\omega = 2.81$. We believe that only the second choice is reasonable. In this case, the gains claimed in [FK24] over the hybrid-XL-Wiedemann algorithm are modest (a factor of two for the largest examples).

What PXL and Crossbred have in common is that they have a preprocessing step (based on linear algebra in Macaulay matrices) that finds "special" polynomials in the ideal spanned by the input equation. These special polynomials are restricted to only have certain monomials.

In Crossbred, the only allowed monomials are those where the z's occur with degree at most d. Thus, once the y's are fixed, we are left with a degree-d polynomial system in $n-k$ variables. Existing practical implementations use $d = 1$, so the resulting linear system is small and easy to solve.

In PXL, the choice of allowed monomials is a bit more flexible, as there is no fixed upper-bound on their degree. The only condition is that their number must not be too large (once the y's are erased). In [FK24], the authors of PXL suggest a specific algorithm to select them, but in fact they could be chosen somewhat arbitrarily. In most cases, there is a value of d that yields almost the same number of polynomials with the Crossbred algorithm. The complexity of both algorithms therefore cannot be very different.

Parameters, estimations and discussion. Table 17 shows our choice of parameters for $q = 256$, along with our estimations of the complexity of running the (hybrid-)XL-Wiedemann (WXL) algorithm and the "Polynomial XL" (PXL) algorithm.

Even though an implementation of WXL is available, it is both quite difficult and a bit meaningless to predict its actual running time on a specific platform (e.g. "100 billion years on a single core of an Intel Xeon Gold 6230"), if only because the computation is meant to

Level		I	III	V
n		48	72	96
WXL	k	3	5	8
	D	22	28	33
	$\log_2 N$	57.9	79.6	98.7
	$\log_2 \lvert A \rvert$	68.0	90.8	110.6
	cost	157.0	217.5	280.4
PXL	k	5	7	9
	D	17	24	30
	$\log_2 \alpha$	36	54.6	73
	$\log_2 \lvert A \rvert$	86.5	128.9	169
	cost	148	216	283

Table 16: Parameter choice with $q = 256$. For WXL, N denotes the size of the (sparse) matrix and $|A|$ denotes its number of non-zero coefficients. For PXL, α denotes the size of the (dense) matrix with polynomial entries resulting from the preprocessing and $|A|$ denotes its number of field coefficients. In both cases, $|A|$ is thus a reasonable estimate of the size of the matrix.

Level		I	III	V
n		56	84	116
WXL	k	13	17	24
	D	13	19	24
	$\log_2 N$	40.8	62.2	81.9
	$\log_2 \lvert A \rvert$	50.7	73.5	94.0
	cost	150.6	210.8	278.9
PXL	k	12	17	26
	D	14	19	23
	$\log_2 \alpha$	32	48.6	62.7
	$\log_2 \lvert A \rvert$	79.3	116.3	149.2
	cost	142.8	209.3	284.9

Table 17: Parameter choice with $q = 16$. N denotes the size of the (sparse) matrix and $|A|$ denotes its number of non-zero coefficients.

be infeasible. The actual obstacle to this more concrete estimate is the block-Wiedemann algorithm.

In the context of the Number Field Sieve, the block-Wiedemann algorithm has been executed in practice on a matrix of size 36M with 250 element per rows over a large finite field (to compute a discrete log), and on a matrix of size 400M with 250 elements per row over $\mathbb{F}_2$ (to factor RSA-250). Details of these computations are reported in [BGG+20]. In the context of the XL-Wiedemann, it was executed on a matrix of size 45M over $\mathbb{F}_{31}$. Details of the computation have been inferred by us, with some information available on the MQchallenge website. The BW1 step requires days of sequential processing (100, 18 and 19 days for the three described computations, respectively). By itself, this is a serious practical hurdle, and it is not completely obvious that the algorithm "practically" scales to larger sizes. In [BGG+20], the authors conclude:

> [...] with adequate parameter choices, large sparse linear systems occurring in NFS computations can be handled, and at this point we are not facing a technology barrier.

However, the matrix sizes considered above are many orders of magnitude larger than those that have been dealt with in practice.

From a practical point of view, it is difficult to predict the actual running time (in hours) of the block-Wiedemann algorithm, even when the computation is practical. The process is well-known to be memory-bound or communication-bound, so the number of operations is not necessarily well-correlated to the actual running time. Choosing the blocking factors is not completely obvious either. If it is possible to measure the actual running time of one iteration, then the actual running time of the algorithm can be fairly well evaluated. However, predicting the time taken by the matrix-vector product is difficult: it depends on the hardware, on the shape of the matrix, on the clustering of entries inside it, etc.

4.2.3 Special case of Boolean systems

Estimating the difficulty of solving Boolean polynomial system is challenging because of the tension between "galactic" algorithms with the best asymptotic complexity and practically efficient ones.

Exhaustive search is the baseline method to solve systems of Boolean quadratic polynomial equations, with a running time $\tilde{\mathcal{O}}(2^n)$ and negligible space complexity. An FPGA implementation of exhaustive search [BCC+13] was used to break LUOV in practice [DDV+21].

Yang and Chen [YC04] discussed the asymptotic complexity of the hybrid method applied to Boolean system (along with the optimal number of variables to guess). The BooleanSolve algorithm of Bardet, Faugère, Salvy and Spaenlehauer [BFS+13] is the best embodiment of the hybrid method at this point, with running time $\tilde{\mathcal{O}}\left(2^{0.792n}\right)$ on average, under algebraic assumptions. It guesses some variables, then checks if a polynomial combination of the remaining polynomials is equal to 1. If it is the case, then the guessed values are incorrect (by Hilbert's Nullstellensatz). Checking this is accomplished by deciding whether large sparse linear systems have a solution (using the block-Wiedemann algorithm). The inventors of BooleanSolve claim that it is slower than exhaustive search when $n \leq 200$. However, this threshold should be treated with caution in the absence of an implementation.

The Crossbred algorithm of Joux and Vitse [JV17] also belongs to the "guess variables then solve a linear system" family of algorithms. Its asymptotic complexity is not precisely known, but its practical efficiency is spectacular: it has been used to solve record-size random systems

with $n = 83$ variables and $m = 186$ equations, and with $m = 76$ equations in $n = 114$ variables. These are the current record. It is the first algorithm that has beaten brute-force in practice on random non-overdetermined systems. The original implementation by Joux and Vitse is not public. However, there are two public implementations: one that uses GPUs by Niederhagen, Ning and Yang [NNY18], and another more competitive one by Bouillaguet and Sauvage (`https://gitlab.lip6.fr/almasty/hpXbred` — this one holds the current records).

A completely different family of algorithms emerged in 2017 when Lokshtanov, Paturi, Tamaki, Williams and Yu [LPT+17] presented a randomized algorithm of complexity $\tilde{\mathcal{O}}\left(2^{0.8765n}\right)$ based on the "polynomial method". In strong contrast with almost all the previous ones, it does not require any assumption on the input polynomials, which is a theoretical breakthrough. The algorithm works by assembling a high-degree polynomial that evaluates to 1 on partial solutions, then approximates it by lower-degree polynomials. The technique was later improved by Björklund, Kaski and Williams [BKW19], reaching $\tilde{\mathcal{O}}\left(2^{0.804n}\right)$, then again by Dinur [Din21c], reaching $\tilde{\mathcal{O}}\left(2^{0.6943n}\right)$ — this is "Dinur's first algorithm".

Noting that the self-reduction that results in this low asymptotic complexity only kicks in for very large values of n, Dinur proposed a simpler, lightweight version of his algorithm for the crypto community with complexity $\mathcal{O}\left(n^2 2^{0.815n}\right)$ using less than $n^2 2^{0.63n}$ bits of memory [Din21a]. This one is known as "Dinur's second algorithm".

The main problem in choosing parameters is to estimate the number of operations of Dinur's algorithms (the first one in particular). It would be possible to "play safe" by choosing $n = \lambda/0.6943$, where λ is the desired security level, assuming that the hidden polynomial factors in the "big Oh tilde" are equal to one. This suggests choosing $n = 208$ for security level I. But in fact, the concrete number of operations required to run the algorithm is much higher than just $2^{0.6943n}$.

The crossbred algorithm. Because of its practical success, it seems fair to assess the efficiency of the Crossbred algorithm. We note that it is the first algorithm that has been capable of "beating brute force" in practice.

Just like Polynomial XL, the Crossbred algorithm partitions the n input variables $x = (x_1, \ldots, x_n)$ in two categories. Say that they are relabeled as $x = (y_1, \ldots, y_k, z_1, \ldots, z_{n-k})$. Its preprocessing step returns polynomials in which the z variables only occur with degree d. When the y variables are fixed to some value, we are left with a much smaller polynomial system that can be solved by linearization. In practical implementations, $d = 1$.

Finding these polynomials can be seen as finding vectors in the (left-)kernel of a Macaulay matrix in which some columns have been removed. It follows that there are essentially two cases: if $d = 1$, then the number of polynomials that must be found is small, and they can be found efficiently by the block-Wiedemann algorithm. The Macaulay matrix remains in sparse representation and linear algebra is essentially quadratic. Otherwise, if $d \geq 2$, many kernel vectors must be found and dense Gaussian elimination is the only reasonable way to find them. In this case, the Macaulay matrix is in dense representation and linear algebra takes time $\mathcal{O}\left(N^\omega\right)$.

We consider that the CryptographicEstimators library has several shortcomings in its estimation of the complexity of Crossbred:

- It overestimates the space complexity by assuming a dense representation of the Macaulay matrix in the preprocessing step, even when it considers the possibility of using the Wiedemann algorithm (that allows the use of a sparse matrix). The `hpXbred` implementation uses a sparse matrix.

- It underestimate the running time of the exhaustive search phase by assuming that linear algebra runs in n^ω operations, even when the matrices are very small (when $d = 1$), when only the cubic algorithm makes sense.
- It overestimate the running time by ignoring the beneficial effect of external hybridation (it allows to increase the number of variables that are not exhaustively searched — see below).
- It overestimates the running time of the preprocessing step by assuming that the Wiedemann algorithm requires $3N$ matrix-vector products, when the block-Wiedemann algorithm with proper parameter choice ($m = 2n$, $n \geq 4$) can require $\leq 1.75N$.

Here is an example of a slight overestimation by the `CryptographicEstimators` library (`v2.0.0`, git commit `0d9bd3f925e`):

```
>>> from cryptographic_estimators import MQEstimator
>>> pb = MQEstimator.MQProblem(n=160, m=160, q=2)
>>> MQEstimator.Crossbred(pb).time_complexity()       # no external hybridation
151.16564211027884
>>> MQEstimator.Crossbred(pb, h=3).time_complexity()  # start by guessing 3 variables
150.43226492985866                                    # the result is better
```

We have some practical experience with the Crossbred algorithm, acquired by assembling the `hpXbred` high-performance implementation and using it to obtain all the current computational records of the MQChallenge website over $\mathbb{F}_2$. In the process, we have developped our own estimator (if only to choose parameters for actual computations).

An (unpublished) reduced-space hybrid method. It is well-known that, given a Boolean quadratic polynomial f, it is easy to find an invertible matrix S (a linear change of variables) such that $(Sx) = x_1x_2 + x_3x_4 + \cdots + x_{n-1}x_n + (\text{linear terms})$. If all the variables with odd index are "guessed", then $f(Sx)$ becomes linear. This allows to express one of the variables as a linear function of the others, and reduces the number of variables (and of polynomial equations) by one. It follows that a quadratic system with n equations in n variables can be solved by solving $2^{n/2}$ systems with $n - 1$ equations in $n/2 - 1$ variables.

This technique can be improved. It follows from [MPG13, Proposition 3] that, given *two* Boolean quadratic polynomials f and g, there is (often) a linear change of variables S such that $f(Sx)$ and $g(Sx)$ are simultaneously *simplectic*. It follows that guessing half of the variables simultaneously turn $f(Sx)$ and $g(Sx)$ into linear functions. It follows that a quadratic system with n equations in n variables can be solved by solving $2^{n/2}$ systems with $n - 2$ equations in $n/2 - 2$ variables.

This (unpublished) trick was used by the `hpXbred` implementation to obtain computational records in the "underdetermined" challenges category (where many variables can be "guessed" without reducing the success probability of the computation). The resulting subsystems are quite overdetermined, and the Crossbred algorithm performs well in this case. We call the resulting combination Crossbred$^+$. It always requires much less space than the "normal" Crossbred and is usually almost as fast.

Dinur's second algorithm. Because of the lack of any serious implementation, Dinur's algorithms pose the greatest challenge to a concrete estimation. This is probably not going to

change because it seems likely that these algorithms cannot be competitive for any computation that can be carried out in practice. Dinur's second algorithm takes a parameter named n_1 in [Din21b]. Write:

$$N = \sum_{i=0}^{n_1+3} \binom{n-n_1}{i}$$

The algorithm has two dominating phases:

1. It needs to find all solutions of N quadratic systems of n_1+1 equations in n_1 variables (by brute force).
2. Then, a collection of n_1 polynomials of degree n_1+3 in $n-n_1$ variables must be interpolated and evaluated on all the 2^{n-n_1} possible inputs. Each such polynomial has N coefficients.

The space requirement of the algorithm is essentially $(n_1+1)N$ bits (to store these large polynomials). The value of n_1 is chosen to balance the costs of these two phases. The first phase is executed using the FES algorithm. To perform the second phase, Dinur described a memory-efficient version of the Moebius transform that evaluates a degree-d polynomial in n variables on all the 2^n possible inputs in time less than $n2^n$, using only twice the amount of memory needed to store the polynomial. We believe that the number of bit operations needed to complete the interpolation is quite underevaluated in [Din21b], for the following reason. It is stated in [Din21b] that:

> We estimate the complexity of a straight-line implementation of our algorithm by counting the number of bit operations (e.g., AND, OR, XOR) on pairs of bits. This ignores bookkeeping operations such as moving a bit from one position to another (which merely requires renaming of variables in straight-line programs).

In other terms, a statement such as:

$$A[2015494782137237151] \leftarrow A[8910305899308506505] \oplus A[14034715819129815024]$$

counts as a single bit operation. The time complexity of the attack is taken as the number of such statements. The problem is that this computational model is non-uniform: each statement representing a single bit operation contains three n-bit memory adresses that are "hard-coded" into the "code" of the procedure. The size of the procedure itself, measured in bits, is then larger than its number of statement by a factor of about $3n$. Generating the code of the procedure is clearly more costly than executing it (in fact, the code may contain an "advice" of size linear in that of the input). At first glance, it is not really obvious how to compute the array indices "on the fly".

Bouillaguet [Bou24] has shown that the memory-efficient Möbius transform described by Dinur in [Din21b] can be implemented in the C language (with a single, fixed program for all possible input sizes) with a running time of $\mathcal{O}(d2^n)$ "elementary" operations on n-bit words (mostly additions). But this clearly requires more bit operations than the number claimed in [Din21b]. Experiments in [Bou24] suggest at least 20 CPU cycles per "bit operation". Therefore, we (optimistically) consider that the cost of the memory efficient Möbius transform is about $20nd2^n$ "gates" (this assumes that an elementary operation on n-bit words translates to exactly n gates).

In addition, we expect the space requirements to make the algorithm completely impractical.

Level		I	III	V
n		160	240	320
Crossbred	h	3	4	3
	D	13	20	27
	k	31	44	56
	$\log_2 N$	61.7	95.9	130
	$\log_2 \lvert A \rvert$	75.3	111	145
	Cost	144	213	282
Crossbred$^+$	h	86	122	160
	D	5	8	11
	k	26	38	51
	$\log_2 N$	23.6	39.2	54.6
	$\log_2 \lvert A \rvert$	37.3	54	70.4
	Cost	147	216	285
Dinur 1st	n_1	39	58	80
	n_2	33, 0	52, 41, 33, 0	74, 61, 51, 43, 36, 31, 0
	Space	129	190	248
	Cost	160	223	283
Dinur 2nd	n_1	34	49	64
	Space	107	158	208
	Cost	148	214	280

Table 18: Parameter choice with $q = 2$.

Dinur's first algorithm. While having the best asymptotic complexity, Dinur's first algorithm suffer from a high concrete complexity for relevant instance sizes. In general, the algorithm returns the parity of the number of solutions ("does the polynomial system have an odd number of solutions?"). If we assume that the polynomial system has at most one solution, then this solves the decisional version of the problem ("does the system have a solution?"). The search-to-decision reduction "guesses" the first variable and checks if a solution still exists. It then proceeds with one less variable.

The algorithm is recursive, and each recursive calls need to choose a parameter (n_1 at the root, n_2 below). We searched for the best values exhaustively and implemented an estimator to determine its number of operations.

We applied the same penalty of a factor $20n$ to the Möbius transform as in Dinur's first algorithm.

We believe that, because the algorithm is complex and has never been implemented, any concrete estimation of its complexity should be taken with caution. Further "practical" improvements may be discovered if an implementation is ever attempted. However, the huge space complexity of the algorithm makes this unlikely.

Parameters, estimations and discussion. Using the `hpXbred` software, the running time of the Crossbred$^+$ algorithm on the level-I parameter set can be determined on currently existing hardware. It solves 2^{86} subsystems of 158 quadratic equations in 72 variables. Solving each

subsystem requires 2375 CPU.h on a single machine (a PowerEdge C6420 blade equipped with two Intel Xeon Gold 6130 CPUs). This makes a total of 2×10^{25} CPU-years on this hardware platform. More precisely, the running times breaks down as follows:

1. BW1: 685 CPU.h
2. BW2: 25 CPU.h
3. BW3: 140 CPU.h
4. Enumeration: 1525 CPU.h

The matrix processed by the block-Wiedemann algorithm has dimension 8.86M and 6.5G non-zero entries. The BW1 and BW3 step total 2^{58} operations, that are executed at about 99.25Gop/s by the machine. The enumeration step has $2^{60.3}$ operations that are executed at 260.6Gop/s by the machine. The difference is most likely explained by the fact that the block-Wiedemann algorithm suffers more from the cost of memory accesses. Note that the peak performance of a single core is about 2150Gop/s ($2 \times$ 512-bit AND per cycle at 2.1GHz).

5 Design choices

This section presents the design rationale of MQOM v2 in relation to the existing literature. Recent advancements in the field have led to signature schemes that are more efficient, more compact, and (sometimes) inherently simpler than their predecessors. We explain the rationale behind our design choices, which were made with an emphasis on simplicity in both design and implementation.

5.1 Threshold-Computation-in-the-Head

The design of MQOM v1 relied on the MPC-in-the-Head paradigm with additive sharings. Since then, two new frameworks have been introduced: the VOLE-in-the-Head (VOLEitH) framework [BBD+23] and the Threshold-Computation-in-the-Head (TCitH) framework [FR23b]. These new frameworks provide MQ-based signatures that are roughly half the size of MQOM v1 signatures, while also reducing computational costs. For these reasons, we decided to adopt one of these two frameworks in the development of MQOM v2.

TCitH vs. VOLEitH. While the line commitment scheme in TCitH-GGM only supports opening evaluations over a small domain Ω (with $|\Omega| = N$ being the size of the GGM tree), the VOLEitH framework supports evaluations over a domain of size N^τ by combining τ instances of the small-domain line commitment scheme. As a result, VOLEitH achieves a soundness error of $\frac{2}{N^\tau}$, compared to $\left(\frac{2}{N}\right)^\tau$ with the TCitH-based protocol repeated τ times. This implies that, for a given security level, τ can be slightly smaller in VOLEitH, often leading to reduced communication costs compared to TCitH-GGM.

On the other hand, the resulting large-domain line commitment scheme of VOLEitH requires a statistical consistency test, introducing an additional round of interaction between the prover and verifier in the underlying ZK PoK protocol. This slightly increases the overall communication and necessitates working over a large field extension (typically a λ-bit extended field). For signature schemes with a small secret witness –which is the case of the MQ solution x in MQOM–, this slight increase mitigates the TCitH overhead. As a consequence, the TCitH framework remains competitive in terms of signature size while enjoying a structurally simpler design.

In Table 19, we present the signature sizes for a variant of MQOM v2 based on the VOLEitH framework. We apply the same optimizations to this variant as in the TCitH-based version, including correlated trees and grinding (see the following subsections). Our results show that the short signature variants yield comparable sizes across both frameworks, while the fast signature variants are slightly smaller with the VOLEitH framework. Given this close proximity in signature size and the greater simplicity of the TCitH framework (no consistency check, smaller field extension), we ultimately chose to adopt the TCitH framework.

The sigma variant. In the considered PIOP protocol (see Section 2.1.2), the first verifier challenge is designed to batch multiple polynomials in order to reduce their communication cost. Instead of sending the $\hat{m}$ coordinates of the vector polynomial P_z (masked with P_u), the prover sends $\eta < \hat{m}$ random linear combinations of them, that is the vector polynomial $\Gamma \cdot P_z$ (still masked with P_u, which is the vector polynomial P_α). We observed that the size saving due to this batching interaction is rather small for MQOM, in particular for the $\mathbb{F}_2$ instances. On the other hand, skipping the batching interaction results in a protocol with lower round complexity,

Framework	MQOM2 – TCitH		VOLEitH	
Statistical Batching	Without (3r)	With (5r)	Without (3r)	With (5r)
MQOM2-L1-gf2-short	2 868	2 820	2 966 (+3%)	2 790 (-1%)
MQOM2-L1-gf16-short	3 060	2 916	3 054 (-0%)	2 878 (-1%)
MQOM2-L1-gf256-short	3 540	3 156	3 450 (-3%)	3 098 (-2%)
MQOM2-L1-gf2-fast	3 212	3 144	3 294 (+3%)	3 054 (-3%)
MQOM2-L1-gf16-fast	3 484	3 280	3 414 (-2%)	3 174 (-3%)
MQOM2-L1-gf256-fast	4 164	3 620	3 954 (-5%)	3 474 (-4%)
MQOM2-L3-gf2-short	6 388	6 280	6 788 (+6%)	6 380 (+2%)
MQOM2-L3-gf16-short	6 820	6 496	6 992 (+3%)	6 584 (+1%)
MQOM2-L3-gf256-short	7 900	7 036	7 910 (+0%)	7 094 (+1%)
MQOM2-L3-gf2-fast	7 576	7 414	7 484 (-1%)	6 932 (-7%)
MQOM2-L3-gf16-fast	8 224	7 738	7 760 (-6%)	7 208 (-7%)
MQOM2-L3-gf256-fast	9 844	8 548	9 002 (-9%)	7 898 (-8%)
MQOM2-L5-gf2-short	11 764	11 564	12 170 (+3%)	11 434 (-1%)
MQOM2-L5-gf16-short	12 664	12 014	12 584 (-1%)	11 848 (-1%)
MQOM2-L5-gf256-short	14 564	12 964	14 194 (-3%)	12 722 (-2%)
MQOM2-L5-gf2-fast	13 412	13 124	13 370 (-0%)	12 378 (-6%)
MQOM2-L5-gf16-fast	14 708	13 772	13 928 (-5%)	12 936 (-6%)
MQOM2-L5-gf256-fast	17 444	15 140	16 098 (-8%)	14 114 (-7%)

Table 19: Comparison of MQOM v2 with its variant over VOLEitH. All the signature size are in bytes. The trade-off "short" relies on GGM trees with 2048 leaves, while the trade-off "fast" relies on GGM trees with 256 leaves. While τ would be larger using TCitH than using VOLEitH, the number of the expanded bits using PRG on tree leaves is larger using VOLEitH than using TCitH (until a factor +90%), because of the mask for the consistency check.

3 instead of 5, and arguably simpler design.[4] We have chosen to propose both options –with and without batching interaction– in the development of MQOM v2. Namely, we propose a 3-round variant (the "sigma variant") and a 5-round variant of MQOM. The 5-round variant features smaller signature sizes while the 3-round variant is simpler, easier to implement and could be more amenable in some specific contexts due to its lower round complexity. To the best of our knowledge, the sigma variant of MQOM v2 is the first signature scheme built upon a sigma protocol with recent MPCitH techniques (i.e., not relying on a protocol with helper [KKW18; Beu20] or suffering high soundness error as early MPCitH schemes [GMO16; CDG+17]).

Witness encoding as constant term versus as leading term. In the TCitH and VOLEitH frameworks, we encode the secret witness x in a polynomial P_x. There are two main options for encoding: either we construct P_x so that $P_x(0) = x$, encoding the witness as the constant term, or we define P_x so that $P_x(\infty) = x$, encoding the witness as the leading term.

The TCitH framework [FR23b] originally suggested encoding the witness as the constant term,

[4] With the VOLEitH framework, skipping the batching interaction also lowers the round complexity from 7 to 5.

which is the most traditional approach in the literature when using Shamir's secret sharing. In contrast, the VOLEitH framework suggests encoding the witness as the leading term of the (degree-1) polynomial. However, both frameworks do not mandate a specific encoding; we can choose to encode the witness as the leading term in TCitH and as the constant term in VOLEitH.

Each option has its advantages and disadvantages. Encoding the witness as the constant term requires special handling to avoid evaluation at the zero point, and we must use "infinity" point when $N = |\mathbb{F}|$. It also necessitates dealing with the inversion of some publicly known field elements. On the other hand, encoding the witness as the leading term results in a simpler implementation since no inversion is required and we avoid the special "infinity" point when $N = |\mathbb{F}|$. This makes it possible to use the canonical injection of $\{0, \ldots, N-1\}$ into field elements for Ω. However, this approach results in a slightly higher number of field multiplications, as we need to account for the homogeneous form of the MQ constraints. For the sake of implementation simplicity, we have chosen to encode the witness as the *leading term* of P_x in MQOM v2.

5.2 GGM trees

Recent improvements have made the arithmetic part of MPCitH-based signature schemes more efficient, shifting the computational and communication bottleneck to the symmetric part, particularly GGM trees. Consequently, several recent works have focused on optimizing the symmetric part, primarily by improving all-but-one vector commitments based on GGM trees.

Half-Tree technique [GYW+23; CLY+24; BCD24]. The half-tree technique has been proposed in [GYW+23] and has been first introduced in to the MPCitH context in [CLY+24; BCD24]. This technique aims to optimize the tree derivation, *i.e.* how two children nodes are generated from the parent node. Instead of using a double-length pseudorandom generator, it consists of deriving the first child y from the parent x using a symmetric primitive and building the second child z as $z := x \oplus y$, where $\oplus$ is the XOR operation. This derivation maintains the core security property of tree derivation: revealing one child node should not disclose any information about its sibling. Specifically, if revealing y does not leak information about x, then it also does not reveal anything about $z = y \oplus x$, as x masks it. Likewise, revealing z does not disclose any information about $y = x \oplus z$.

In MQOM v2, we use the half-tree optimization to halve the cost of the tree derivation and because it unlocks a second optimization described below.

Correlated Trees [HJ24; KLS24]. Besides the computational advantage of the half-tree technique, the latter has an interesting property: a tree derivation when using the half-tree preserves the XOR. It implies that the XOR of all the nodes at a same depth is the same across the entire tree. This means that the committer can control the XOR-sum δ of all the leaf seeds (by originally introducing this difference between the two child nodes of the root). Then, replacing the pseudorandom tape $\mathsf{PRG}(\mathsf{seed})$ by $\mathsf{seed} \,\|\, \mathsf{PRG}(\mathsf{seed})$, the XOR-sum δ is further enforced to the λ first bits of the random tapes. This makes it possible to save λ bits of communication in the correction value Δ_x by fixing δ to the λ first bits of x, thus leading to shorter signatures.

In MQOM v2, we use this optimization, namely we use correlated trees to save $\tau \cdot \lambda$ bits in the signature.

One-tree optimization [BBM+24]. Some combinatorial optimizations of the GGM trees has been proposed in [BBM+24]. The MPCitH/TCitH/VOLEitH-based schemes always use τ GGM trees. For each of them all the leaves except one are opened. Instead of considering τ independent GGM trees of N leaves in parallel, the authors of [BBM+24] suggest using a unique large GGM tree of $\tau \cdot N$ leaves. The i^{th} leaf of the e^{th} tree becomes the $(e \cdot N + i)^{\text{th}}$ leaf of the large unique tree. As explained in [BBM+24], "opening all-but-τ leaves of the big tree is more efficient than opening all-but-one leaves in each of the τ small trees because with high probability some of the active paths in the tree will merge relatively close to the leaves, which reduces the number of internal nodes that need to be revealed." Then, the authors propose to improve the previous point using some rejection sampling and grinding. When the last Fiat-Shamir challenge is such that the number of releaved nodes in the revealed sibling paths exceeds a threshold, the signer rejects the challenge and recompute the hash with an incremented counter. This process is repeated until the number of revealed nodes is below the fixed threshold. One can show that the approach leads to secure scheme even if the challenge space is reduced, because the security loss is compensated by the computational cost of searching a valid challenge.

Let us stress that this optimization is not compatible with the correlated-tree optimization. In MQOM v2, we did not consider this optimization because it complicates the design and implementation. First, using this large tree of $\tau \cdot N$ prevents from using a complete binary tree (since τ is usually not a power of 2), and so one needs to handle leaves of different depths. Then, while conceptually easy to understand, this optimization requires dealing with path merging which is tricky in terms of implementation. Finally, while path merging saves communication, it introduces variability in the signature size, which we prefer to avoid. For completeness, we present in Table 20 the signature sizes we would obtain if we used the one-tree optimization, instead of correlated trees.

Relaxed vector commitment [KLS24]. A recent work [KLS24] proposes a new idea to slightly improve the efficiency of GGM-tree all-but-one vector commitments. It consists in relaxing the vector commitment scheme by committing each leaf of the GGM trees using λ-bit digests instead of 2λ-bit digests. While this relaxation breaks the standard notion of binding, the authors show that using such a relaxed commitment scheme within a signature scheme still leads to the desired security. The high-level principle is the following: instead of properly binding the tree leaves, this relaxed commitment scheme *binds the height-1 nodes* (the parent nodes of the leaves) using the fact that the 2 (λ-bit) commitment digests of the two children form a 2λ-bit commitment digest for the parent node, which prevents the prover to get collisions over those nodes. Moreover, the authors show that the prover can have at most $2\lambda/\log_2 \lambda$ *preimages of the leaf commitment*. By counting the number of possible openings, the authors show that the relaxed vector commitment can be opened to at most $u := 2N(\lambda/\log 2\lambda)^2$ different witnesses. This relaxed opening degrades the soundness of the proof system by an offset of $\log_2 u$ bits. This security loss can be compensated by increasing the scheme parameters while still benefitting from a decreased signature size.

We did not include this optimization in MQOM v2 but we will consider it for a future update after careful analysis of its security and adaptation to the TCitH context. We could expect a saving of around 200 bytes in the signature size (for the first security level).

Framework	TCitH		VOLEitH	
Statistical Batching	Without (3r)	With (5r)	Without (3r)	With (5r)
L1-gf2-short	2 852	2 804	2 950 (+3%)	2 774 (-1%)
L1-gf16-short	3 044	2 900	3 038 (-0%)	2 862 (-1%)
L1-gf256-short	3 524	3 140	3 434 (-3%)	3 082 (-2%)
L1-gf2-fast	3 204	3 132	3 326 (+4%)	3 086 (-1%)
L1-gf16-fast	3 492	3 276	3 446 (-1%)	3 206 (-2%)
L1-gf256-fast	4 212	3 636	3 986 (-6%)	3 506 (-4%)
L3-gf2-short	6 376	6 262	6 620 (+4%)	6 212 (-1%)
L3-gf16-short	6 832	6 490	6 824 (-0%)	6 416 (-1%)
L3-gf256-short	7 972	7 060	7 742 (-3%)	6 926 (-2%)
L3-gf2-fast	7 240	7 078	7 556 (+4%)	7 004 (-1%)
L3-gf16-fast	7 888	7 402	7 832 (-1%)	7 280 (-2%)
L3-gf256-fast	9 508	8 212	9 074 (-5%)	7 970 (-3%)
L5-gf2-short	11 540	11 340	11 786 (+2%)	11 050 (-3%)
L5-gf16-short	12 440	11 790	12 200 (-2%)	11 464 (-3%)
L5-gf256-short	14 340	12 740	13 810 (-4%)	12 338 (-3%)
L5-gf2-fast	12 996	12 708	13 498 (+4%)	12 506 (-2%)
L5-gf16-fast	14 292	13 356	14 056 (-2%)	13 064 (-2%)
L5-gf256-fast	17 028	14 724	16 226 (-5%)	14 242 (-3%)

Table 20: Signature sizes when using the one-tree technique, instead of correlated trees. All the signature sizes are in bytes. The trade-off "short" relies on GGM trees with 2048 leaves, while the trade-off "fast" relies on GGM trees with 256 leaves. For all instances, the proof-of-work is roughly of 10 bits. While τ would be larger using TCitH than using VOLEitH, the number of the expanded bits using PRG on tree leaves is larger using VOLEitH than using TCitH (up to a +50% overhead), because of the mask for the consistency check.

5.3 Grinding

Together with the one-tree optimization, [BBM+24] suggests using an explicit proof-of-work to the Fiat-Shamir hash computation of the query challenge, whihc is known as *grinding* [Sta21]. Together with the query challenge, the signer samples a w-bit value which should be zero, for w a parameter of the scheme. If this value is not zero, the signer rejects the query challenge and recompute the hash with an incremented counter, until a zero value is found. This strategy increases the cost of hashing the last challenge by a factor 2^w which translates to decreasing the soundness error by a factor 2^{-w}. As a consequence, one can lower the GGM tree parameters to achieve a soundness of $\lambda - w$ bits instead of λ.

We use the grinding optimization in MQOM v2. We chose the grinding parameter w in order to decrease the number of repetitions (τ).

5.4 Symmetric primitives

For most of the symmetric primitives involved in the signature scheme, there are two possible options to instantiate them: either we use an extendable output hash function (XOF), or we use a block cipher. While the first version of MQOM solely relied on XOF, we changed for mainly using a block cipher in MQOM v2 for performance reasons. Specifically, we aim to leverage the AES hardware instructions available on modern CPUs. While the easiest choice would then be to use AES-λ as block cipher (e.g. as counter mode for the PRG), this choice implies a 128-bit distinguisher whatever λ because of the fixed 128-bit block-size of AES. As a result, the EUF-CMA advantage can only be upper bounded by 2^{-128} whatever the target security λ.

To avoid this issue, we use a block cipher with higher block size for Categories III and V, namely Rijndael-256-256 (with truncation for $\lambda = 192$). The latter cipher also benefits from fast implementation using AES hardware instructions. Moreover, using a cipher with a λ-bit key-size and λ-bit block-size, we can use a (partial) fixed-key mode in the seed derivation with a Davies-Meyer construction. This further improves the performances by saving some costly key schedules.

6 Advantages and limitations

Bad news first, the MQOM signature scheme suffers the following limitations:

- **Relatively slow:** As other MPCitH based scheme, MQOM is relatively slow, with signing and verification time ranging between 2 and 14 megacycles (0.9 – 5.6 ms AMD Ryzen Threadripper PRO 7995WX processor) for NIST security category I. This is slow compared to lattice-based signatures. One of the reason is the greedy use of symmetric cryptography.
- **Quadratic growth in the security level:** As other MPCitH-based signature schemes, or, more generally, as other schemes applying the Fiat-Shamir transform to a parallelly repeated ZK-PoK with non-negligible soundness error, MQOM suffers a quadratic growth of the signature size. In practice, the size of MQOM signatures roughly doubles while going from Category I to Category III and while going from Category III to Category V as well.

On the other hand, MQOM benefits of the following advantages:

- **Conservative hardness assumption:** Being generic, the MPCitH approach can be applied to any problem on does not rely on structured problems to introduce a trapdoor. MQOM benefits this by relying on a full random instance of the MQ problem which is believe to be a conservative hardness assumption.
- **Small (public) keys:** Thanks to the unstructured feature of the MQ instance, it can be mostly derive from a random seed. Hence the public key is only composed of a λ-bit seed and the relatively-short output y of the MQ system. The secret key additionally includes the relatively-short input x of the MQ system (which can further be fully compressed as the root seed of the key generation).
- **Highly parallelizable:** As other schemes based on the MPCitH paradigm, MQOM is highly parallelizable. Most of the computation can be done in parallel for the τ repetitions and computation can be further parallelized inside a repetition (arithmetic computation, seed trees and commitments).
- **Good public key + signature size:** As other schemes based on the MPCitH paradigm, MQOM achieves a good score in terms of "public key + signature size" metric compared to other candidate post-quantum signature schemes.
- **Relatively small signatures:** The last generation of MPCitH-based signature schemes in the literature (at time of writing) achieves signature sizes ranging on 2.5–5 KB (for 128-bit of security). MQOM is on the lower side of this range, with 2.8–3.6 KB. MPCitH-based signatures achieving lower sizes are arguably based on less conservative assumptions (*e.g.* recent dedicated symmetric designs). Among the MPCitH-based NIST candidates selected for Round 2, MQOM has the smallest signatures.
- **Fairly embedded friendly:** For an MPCitH-based scheme, MQOM is fairly well-suited for implementation on embedded devices. Benchmarks on Cortex-M4 demonstrate that MQOM can be implemented with low memory requirements (under 10 KB for L1). Among the MPCitH-based NIST candidates selected for Round 2, MQOM requires the fewest symmetric primitive calls, and natively achieves the lowest memory footprint. Moreover,

protecting MQOM against side-channel attacks using masking is simple: it avoids costly Arithmetic-Boolean masking conversions (common in lattice-based schemes), does not require any divisions (even with public divisors) or Gaussian elimination (as in UOV-like schemes).

References

[AB24] M. Albrecht and G. Bard. *The M4RI Library*. The M4RI Team. 2024. URL: https://bitbucket.org/malb/m4ri (cited on page 48).

[AFG+24] C. Aguilar-Melchor, T. Feneuil, N. Gama, S. Gueron, J. Howe, D. Joseph, A. Joux, E. Persichetti, T. H. Randrianarisoa, M. Rivain, and D. Yue. SDitH — Syndrome Decoding in the Head. Technical report, National Institute of Standards and Technology, 2024. available at https://csrc.nist.gov/Projects/pqc-dig-sig/round-2-additional-signatures (cited on page 24).

[AP21] A. Adomnicai and T. Peyrin. Fixslicing AES-like ciphers. *IACR TCHES*, (1):402–425, 2021. URL: https://tches.iacr.org/index.php/TCHES/article/view/8739 (cited on page 42).

[AW21] J. Alman and V. V. Williams. A refined laser method and faster matrix multiplication. In D. Marx, editor, *Proceedings of the 2021 ACM-SIAM Symposium on Discrete Algorithms, SODA 2021, Virtual Conference, January 10 - 13, 2021*, pages 522–539. SIAM, 2021 (cited on page 48).

[Bar04] M. Bardet. *Étude des systèmes algébriques surdéterminés. Applications aux codes correcteurs et à la cryptographie*. PhD thesis, Pierre and Marie Curie University, Paris, France, 2004. URL: https://tel.archives-ouvertes.fr/tel-00449609 (cited on page 50).

[BBD+23] C. Baum, L. Braun, C. Delpech de Saint Guilhem, M. Klooß, E. Orsini, L. Roy, and P. Scholl. Publicly verifiable zero-knowledge and post-quantum signatures from VOLE-in-the-head. In pages 581–615, Santa Barbara, CA, USA, 2023 (cited on pages 2–4, 8, 61).

[BBM+24] C. Baum, W. Beullens, S. Mukherjee, E. Orsini, S. Ramacher, C. Rechberger, L. Roy, and P. Scholl. One tree to rule them all: optimizing GGM trees and OWFs for post-quantum signatures. In *ASIACRYPT 2024, Part I*, pages 463–493, 2024 (cited on pages 4, 64, 65).

[BCC+13] C. Bouillaguet, C. Cheng, T. Chou, R. Niederhagen, and B.-Y. Yang. Fast Exhaustive Search for Quadratic Systems in $\mathbb{F}_2$ on FPGAs. In *Selected Areas in Cryptography*, pages 205–222. Springer, 2013. https://eprint.iacr.org/2013/436.pdf (cited on page 55).

[BCD24] D. Bui, K. Cong, and C. Delpech de Saint Guilhem. Improved all-but-one vector commitment with applications to post-quantum signatures. Cryptology ePrint Archive, Report 2024/097, 2024. URL: https://eprint.iacr.org/2024/097 (cited on page 63).

[Beu20] W. Beullens. Sigma protocols for MQ, PKP and SIS, and Fishy signature schemes. In A. Canteaut and Y. Ishai, editors, *EUROCRYPT 2020, Part III*, pages 183–211, Zagreb, Croatia, 2020 (cited on page 62).

[Beu22] W. Beullens. Breaking rainbow takes a weekend on a laptop. In Y. Dodis and T. Shrimpton, editors, *Advances in Cryptology - CRYPTO 2022 - 42nd Annual International Cryptology Conference, CRYPTO 2022, Santa Barbara, CA, USA, August 15-18, 2022, Proceedings, Part II*, pages 464–479. Springer, 2022. URL: https://doi.org/10.1007/978-3-031-15979-4_16 (cited on page 52).

[BFP09] L. Bettale, J. Faugère, and L. Perret. Hybrid approach for solving multivariate systems over finite fields. *J. Math. Cryptol.*, (3):177–197, 2009 (cited on page 52).

[BFP12] L. Bettale, J. Faugère, and L. Perret. Solving polynomial systems over finite fields: improved analysis of the hybrid approach. In J. van der Hoeven and M. van Hoeij, editors, *International Symposium on Symbolic and Algebraic Computation, ISSAC'12, Grenoble, France - July 22 - 25, 2012*, pages 67–74. ACM, 2012 (cited on pages 52, 53).

[BFR24] R. Benadjila, T. Feneuil, and M. Rivain. MQ on my mind: post-quantum signatures from the non-structured multivariate quadratic problem. In pages 468–485, 2024 (cited on pages 2, 47).

[BFS15] M. Bardet, J. Faugère, and B. Salvy. On the complexity of the F5 gröbner basis algorithm. *J. Symb. Comput.*:49–70, 2015 (cited on page 50).

[BFS+13] M. Bardet, J. Faugère, B. Salvy, and P. Spaenlehauer. On the complexity of solving quadratic boolean systems. *J. Complexity*, (1):53–75, 2013. URL: https://doi.org/10.1016/j.jco.2012.07.001 (cited on page 55).

[BGG+20] F. Boudot, P. Gaudry, A. Guillevic, N. Heninger, E. Thomé, and P. Zimmermann. Comparing the difficulty of factorization and discrete logarithm: A 240-digit experiment. In D. Micciancio and T. Ristenpart, editors, *CRYPTO 2020, Part II*, pages 62–91, Santa Barbara, CA, USA, 2020 (cited on pages 51, 55).

[BKW19] A. Björklund, P. Kaski, and R. Williams. Solving systems of polynomial equations over GF(2) by a parity-counting self-reduction. In C. Baier, I. Chatzigiannakis, P. Flocchini, and S. Leonardi, editors, *46th International Colloquium on Automata, Languages, and Programming, ICALP 2019, July 9-12, 2019, Patras, Greece*, 26:1–26:13. Schloss Dagstuhl - Leibniz-Zentrum für Informatik, 2019. URL: https://doi.org/10.4230/LIPIcs.ICALP.2019.26 (cited on page 56).

[BMS+22] E. Bellini, R. H. Makarim, C. Sanna, and J. A. Verbel. An estimator for the hardness of the MQ problem. In L. Batina and J. Daemen, editors, *Progress in Cryptology - AFRICACRYPT 2022: 13th International Conference on Cryptology in Africa, AFRICACRYPT 2022, Fes, Morocco, July 18-20, 2022, Proceedings*, pages 323–347. Springer Nature Switzerland, 2022 (cited on page 47).

[Bou24] C. Bouillaguet. Algorithm xxx: evaluating a boolean polynomial on all possible inputs. *ACM Trans. Math. Softw.*, 2024. URL: https://doi.org/10.1145/3699957. Just Accepted (cited on page 58).

[CCN+12] C. Cheng, T. Chou, R. Niederhagen, and B. Yang. Solving quadratic equations with XL on parallel architectures. In E. Prouff and P. Schaumont, editors, *Cryptographic Hardware and Embedded Systems - CHES 2012 - 14th International Workshop, Leuven, Belgium, September 9-12, 2012. Proceedings*, pages 356–373. Springer, 2012 (cited on pages 51, 52).

[CDG+17] M. Chase, D. Derler, S. Goldfeder, C. Orlandi, S. Ramacher, C. Rechberger, D. Slamanig, and G. Zaverucha. Post-quantum zero-knowledge and signatures from symmetric-key primitives. In B. M. Thuraisingham, D. Evans, T. Malkin, and D. Xu, editors, *ACM CCS 2017*, pages 1825–1842, Dallas, TX, USA. ACM Press, 2017 (cited on page 62).

[CDI05] R. Cramer, I. Damgård, and Y. Ishai. Share conversion, pseudorandom secret-sharing and applications to secure computation. In J. Kilian, editor, *TCC 2005*, pages 342–362, Cambridge, MA, USA, 2005 (cited on page 8).

[CG23] A. Caminata and E. Gorla. Solving degree, last fall degree, and related invariants. *J. Symb. Comput.*:322–335, 2023. URL: https://doi.org/10.1016/j.jsc.2022.05.001 (cited on page 50).

[CKP+00] N. T. Courtois, A. Klimov, J. Patarin, and A. Shamir. Efficient algorithms for solving overdefined systems of multivariate polynomial equations. In B. Preneel, editor, *Advances in Cryptology - EUROCRYPT 2000, International Conference on the Theory and Application of Cryptographic Techniques, Bruges, Belgium, May 14-18, 2000, Proceeding*, pages 392–407. Springer, 2000. URL: https://doi.org/10.1007/3-540-45539-6_27 (cited on page 51).

[CLY+24] H. Cui, H. Liu, D. Yan, K. Yang, Y. Yu, and K. Zhang. ReSolveD: shorter signatures from regular syndrome decoding and VOLE-in-the-head. In *PKC 2024, Part I*, pages 229–258, 2024 (cited on page 63).

[DDV+21] J. Ding, J. Deaton, Vishakha, and B. Yang. The nested subset differential attack - A practical direct attack against LUOV which forges a signature within 210 minutes. In A. Canteaut and F. Standaert, editors, *Advances in Cryptology - EUROCRYPT 2021 - 40th Annual International Conference on the Theory and Applications of Cryptographic Techniques, Zagreb, Croatia, October 17-21, 2021, Proceedings, Part I*, pages 329–347. Springer, 2021. URL: https://doi.org/10.1007/978-3-030-77870-5_12 (cited on page 55).

[DGP08] J.-G. Dumas, P. Giorgi, and C. Pernet. Dense linear algebra over word-size prime fields: the fflas and ffpack packages. *ACM Trans. on Mathematical Software (TOMS)*, (3):1–42, 2008 (cited on page 48).

[Din21a] I. Dinur. Cryptanalytic applications of the polynomial method for solving multivariate equation systems over GF(2). In A. Canteaut and F. Standaert, editors, *Advances in Cryptology - EUROCRYPT 2021 - 40th Annual International Conference on the Theory and Applications of Cryptographic Techniques, Zagreb, Croatia, October 17-21, 2021, Proceedings, Part I*, pages 374–403. Springer, 2021. URL: https://doi.org/10.1007/978-3-030-77870-5_14 (cited on page 56).

[Din21b] I. Dinur. Cryptanalytic applications of the polynomial method for solving multivariate equation systems over GF(2). In A. Canteaut and F.-X. Standaert, editors, *EUROCRYPT 2021, Part I*, pages 374–403, Zagreb, Croatia, 2021 (cited on page 58).

[Din21c] I. Dinur. Improved algorithms for solving polynomial systems over GF(2) by multiple parity-counting. In D. Marx, editor, *Proceedings of the 2021 ACM-SIAM Symposium on Discrete Algorithms, SODA 2021, Virtual Conference, January 10 - 13, 2021*, pages 2550–2564. SIAM, 2021. URL: https://doi.org/10.1137/1.9781611976465.151 (cited on page 56).

[EVZ+24] A. Esser, J. A. Verbel, F. Zweydinger, and E. Bellini. Sok: cryptographicestimators - a software library for cryptographic hardness estimation. In J. Zhou, T. Q. S. Quek, D. Gao, and A. A. Cárdenas, editors, *Proceedings of the 19th ACM Asia Conference on Computer and Communications Security, ASIA CCS 2024, Singa-*

pore, July 1-5, 2024. ACM, 2024. URL: https://doi.org/10.1145/3634737.3645007 (cited on page 47).

[FK24] H. Furue and M. Kudo. Polynomial XL: A variant of the XL algorithm using macaulay matrices over polynomial rings. In M. O. Saarinen and D. Smith-Tone, editors, *Post-Quantum Cryptography - 15th International Workshop, PQCrypto 2024, Oxford, UK, June 12-14, 2024, Proceedings, Part II*, pages 109–143. Springer, 2024. URL: https://doi.org/10.1007/978-3-031-62746-0_6 (cited on page 53).

[FR23a] T. Feneuil and M. Rivain. MQOM: MQ on my Mind – Algorithm Specifications and Supporting Documentation. Version 1.0 – 31st May 2023, 2023. https://mqom.org/docs/mqom-v1.0.pdf (cited on pages 2, 47).

[FR23b] T. Feneuil and M. Rivain. Threshold computation in the head: improved framework for post-quantum signatures and zero-knowledge arguments. Cryptology ePrint Archive, Report 2023/1573, 2023. URL: https://eprint.iacr.org/2023/1573 (cited on pages 2–4, 8, 9, 61, 62).

[FR23c] T. Feneuil and M. Rivain. Threshold linear secret sharing to the rescue of MPC-in-the-head. In *ASIACRYPT 2023, Part I*, pages 441–473, 2023 (cited on page 3).

[GKW+20] C. Guo, J. Katz, X. Wang, and Y. Yu. Efficient and secure multiparty computation from fixed-key block ciphers. In *2020 IEEE Symposium on Security and Privacy*, pages 825–841, San Francisco, CA, USA. IEEE Computer Society Press, 2020 (cited on page 13).

[GMO16] I. Giacomelli, J. Madsen, and C. Orlandi. ZKBoo: faster zero-knowledge for Boolean circuits. In T. Holz and S. Savage, editors, *USENIX Security 2016*, pages 1069–1083, Austin, TX, USA. USENIX Association, 2016 (cited on page 62).

[GYW+23] X. Guo, K. Yang, X. Wang, W. Zhang, X. Xie, J. Zhang, and Z. Liu. Half-tree: halving the cost of tree expansion in COT and DPF. In C. Hazay and M. Stam, editors, *EUROCRYPT 2023, Part I*, pages 330–362, Lyon, France, 2023 (cited on pages 9, 63).

[HJ24] J. Huth and A. Joux. MPC in the head using the subfield bilinear collision problem. In *CRYPTO 2024, Part I*, pages 39–70, Santa Barbara, CA, USA, 2024 (cited on page 63).

[IKO+07] Y. Ishai, E. Kushilevitz, R. Ostrovsky, and A. Sahai. Zero-knowledge from secure multiparty computation. In D. S. Johnson and U. Feige, editors, *39th ACM STOC*, pages 21–30, San Diego, CA, USA. ACM Press, 2007 (cited on page 2).

[JV17] A. Joux and V. Vitse. A Crossbred Algorithm for Solving Boolean Polynomial Systems. In *NuTMiC*, pages 3–21. Springer, 2017. https://eprint.iacr.org/2017/372.pdf (cited on page 55).

[KKW18] J. Katz, V. Kolesnikov, and X. Wang. Improved non-interactive zero knowledge with applications to post-quantum signatures. In D. Lie, M. Mannan, M. Backes, and X. Wang, editors, *ACM CCS 2018*, pages 525–537, Toronto, ON, Canada. ACM Press, 2018 (cited on pages 2, 8, 62).

[KLS24] S. Kim, B. Lee, and M. Son. Relaxed vector commitment for shorter signatures. Cryptology ePrint Archive, Report 2024/1004, 2024. URL: https://eprint.iacr.org/2024/1004 (cited on pages 47, 63, 64).

[KPR+] M. J. Kannwischer, R. Petri, J. Rijneveld, P. Schwabe, and K. Stoffelen. PQM4: post-quantum crypto library for the ARM Cortex-M4. https://github.com/mupq/pqm4 (cited on page 42).

[Laz83] D. Lazard. Gröbner-bases, gaussian elimination and resolution of systems of algebraic equations. In J. A. van Hulzen, editor, *EUROCAL*, pages 146–156. Springer, 1983. ISBN: 3-540-12868-9 (cited on pages 49, 51).

[LPT+17] D. Lokshtanov, R. Paturi, S. Tamaki, R. R. Williams, and H. Yu. Beating brute force for systems of polynomial equations over finite fields. In P. N. Klein, editor, *Proceedings of the Twenty-Eighth Annual ACM-SIAM Symposium on Discrete Algorithms, SODA 2017, Barcelona, Spain, Hotel Porta Fira, January 16-19*, pages 2190–2202. SIAM, 2017. ISBN: 978-1-61197-478-2. URL: https://doi.org/10.1137/1.9781611974782.143 (cited on page 56).

[MPG13] G. Macario-Rat, J. Plût, and H. Gilbert. New insight into the isomorphism of polynomial problem IP1S and its use in cryptography. In K. Sako and P. Sarkar, editors, *ASIACRYPT 2013, Part I*, pages 117–133, Bengalore, India, 2013 (cited on page 57).

[NIS22] N. I. of Standards and T. (NIST). Call for Additional Digital Signature Schemes for the Post-Quantum Cryptography Standardization Process, 2022. https://csrc.nist.gov/csrc/media/Projects/pqc-dig-sig/documents/call-for-proposals-dig-sig-sept-2022.pdf (cited on page 2).

[NNY18] R. Niederhagen, K. Ning, and B. Yang. Implementing joux-vitse's crossbred algorithm for solving MQ systems over GF(2) on gpus. In T. Lange and R. Steinwandt, editors, *Post-Quantum Cryptography - 9th International Conference, PQCrypto 2018, Fort Lauderdale, FL, USA, April 9-11, 2018, Proceedings*, pages 121–141. Springer, 2018. URL: https://doi.org/10.1007/978-3-319-79063-3_6 (cited on page 56).

[Ope] OpenBenchmarking.org. https://openbenchmarking.org/processors (cited on page 37).

[Roy22] L. Roy. SoftSpokenOT: quieter OT extension from small-field silent VOLE in the minicrypt model. In Y. Dodis and T. Shrimpton, editors, *CRYPTO 2022, Part I*, pages 657–687, Santa Barbara, CA, USA, 2022 (cited on pages 8, 24).

[SS16] P. Schwabe and K. Stoffelen. All the AES you need on Cortex-M3 and M4. In R. Avanzi and H. M. Heys, editors, *SAC 2016*, pages 180–194, St. John's, NL, Canada, 2016 (cited on page 42).

[Sta21] StarkWare. ethSTARK documentation. Cryptology ePrint Archive, Report 2021/582, 2021. URL: https://eprint.iacr.org/2021/582 (cited on pages 12, 65).

[SZ22] A. Szepieniec and Y. Zhang. Polynomial IOPs for linear algebra relations. In G. Hanaoka, J. Shikata, and Y. Watanabe, editors, *PKC 2022, Part I*, pages 523–552, Virtual Event, 2022 (cited on page 3).

[Tha23] J. Thaler. *Proofs, Arguments, and Zero-Knowledge*. 2023. https://people.cs.georgetown.edu/jthaler/ProofsArgsAndZK.pdf (cited on page 3).

[Wik] Wikipedia. AVX-512. Note: Intel fusing off AVX-512 support on Alder Lake. https://en.wikipedia.org/wiki/AVX-512#endnote_adl-avx512-note (cited on page 37).

[YC04] B. Yang and J. Chen. Theoretical analysis of XL over small fields. In H. Wang, J. Pieprzyk, and V. Varadharajan, editors, *Information Security and Privacy: 9th Australasian Conference, ACISP 2004, Sydney, Australia, July 13-15, 2004. Proceedings*, pages 277–288. Springer, 2004. URL: https://doi.org/10.1007/978-3-540-27800-9_24 (cited on page 55).

[YSW+21] K. Yang, P. Sarkar, C. Weng, and X. Wang. QuickSilver: efficient and affordable zero-knowledge proofs for circuits and polynomials over any field. In G. Vigna and E. Shi, editors, *ACM CCS 2021*, pages 2986–3001, Virtual Event, Republic of Korea. ACM Press, 2021 (cited on page 4).